Determining Predictive Metabolomic Biomarkers of Meniscal Injury in Dogs with Cranial Cruciate Ligament Disease Using Stifle Joint Synovial Fluid

Thesis submitted in accordance with the requirements of the University of Liverpool for the degree of Master of Philosophy

By

Christine Rebecca Pye

September 2021

Table of Contents

Acknowledgements.

Firstly, I would like to acknowledge and give my thanks to my two supervisors, Professor Mandy Peffers and Professor Eithne Comerford, for their help and support over this past year. Both have been an inspiration to me as a veterinary surgeon entering the world of academia from a clinical background, and their knowledge and skills have been invaluable to me throughout this project.

I would also like to sincerely thank Marie Phelan from the NMR Centre at the University of Liverpool. For teaching me and helping answer any query I might have had along the way.

Thanks to Dan Green from the computational biology facility for his help with statistical analyses and R scripts, and thanks to Bas Housmans from the University of Maastricht for his work on the luciferase reporter assays.

Thanks also to all the staff at the University of Liverpool Small Animal Teaching Hospital and the Animal Trust, for their help with collecting samples for this project amongst all their other duties, and to the Animal Trust staff for helping me get through those long hot days in theatre!

I would also like to acknowledge my funders for this project, BSAVA PetSavers, for enabling this work to happen.

Lastly, to all of the Peffers group past and present, for helping me find my feet in research during a global pandemic.

Abstract

Canine cruciate ligament rupture is one of the most common causes of pelvic limb lameness in dogs, leading to stifle instability, pain, lameness and osteoarthritis. Meniscal injuries arise as a sequelae of stifle joint instability due to cranial cruciate ligament rupture, and can be challenging to diagnose without surgical means in veterinary practice. Nuclear magnetic resonance spectroscopy of synovial fluid is a relatively inexpensive, accurate and reproducible technique that has been used to identify metabolites that are significantly altered in joint pathologies. The aim of this study was to define the metabolomic profile of synovial fluid from canine stifle joints with and without meniscal injuries in order to investigate biomarkers of meniscal injuries. We hypothesised that the metabolomic profile of synovial fluid in dogs will change according to the presence of cranial cruciate ligament rupture and with or without meniscal injury.

In this thesis, firstly, an optimisation study was undertaken examining the effects of increased refrigerated storage time prior to processing on the metabolomic profile of equine and canine synovial fluid. Secondly, nuclear magnetic resonance spectroscopy was undertaken on canine synovial fluid and the metabolomic profile established and compared to different clinical variables and joint pathologies, including cranial cruciate ligament rupture and meniscal injuries. Thirdly, a lipidomic study was undertaken to examine whether any lipids could be identified as being significantly altered depending on meniscal injury status. Finally, other differential signalling pathways were also examined, as well as examining protein abundances in canine synovial fluid.

An increase in mobile lipids was found in canine synovial fluid with meniscal injuries compared to without meniscal injuries using nuclear magnetic resonance spectroscopy. Nuclear magnetic resonance analysis of lipid extracts from a subset of samples found an increase in most lipids with meniscal injury, although no lipids reached the significance threshold. Three reporter elements were significantly upregulated when stimulated by canine synovial fluid with meniscal injury compared to without meniscal injury, including glucocorticoid response element. However, using ELISA there was no significant difference in cortisol concentrations in the canine synovial fluid between groups.

As far as the authors are aware, this is the first study to examine metabolomic changes of synovial fluid depending on meniscal injury status in any species. The finding of increases in lipids in the synovial fluid of dogs with meniscal injury is of interest in determining potential future biomarkers of meniscal injury, as well as understanding the metabolic processes that occur with meniscal injury.

List of Tables

List of Figures

List of Abbreviations

11β-HSD1	11β-hydroxysteroid dehydrogenase 1
1D	One dimensional
2D	Two dimensional
AA	Adjuvant arthritis
ACL	Anterior cruciate ligament
ANCOVA	Analysis of co-variance
ANOVA	Analysis of variance
AP-1	Activator protein 1
BCS	Body condition score
BD	Bechet's disease
CaCL	Caudal cruciate ligament
CCL	Cranial cruciate ligament
CCLD	Cranial cruciate ligament disease
CCLR	Cranial cruciate ligament rupture
CCWO	Cranial closing wedge osteotomy
CT	Computed tomography
CXCL6	C-X-C Motif Chemokine Ligand 6
ECM	Extra-cellular matrix
EGF	Epidermal growth factor
ELISA	Enzyme linked immunosorbent assay
ERK	Extracellular-signal related kinase
FCS	Fetal calf serum
FDR	False discovery rate
FE	Female entire
FID	Free induction decay
FN	Female neutered
GC	Gas chromatography
GC	Gas chromatography
GC/TOF-MS	Gas chromatography/time of flight mass spectrometry
GC-MS	Gas chromatography- mass spectrometry
GRE	Glucocorticoid response element
GRE	Glucocorticoid receptor
HA	Hyaluronic acid
HILIC-HRMS	Hydrophilic interaction liquid chromatography - high-resolution mass spectrometry
HMDB	Human metabolite database
HRG	Histidine rich glycoprotein
HSD	Honestly significantly different
IA	Intra-articular
ID	Identification
IL-1β	Interleukin 1 beta
IL-8	Interleukin 8
kg	Kilogram
LC-MS	Light chromatography- mass spectrometry
LC-MS	Light chromatography
LMI	Late meniscal injuries

LWHH	Line width half height
MAPK	Mitogen activated protein kinase
MCP-1	Monocyte chemoattractant protein 1
ME	Male entire
MIP-1β	Macrophage inflammatory protein-1β
MMP	Matrix metalloproteinase 2
MN	Male neutered
MRI	Magnetic resonance imaging
MS	Mass Spectrometry
N/A	Not applicable
NIH	National Institutes of Health
NMR	Nuclear magnetic resonance
OA	Osteoarthritis
OCD	Osteochondritis dissecans
PCA	Principal component analysis
PCA	Principle component
PGE2	Prostaglandin E2
Phe/Tyr	Phenylalanine/Tyrosine ratio
pSpA	Peripheral spondyloarthritis
PTAA	Post-traumatic ankle arthritis
PTOA	Post-traumatic osteoarthritis
RA	Rheumatoid arthritis
ReA	Reactive arthritis
RNA	Ribonucleic acid
SD	Standard deviation
SF	Synovial fluid
SNA	Seronegative arthritis
SRE	Serum response element
TIMP	Tissue inhibitors of metalloproteinases
TNFα	Tumour necrosis factor alpha
TPA	Tibial plateau angle
TPLO	Tibial plateau levelling osteotomy
TSE	Turbo spin echo
TSP	Sodium trimethyl propionate
TTA	Tibial tuberosity advancement
UPLC-QTOF-MS	Ultra-performance liquid chromatography to quadrupole time-of-flight mass spectrometry,
uSpA	Unspecified arthritis
VEGF	Vascular endothelial growth factor

1. Introduction

1.1. The canine stifle joint

1.1.1. Introduction

The canine stifle joint (analogous to the human knee joint) is a synovial joint situated within the pelvic limb. It constitutes the articulation of the distal femur and proximal tibia (the femorotibial articulation), the distal femur and patella (the femoropatellar articulation) and the proximal fibular and tibia (the tibiofibular articulation)(Carpenter Jr and Cooper, 2000). The patella is a large sesamoid bone connecting the quadriceps muscle group to the cranio-proximal tibia via the patella ligament (Burks *et al*., 1990). There are three other sesamoid bones, namely the lateral, medial and popliteal fabellae (Park, 1979). The joint is encapsulated by a joint capsule, which consists of an outer fibrous layer, and an inner synovial membrane (Galloway and Lester, 1995). The patella ligament is separated from the joint capsule by a pad of adipose tissue, the infrapatellar fat pad (Schmidli *et al*., 2018). A viscous fluid, synovial fluid (SF), is present within the stifle joint (Leeson *et al*., 1988). The articular surfaces of the bones are covered in articular cartilage, a highly specialised connective tissue of diarthrodial joints (Dunham *et al*., 1988). Two semi-lunar fibrocartilaginous discs of tissue, called the menisci lie between the proximal tibia and distal femoral condyles (Arnoczky *et al*., 1980). There are four femorotibial ligaments providing ligamentous support within the canine stifle joint. These are the medial and lateral collateral ligaments, and the cranial and caudal cruciate ligaments (Arnoczky and Marshall, 1977, Vasseur and Arnoczky, 1981). Multiple pelvic limb muscles also constitute a component of the stifle joint organ, playing a role in joint function (Evans and De Lahunta, 2013).

The stifle joint can be thought of as an organ, in that all the components act in synergy with each other, and if one component were to fail, then failure of the stifle joint organ can ensue (Heffron and Campbell, 1978, Innes *et al*., 2004, Pozzi *et al*., 2010b).

1.1.2. The canine cranial cruciate ligament

The two cruciate ligaments are named after their anatomical arrangement, as they cross over each other within the joint (Arnoczky and Marshall, 1977). The caudal cruciate ligament (CaCL) runs caudodistal from the lateral medial femoral condyle to the medial aspect of the

popliteal notch of the tibia. The cranial cruciate ligament (CCL) attaches from the caudomedial aspect of the lateral femoral condyle and the caudolateral aspect of the intercondylar fossa of the femur, and runs cranially, medially and distally in an outward spiral to insert onto the cranial intercondyloid area of the tibial plateau (Arnoczky and Marshall, 1977). There are two distinct bands of the CCL, the craniomedial (CrM) band and the caudolateral (CaL) band, named after their relative area of insertion on the tibial plateau (Figure 1.1). The CaL band is the larger of the two, forming the bulk of the CCL (Tanegashima *et al*., 2019). The CCL has a core region, which is its main tissue component, and an epiligamentous region (Hayashi *et al*., 2003). Although the cruciate ligaments are located within the joint, they are deemed to be extra-synovial as they are covered in a layer of synovium (Heffron and Campbell, 1978).

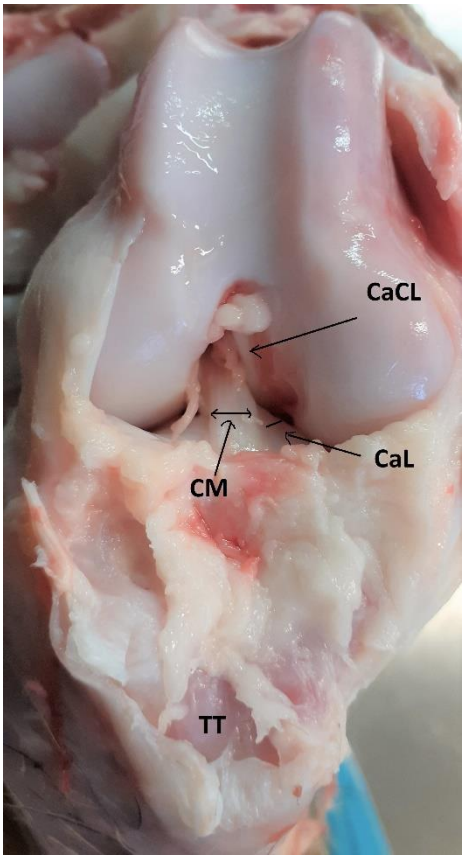

Figure 1.1. Cranial view of the canine stifle joint*. The caudal cruciate ligament (CaCL), and the two bands of the cranial cruciate ligament, the caudolateral band (CaL) and the craniomedial band (CrM) are shown. The tibial tuberosity (TT) is also labelled.*

The cruciate ligaments are composed of twisted collagenous fascicles and fibre bundles, subdivided into fascicles, subfascicular units, fibres and fibrils (Arnoczky and Marshall, 1977). The fibrils have a crimped appearance, and upon tensile loading of the ligaments these

crimped fibrils straighten out, increasing in length (Yahia and Drouin, 1989, Readioff *et al*., 2020). The CCL is composed of 60-70% water, with collagen constituting approximately 90% of the dry weight of the CCL, and the remaining dry weight being composed of other proteins such as elastin (5-10%) (Smith et al., 2014), proteoglycans, glycoproteins and lipoproteins (Comerford et al., 2006, Comerford et al., 2011). Collagen type I is the predominant collagen type in the cruciate ligaments, representing over 90% of the collagen in the CCL, with type III collagen making up the rest (Amiel *et al*., 1984). The main cell type present in the CCL is the fibroblast, and three different types have been described, with type A cells having long, thin cytoplasmic processes, type B cells having shorter, thicker, frequently branching processes, and type C cells with rounded nuclei and no cytoplasmic processes (Smith *et al*., 2012). Mechanoreceptors and proprioceptors are present in the centre of the cruciate ligaments, and axons course from these receptors through the synovium that encases the ligaments, and proximally towards the spinal cord (Arcand *et al*., 2000, Adachi *et al*., 2002). The blood supply to the CCL arises from the periligamentous tissue, and is relatively tenuous (Testuz *et al*., 2016).

The cruciate ligaments are critical for stabilisation of the stifle joint. The primary function of the CCL is to prevent cranial tibial subluxation, but it also plays a role in preventing stifle hyperextension and internal rotation (Arnoczky and Marshall, 1977, Heffron and Campbell, 1978). Both the CrM and CaL bands of the CCL are taut during extension of the stifle joint, but only the CrM band is taut during flexion of the stifle joint, making this band the main safeguard against cranial tibial subluxation (Heffron and Campbell, 1978).

1.1.3. The menisci

The menisci are a pair of fibrocartilaginous crescent shaped discs within the stifle joint, situated on the peripheral weight bearing aspects of the proximal tibia, between the femoral and tibial condyles (Figure 1.2). There are two menisci: the medial and lateral meniscus (Dyce *et al*., 2002). The medial meniscus is firmly attached to the tibia by a cranial meniscotibial ligament, and a caudal meniscotibial ligament, as well as attachments of the abaxial medial meniscus to the medial collateral ligament. The lateral meniscus is attached to the tibia cranially via a cranial meniscotibial ligament, but caudally it attaches to the femur via the meniscofemoral ligament (Carpenter Jr and Cooper, 2000, Arnoczky and Warren, 1983). Both menisci are wedge shaped in cross section, being thicker abaxially and becoming thinner axially (Stephan *et al*., 1998, Dyce *et al*., 2002).

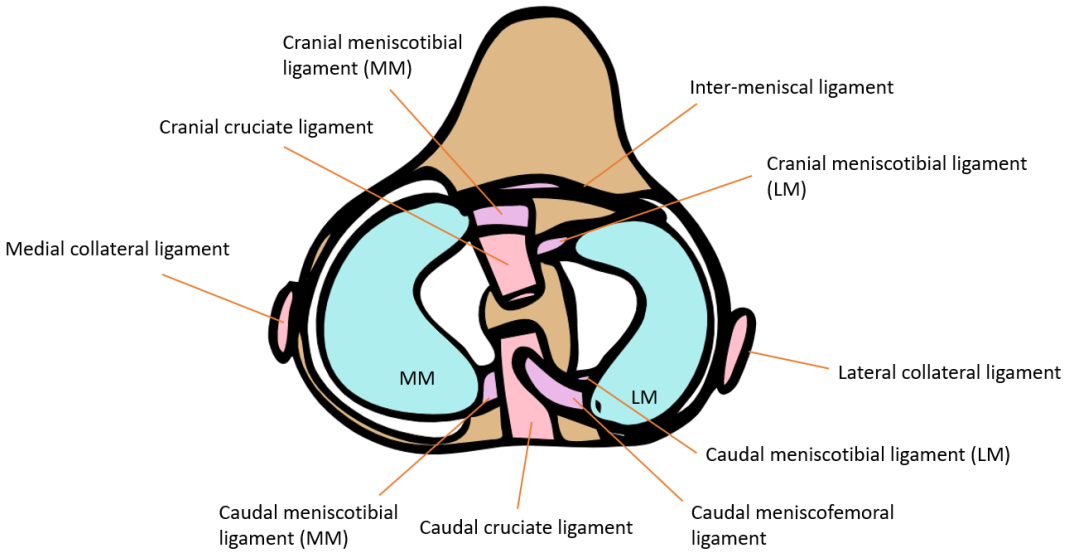

Figure 1.2. Schematic illustration of the anatomy of the proximal tibia, menisci, and associated ligaments of the stifle joint. *MM=medial meniscus, LM=lateral meniscus. Adapted from Franklin et al. (2010)*

The menisci are composed of an interlacing network of collagen fibres, mainly type I collagen with smaller amounts of type II collagen, interspersed with cells (chondrocytes and fibrochondrocytes) and an extra-cellular matrix (ECM) of proteoglycans and glycoproteins (Kambic and McDevitt, 2005). They contain approximately 70% water to 30% dry weight (Kambic and McDevitt, 2005). The surface layer of the collagen matrix has randomly arranged collagen bundles, in a composition similar to hyaline cartilage, to reduce friction between the menisci and the femur and tibia. Deep to this, the collagen bundles in the innermost third of the menisci are orientated in a radial fashion, whilst in the outer two thirds they are arranged in layers of circumferential bundles, with occasional radial fibres (Bullough *et al*., 1970, Bansal *et al*., 2020). The blood supply to the menisci originates from the medial and lateral genicular arteries and supply the peripheral rim of the medial and lateral menisci. Approximately 25% of the menisci are vascularised, with the rest of the menisci being relatively avascular (Arnoczky and Warren, 1983).

The menisci have several important functions in the stifle joint:

1) They are involved in load bearing, load distribution and shock absorption. As the menisci lie between the tibia and femoral condyles, they limit direct contact between the articular surfaces, reducing stress on the articular cartilage and increasing the surface area for load distribution (Krause *et al*., 1976). As load is applied to the stifle, the joint is compressed, and contact between the femur and the menisci increases. The compressive loads are redistributed radially as tensile forces across the menisci, and the circumferentially organised collagen fibres elongate causing the wedge-shaped menisci to extrude peripherally (Krause *et al*., 1976, Anderson *et al*., 1993, Jones *et al*., 1996). These hoop forces are then transmitted to the tibia via the meniscotibial ligaments and attachments to the medial collateral ligament, thus protecting the articular cartilage (Pozzi *et al*., 2010a).

2) They contribute to joint stability. The menisci add to cranial-caudal, varus-valgus, and rotational joint stability by increasing the congruency between the femoral condyles and tibial plateau (Pozzi *et al*., 2010a).

3) They contribute to proprioception. As they are well innervated, they contribute to sensory feedback assisting in proprioception and muscle co-ordination (Akgun *et al*., 2008, Saygi *et al*., 2005).

4) They have a beneficial effect on joint lubrication, by aiding with the transmission of SF through micro-canals to the articular cartilage surface (Bird and Sweet, 1988).

1.1.4.The synovium and synovial fluid

Synovial fluid is produced by the synovial membrane, which lines the innermost layer of the joint capsule. The synovial membrane consists of a one to three cell thick layer of synoviocytes within an ECM of collagen and hyaluronic acid (Galloway and Lester, 1995). This matrix acts as a semi-permeable membrane, allowing diffusion of plasma proteins, electrolytes and small molecules from the plasma to the SF, which can be described as a dialysate of plasma (Ropes *et al*., 1940). SF has several important functions. It primarily acts as a lubricant of the joint, containing molecules with low-friction and low-wear properties to

articular cartilage, such as hyaluronic acid, lubricin and surface-active phospholipids (Schwarz and Hills, 1996b, Plickert *et al*., 2013, Siódmiak *et al*., 2017). It also permits transport of nutrients, as well as regulatory substances such as cytokines and growth factors secreted by synoviocytes, from the synovial membrane to the articular cartilage, and allows the transport of intra-articular waste products to the lymph (Blewis *et al*., 2007, Gibson and Rooney, 2007)

1.2. Canine Cranial Cruciate Ligament Rupture

1.2.1. Overview of cranial cruciate ligament rupture

Cranial cruciate ligament rupture (CCLR) is a common cause of pelvic limb lameness in the dog, and the most common cause of lameness and osteoarthritis (OA) in the canine stifle (Wilke *et al*., 2005). A recent study estimated the prevalence of CCLR be 0.56% of all dogs presented to primary care practices in England (Taylor-Brown *et al*., 2015).

Although acute rupture of the CCL from a single traumatic event has been described (Aron, 1988, Reinke, 1982), the majority of cases of CCLR are due to a degenerative disease process, cranial cruciate ligament disease (CCLD), with progressive degeneration of the ECM of the ligament leading to partial or complete rupture after a minor or non-contact injury (Paatsama, 1952, Hayashi *et al*., 2003). This partial or complete rupture of the CCL in turn leads to joint instability, pain, lameness and OA, and can have a significant impact on the welfare of the affected dog (Brydges *et al*., 2012). The economic impact of CCLR has also been reported to be significant, with an estimated $1.32 billion spent on the management and treatment of the disease in the USA alone in 2003 (Wilke *et al*., 2005).

1.2.2. Aetiopathogenesis and risk factors for cranial cruciate ligament rupture

The pathogenesis of CCLR is complex and likely multifactorial, including genetic, conformational and inflammatory components (Comerford *et al*., 2011). CCLR can be thought of as “organ failure” of the stifle joint, with biological and biomechanical factors interacting to induce and perpetuate OA, pain, lameness and limb dysfunction (Kuroki *et al*., 2021, Inauen *et al*., 2009). Histological analyses of ruptured CCLs have shown loss of fibroblasts from the core region, increased amounts of chondroid metaplastic cells, and

disruption of the ECM (Hayashi *et al*., 2003). Risk factors for CCLR include breed, age, neuter status, body condition and stifle joint conformation (Comerford *et al*., 2011).

1.2.2.1. Breed

Certain breeds have been found to be more predisposed to CCLR than others, with Labrador Retrievers, Newfoundlands and Rottweilers being overrepresented (Guthrie et al., 2012a, Taylor-Brown et al., 2015).

1.2.2.2. Genetics

Genetic associations with CCLR in certain at-risk breeds have been discovered (Baird *et al*., 2014, Healey *et al*., 2019), and recent work has discovered novel loci that appear to influence the development of CCLR by the use of RNA sequencing of CCL tissue from non-affected and CCLR affected dogs (Baker et al., 2018, Baker et al., 2021).

1.2.2.3. Age

CCLR is most common in dogs over four years of age (Witsberger *et al*., 2008), with larger breed dogs weighing more than 15kg tending to develop CCLR at a younger age than smaller dogs (Harasen, 2008).

1.2.2.4. Obesity

Another risk factor to the development of CCLR is obesity, with overweight dogs appearing to be more likely to develop CCLR (Santarossa *et al*., 2020). This could be due to the increased load on the stifle joint, or other metabolic factors, with adipose tissue being recognised to be metabolically active and a potential source of inflammatory factors (Schmidli *et al*., 2018, Saengsoi, 2018).

1.2.2.5. Neuter status

Neutering has been found in some studies to increase the risk of developing CCLR (Torres de la Riva *et al*., 2013, Witsberger *et al*., 2008), and in other studies has not found to increase the risk (Adams et al., 2011, Guthrie et al., 2012b). It is uncertain whether neutering could

increase the risk of CCLR developing due to the increased risk of obesity in neutered dogs, or due to the lack of gonadal hormones leading to changes in conformation of the tibial plateau (Duerr *et al*., 2007), delayed growth plate closure (Torres de la Riva *et al*., 2013), and/or changes to the composition of the CCL itself (Slauterbeck *et al*., 2004).

1.2.2.6. Contralateral limb cranial cruciate ligament rupture

Another risk factor for CCLR is pre-existing CCLR in the contralateral limb. Approximately 40% to 60% of dogs with unilateral CCLR will go on to develop bilateral disease within 18 months of diagnosis (de Bruin *et al*., 2007a), with another study finding a median survival time of the contralateral CCL after unilateral CCLR of 947 days (Muir *et al*., 2011).

1.2.2.7. Pelvic limb conformation

The conformation of the stifle joint has also been hypothesised to play a role in the aetiopathogenesis of CCLR. Dogs with a straight (hyperextended) stifle joint and narrow intercondylar notch could be at risk of impingement of the CCL in the joint, increasing the risk of ligament laxity and degeneration (Comerford *et al*., 2006). A steeper tibial plateau angle (TPA) could increase susceptibility to CCLR due to increased strain and shear force on the CCL (Janovec *et al*., 2017, Ichinohe *et al*., 2021). Dogs with patellar luxation, internal rotation of the tibia, and/or a bowlegged appearance (genu varum) can also be more at risk of developing CCLR due to increased stress on the CCL (Griffon *et al*., 2017, Mostafa *et al*., 2018).

1.2.2.8. Inflammatory components

Many studies have investigated the role of inflammation in the pathogenesis of CCLD, although it remains unclear whether this is a primary contributing factor or secondary to changes within the joint (Comerford *et al*., 2011). Anti-collagen type I and II antibodies have been found in the SF of CCLR affected stifle joints (De Rooster *et al*., 2000, de Bruin *et al*., 2007b), however their role in the initiation of CCLR remains unclear. The role of pro-inflammatory cytokines and collagenolytic enzymes and proteases in the pathogenesis of CCLR has also been studied. The expression of collagenolytic enzymes, and the release of

collagenolytic proteases such as matrix metalloproteinase-2 (MMP-2) from the synovium into the SF has shown to lead to an increased risk of CCLR (Muir *et al*., 2005, Boland *et al*., 2014). Interleukin-8 (IL-8) has been found to be increased in the SF to be increased in the SF of CCLR affected stifle joints (de Bruin *et al*., 2007c, Malek *et al*., 2020), although no firm conclusions could be drawn regarding the role of this cytokine in the development of CCLR in these studies. Monocyte chemoattractant protein-1 (MCP-1) has recently been found to be increased in the SF of dogs with OA secondary to CCLR, and MCP-1 concentrations in the SF were also correlated with synovial histopathological grading in this study (Malek et al., 2020).

1.2.3. Diagnosis of cranial cruciate ligament rupture

CCLR is diagnosed by history, clinical signs, clinical examination findings, and imaging modalities such as radiography (Troy and Bergh, 2015, Bogaerts *et al*., 2018). The clinical history of affected dogs is typically a sudden onset pelvic limb lameness after a non-contact injury, although dogs can present with a more insidious history of lameness due to the degenerative nature of CCLD (Muir, 2017). Clinical signs are typically lameness on the affected pelvic limb with pain upon stifle flexion and extension on examination, and stifle instability noted by a positive cranial draw and/or tibial thrust test (Henderson, 1978, Might *et al*., 2013). Stifle instability is not always apparent in partial rupture of the CCL or in chronic cases with a large amount of periarticular fibrosis (Scavelli *et al*., 1990, Barger *et al*., 2016).

Radiography of the affected joint typically reveals compression of the infrapatellar fat pad in the cranial joint space and distention of the caudal fascial planes by an increase in intra-articular soft tissue opacity, consistent with joint effusion (Innes *et al*., 2004, Bogaerts *et al*., 2018). Osteophytosis at various sites in the joint (including the patella, femoral trochlear ridges, medial and lateral femoral condyles, fabella, lateral margin of the lateral tibial condyle and proximomedial margin of the tibia), enthesophytes, subchondral bone sclerosis, and changes in the periarticular soft tissues are also common radiological features (Innes *et al*., 2004, Wessely *et al*., 2017, Bogaerts *et al*., 2018) (Figure 1.3).

Advanced imaging techniques that can be used in diagnosis of CCLR include computed tomography (CT) with positive contrast arthrography, and magnetic resonance imaging (MRI), although these techniques are less widely available in veterinary practice and are more expensive (Samii *et al*., 2009, Sample *et al*., 2017). Diagnosis by ultrasonography has

also been described, but and has been found to be an insensitive method of detecting CCLR (Arnault *et al*., 2009). Surgical methods of diagnosis include arthroscopy or arthrotomy, often used at time of surgical management (Hoelzler *et al*., 2004).

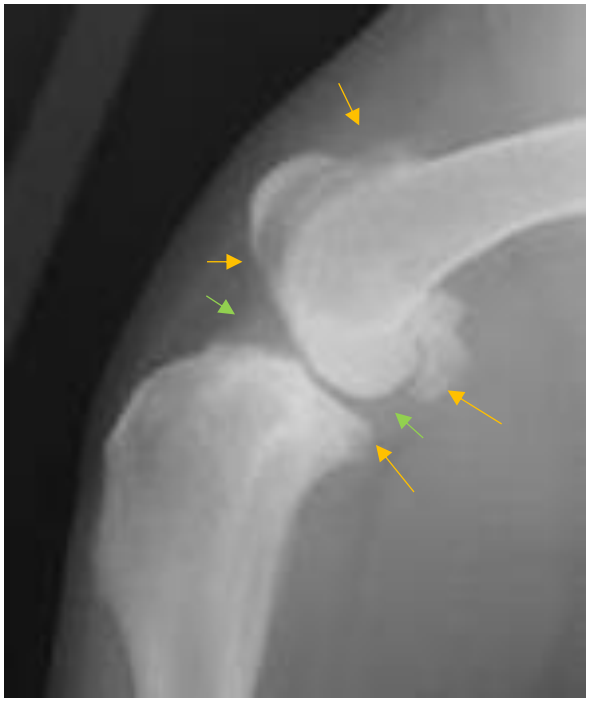

Figure 1.3. Mediolateral projection of a radiograph of a canine stifle joint with radiographic signs of cranial cruciate ligament rupture. *Yellow arrows indicate areas of osteophytosis. Green arrows indicate soft tissue opacity consistent with joint effusion.*

1.2.4. Treatment of cranial cruciate ligament rupture

Treatment of CCLR can be either conservative or surgical. Conservative (medical/non-surgical) methods of treatment include exercise restriction, nonsteroidal anti-inflammatory drugs, weight loss, physiotherapy and hydrotherapy (Comerford *et al*., 2013, Duerr *et al*., 2014). There are many different surgical options for treatment of CCLR, including intra-articular, extra-articular and per-articular techniques (Comerford *et al*., 2013). Intra-articular techniques include fascial grafts (Geels *et al*., 2000). Extra-articular techniques include extra-capsular fabellotibial prosthesis sutures to stabilise the stifle joint (Cook *et al*., 2010, Nelson *et al*., 2013). Periarticular techniques include tibial osteotomies that aim to alter the biomechanics of the affected stifles, such as tibial tuberosity advancement (TTA), cranial

closing wedge osteotomy (CCWO) and tibial plateau levelling osteotomy (TPLO) procedures (Slocum and Slocum, 1993, Lafaver *et al*., 2007, Terreros and Daye, 2020). Importantly, there are currently no treatments aimed specifically at prevention of ligament degeneration in at risk breeds, likely due to the complex and multifactorial nature of the disease (Comerford *et al*., 2011).

1.3. Meniscal injuries

1.3.1. Introduction

Meniscal injuries in dogs typically occur as a consequence of the instability in the stifle joint secondary to CCLR (McCready and Ness, 2016a). Although isolated meniscal tears have been reported in dogs, they are extremely rare (Hulse and Johnson, 1988). The medial meniscus is most commonly affected, as the meniscotibial ligament attaching the caudal horn of the medial meniscus to the tibia makes it more firmly attached to the tibia than the lateral meniscus, which attaches to the femur caudally via the meniscofemoral ligament (Bennett and May, 1991). The result of this attachment of the medial meniscus to the tibia is that it can become trapped between the femoral condyles and tibial plateau during cranial translocation of the tibia after rupture of the CCL, and become torn (Thieman *et al*., 2009). *Ex vivo* studies have demonstrated that the caudal horn of the medial meniscus plays a role as a stabiliser of the stifle joint in the cranial cruciate deficient stifle, increasing the risk of injuries to this area of the meniscus (Kennedy *et al*., 2005). Injuries to the lateral meniscus are less common, as the caudal horn of the lateral meniscus attaches to the femur via the meniscofemoral ligament, allowing movement of the lateral meniscus with cranial translocation of the tibia (Pozzi *et al*., 2006).

1.3.2. Prevalence and risk factors for canine meniscal injuries

The reported prevalence of meniscal injuries at the time of surgery for CCLR varies from 20% to 77 % (Bennett and May, 1991, Fitzpatrick and Solano, 2010). Meniscal injuries can also occur postoperatively weeks or months after surgery for CCLR, due to residual instability in the joint, or due to surgeon error in misdiagnosing meniscal injuries at the time of surgery (Metelman *et al*., 1995b). These late meniscal injuries (LMI) can cause ongoing pain and lameness in the affected joint. The incidence of LMI causing stifle morbidity has been

reported in 2.8% to 13.8% of dogs (Metelman et al., 1995b, Fitzpatrick and Solano, 2010, McCready and Ness, 2016a, Matchwick et al., 2021).

Epidemiological studies into the risk factors for developing meniscal injuries have found no obvious correlation with breed, sex, or tibial plateau angle, but have suggested an increased incidence in overweight dogs with chronic, complete rupture of the CCL (Hayes *et al*., 2010). The risk of developing an LMI post-operatively may increase depending on the procedure undertaken, and whether or not a medial meniscal release was performed at the time of surgery (Wolf et al., 2012, Christopher et al., 2013). Medial meniscal release involves transecting the medial meniscus either at the caudal meniscotibial ligament or at the mid-body level, allowing the meniscus to move and prevent it from becoming trapped during cranial translation of the tibia (Wolf *et al*., 2012). However, it also reduces the ability of the meniscus to withstand hoop stresses and predisposes the medial compartment of the stifle to further cartilage degeneration and OA by altering the biomechanical environment and increasing articular surface stress (Pozzi *et al*., 2010a). In terms of the risk of developing a LMI based on surgical technique, studies have shown varied results, with some finding an increase if TTA is performed over TPLO (Jeong *et al*., 2021) , whilst some finding no difference between treatment groups (Krotscheck et al., 2016, Hans et al., 2017).

1.3.3. Types of meniscal injury

Meniscal injuries can be classified into multiple types (Bennett and May, 1991, Thieman *et al*., 2009). These include radial tears, non-displaced vertical longitudinal tears, displaced vertical longitudinal tears (commonly referred to as “bucket-handle” tears), oblique or flap tears, horizontal tears, complex tears, and degenerative tears (Bennett and May, 1991). Bucket handle tears of the medial meniscus have been reported to have the highest incidence in dogs (Ritzo *et al*., 2014).

1.3.4. Diagnosis of meniscal injuries

Meniscal injuries can be diagnosed through clinical examination findings, imaging, and surgical evaluation. Non-surgical methods of diagnosing meniscal injuries in dogs can be challenging, especially for LMI (Franklin *et al*., 2010). In the case of post-operative LMI, clinical history is often of a sudden recurrence of lameness weeks or months after surgery

for CCLR, with studies finding an average time from surgery to occurrence of LMI of approximately six months (Metelman *et al*., 1995a). Orthopaedic examination can reveal a "meniscal click" on flexion of the stifle joint, however this has been shown to have a low sensitivity of 25-58% depending on the study, and is more commonly associated with bucket handle tears (Neal *et al*., 2015, Gleason *et al*., 2020). Imaging techniques such as radiography, ultrasonography, CT and MRI scans have also been used in the diagnosis of meniscal injuries. Radiographs can be useful in ruling out other causes of lameness, such as implant related problems in recurring lameness post-operatively, however radiographs cannot show meniscal injuries directly. Won *et al.* (2020) recently investigated using radiographic joint space width as an indicator of meniscal injuries in lateral projections of the canine stifle, although this was only 40.5% sensitive. Studies examining the effectiveness of ultrasonography in the detection of meniscal injuries have shown it to be 82-95% sensitive, and 82-93% specific (Mahn *et al*., 2005, Arnault *et al*., 2009). However, this can be dependent on the experience and skill of the ultrasonographer.

CT arthrography is another imaging modality that has been used to diagnose meniscal injuries in dogs, although with varying results, and low sensitivity with some assessors (Samii *et al*., 2009, Tivers *et al*., 2009). One study assessing the use of transverse CT arthrography scans in the diagnosis of CCLR and meniscal injury in 29 canine stifles (4 normal and 25 abnormal) showed the sensitivity of meniscal injury diagnosis between three board-certified radiologists varied from 13.3-73.3%, with specificity of 57.1-100% (Samii *et al*., 2009). Another study of 21 CT arthrograms using dorsal plane scans reported a higher sensitivity and specificity of 57 – 64% and 71-100% respectively (Tivers *et al*., 2009). CT arthrography is a minimally invasive diagnostic method for meniscal injuries, and although it is more available than MRI in veterinary practice, it still requires specialised equipment, and an experienced assessor to achieve the most reliable results (Tivers *et al.,* 2009). It may also have lower accuracy in assessing incomplete or non-displaced meniscal tears (Tivers *et al.,* 2009).

Varying results have also been reported when diagnosing meniscal injuries with the use of both low field and high field MRI. Depending on the study, the sensitivity of low field MRI in diagnosing meniscal injuries in dogs has been found to be 64-100% (Böttcher *et al*., 2010, Gonzalo-Orden *et al*., 2001). High field MRI has been reported to have a sensitivity of 75-100% (Olive *et al*., 2014, Blond *et al*., 2008). When using MRI to diagnose LMI, there is the

possibility of implant related artefacts when assessing stifles post-operatively, although recent studies have found minimal interference with intra-articular structures with titanium implants compared to stainless steel (Feichtenschlager *et al*., 2018). The optimal sequence using MRI in this study for the diagnosis of meniscal injuries in canine stifles was found to be a sagitally orientated T2 weighted turbo spin echo (TSE), complemented by a dorsally orientated T1 weighted TSE (Feichtenschlager *et al*., 2018). Although MRI is a non-invasive method of diagnosing meniscal injuries in dogs, it requires specialist equipment, is expensive, and is not readily available in veterinary practice.

Surgical techniques to diagnose meniscal injuries include arthrotomy and arthroscopy (Böttcher *et al*., 2010). The gold standard at present for the diagnosis of meniscal tears is arthroscopy (Franklin *et al*., 2017a, Kim *et al*., 2017a), however, arthrotomy is still widely performed. Arthroscopy is less invasive than arthrotomy, requiring a smaller incision, and therefore associated with less post-operative morbidity (Hoelzler *et al*., 2004). Arthroscopy has also been found to be better at aiding visualisation of meniscal structures than arthrotomy (Rogatko *et al*., 2018, Plesman *et al*., 2013). The accuracy of diagnosis of both arthroscopy and arthrotomy increases when the menisci are probed for tears (Pozzi *et al*., 2008a). However, arthroscopy has also recently been found to be associated with more iatrogenic cartilage injury than mini-medial arthrotomy (Rogatko *et al*., 2018), and it also requires specialist equipment and training. A benefit of surgical evaluation for diagnosis of meniscal injuries is that it also allows for treatment at the same time, however, there is an inherent risk with any general anaesthesia and surgical procedure (Bille *et al*., 2012).

Currently, there are no biomarkers that allows for the diagnosis of meniscal injuries in any species.

1.3.5. Treatment of meniscal injuries

Meniscal injuries in dogs are usually treated through means of partial meniscectomy, or hemi-meniscectomy via arthrotomy or arthroscopy (Moses, 2002, Seo *et al*., 2017, Rovesti *et al*., 2018). Removal of the meniscus has been found to be associated with an increased risk of OA development (Cox *et al*., 1975, Pozzi *et al*., 2010b). Because of this risk, greater emphasis in recent years have been placed on methods of repairing rather than removing torn menisci in human medicine (Doral *et al*., 2018). As the outer (abaxial) 25% of the meniscus is vascularised, meniscal tears in this area have a higher chance of healing than

tears within the axial avascularised “white zone” (Thieman *et al*., 2010). Although there have been successful cases of meniscal injury repair in dogs, the vast majority of meniscal tears in dogs are treated by removal of the damaged tissue (Moses, 2002, Thieman *et al*., 2010). This is due to a number of factors, including the perception of most tears as being irreparable and the risk of any repair failing leading to further surgery (with the associated risks and costs of this further treatment) (Franklin *et al*., 2010).

1.4. Osteoarthritis related to cranial cruciate ligament rupture and meniscal injuries

1.4.1. Introduction

Osteoarthritis is a multifactorial and progressive degenerative disease affecting whole synovial joints (Showiheen *et al*., 2019). It is characterised by the degradation of articular cartilage, subchondral bone sclerosis, osteophytosis, varying degrees of synovitis and ligament degeneration (Figure 1.4) (Man and Mologhianu, 2014, Berenbaum and Walker, 2020). OA causes pain and lameness, and is a significant cause of morbidity in humans and dogs alike, yet despite the high prevalence of OA, its pathogenesis is still not completely understood, and there is no treatment that can stop the progression of the disease or prevent it from occurring (Mobasheri and Batt, 2016). Broadly, OA can be divided into primary (idiopathic) OA and secondary OA, such as OA secondary to trauma, joint abnormalities or malalignment (Man and Mologhianu, 2014). In dogs, the majority of cases of canine OA believed to be secondary to inciting factors, such as coxofemoral (hip) joint dysplasia, elbow dysplasia, CCLR, patella luxation, limb malformations and articular fractures (Johnston, 1997). A number of risk factors for canine OA have been identified, including genetic predispositions, diet and obesity (Anderson *et al*., 2018c).

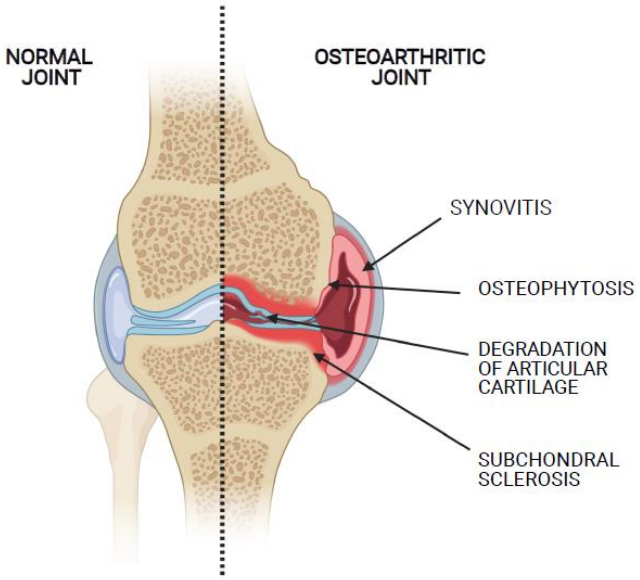

Figure 1.4. An illustration detailing the changes in an osteoarthritic synovial joint. *Degradation of articular cartilage is only one pathophysiological mechanism in osteoarthritic joints, with subchondral bone sclerosis, osteophytosis, ligament degeneration (not pictured) and synovitis also being common features of the disease process.*

1.4.2. Molecular Mechanisms of OA

Osteoarthritis arises due to an imbalance between the synthesis and degradation of ECM components of articular cartilage (Man and Mologhianu, 2014). Although it is primarily a disease of the articular cartilage, the disease process involves the whole of the joint, with understanding of the cross-links between the articular cartilage, the synovium and subchondral bone still developing. Synovitis, subchondral bone sclerosis, periarticular osteophytosis, ligament dysfunction and meniscal degeneration are all associated with osteoarthritis (Gilbertson, 1975, Tan *et al*., 2006, Sellam and Berenbaum, 2010).

At the molecular level, an overexpression of matrix metalloproteases and aggrecanases cause the degradation of type II collagen and aggrecan in the articular cartilage ECM (Yoshihara *et al*., 2000, Scavenius *et al*., 2019). These enzymes are released by chondrocytes in response to proinflammatory cytokines, such as interleukin 1β (IL-1β), interleukin-6 (IL-6) and tumour necrosis factor alpha (TNF-α), which are released from synoviocytes and macrophages (Wojdasiewicz *et al*., 2014, Pearson *et al*., 2017). The breakdown products

from this proteolysis in turn stimulates further cytokine production from synoviocytes and chondrocytes (Sokolove and Lepus, 2013).

In the initial stages of OA, the collagen network is weakened, with reduced stiffness in the cartilage (Mieloch *et al*., 2019). The chondrocytes respond with compensatory anabolic mechanisms such as increasing proliferation of chondrocytes in the deeper layers, and increasing metabolic activity and the synthesis of matrix components, but eventually the chondrocytes cannot keep up their repair activity and the cartilage becomes degraded (Adams and Brandt, 1991, Man and Mologhianu, 2014).

There is likely a complex and multifaceted relationship between OA and CCLR in the dog (Comerford et al., 2011). Historically, it was believed that the instability of the stifle joint caused by CCLR led to the development of OA within the affected joint, but studies have shown that early signs of OA are present in CCLR affected stifles before gross joint instability is noticeable (Comerford *et al*., 2005, de Bruin *et al*., 2007a, Muir *et al*., 2011, Chuang *et al*., 2014). The presence of early signs of OA before joint instability suggests that OA may not just develop as a result of stifle instability and altered biomechanics of the CCL deficient stifle, but also as a result of the inflammatory changes taking place in an affected joint (Bleedorn *et al*., 2011).

1.5. Biomarkers in joint disease

1.5.1. Introduction

Biomarkers are biochemical entities that indicate the presence of a specific disease or pathology, and can be used to measure the progress of disease or the effect of treatment on clinical outcome (Mobasheri and Cassidy, 2010). The National Institutes of Health (NIH) Biomarkers Definitions Working Group has defined a biomarker as “a characteristic that is objectively measured and evaluated as an indicator of normal biological processes, pathogenic processes, or pharmacologic responses to a therapeutic intervention.” (Biomarkers Definitions Working Group, 2001). Biomarkers can be represented by a variety of characteristics, including physiological, histological and molecular (Boffa *et al*., 2020). Molecular biomarkers can be identified and measured in many different biological samples and biofluids, including whole blood, serum, urine, faeces, bile, cerebrospinal fluid, saliva, and SF (Xu and Veenstra, 2008).

1.5.2. Synovial Fluid as a Source of Biomarkers

Synovial fluid holds an important source of biomarkers in the study of diarthrodial joint pathologies (Boffa *et al*., 2020). It is in close contact with joint tissues, such as articular cartilage, bone and the synovial membrane, that can become altered during joint injuries and disease processes, and therefore could allow for the detection of biomarkers that reflect these changes (Anderson *et al*., 2018b, Malek *et al*., 2020). As it is a dialysate of plasma, it could also reflect systemic pathologies in the organism as a whole (Gibson and Rooney, 2007). Although other biofluids such as blood and urine have been used in the detection of biomarkers for joint diseases, biomarkers are in higher concentration in SF, therefore allowing a higher sensitivity and specificity upon analysis (Boffa *et al*., 2020).

Synovial fluid has been found to contain numerous biomarkers of joint diseases, such as OA and rheumatoid arthritis (RA), in a number of species (Anderson *et al*., 2018b, Boland *et al*., 2014, Anderson *et al*., 2018a). For example, in OA, a plethora of biomarkers have been investigated in SF, with 201 SF biomarkers being identified in one recent review (Boffa *et al*., 2020). These biomarkers include the cytokines IL-6, IL-8, TNF-α, vascular endothelial growth factor (VEGF) and adipokine leptin, matrix metalloproteases MMP1 and MMP3 and tissue inhibitors of metalloproteinases (TIMPs) (Ding *et al*., 2017, Kim *et al*., 2016, Heard *et al*., 2012). MicroRNAs present in SF have also been investigated as biomarkers of joint diseases, showing their involvement in disease pathogenesis and progression (Lao and Le, 2021).

1.5.3. Biomarkers of CCLR and meniscal injuries

There are currently no specific biomarkers for CCLR or meniscal injuries in dogs that can be used as a reliable diagnostic tool or used as a treatment target or preventative treatment in at risk breeds. The main research into biomarkers of CCLD in dogs has been related to OA that inevitably arises as a consequence of CCLD, both in naturally occurring and experimental cases (Henrotin *et al*., 2012, Malek *et al*., 2020). Studies researching potential biomarkers of CCLD and OA secondary to CCLD in dogs have found a number of proteins, collagenolytic proteases and pro-inflammatory cytokines that significantly differ in CCLD affected dogs. High levels of proinflammatory cytokines IL-1β, IL-6 and TNF-α were found in the SF of CCLD affected dogs in a study by Fujita *et al*. (2012) indicating the presence of inflammation in these joints. Boland *et al*. (2014) investigated the significance of matrix metalloproteases

MMP-2 and MMP-9, and C reactive protein in the SF of 14 large breed dogs with clinical CCLR compared to their contralateral stifles and stifles of unaffected large breed dogs. They found that MMP-2 was significantly higher in CCLR affected joints compared to contralateral stifles and non-affected dogs, although the levels in the contralateral stifles of affected dogs varied. MMP-2 is produced by chondrocytes and synovial fibroblasts, and is a collagenolytic enzyme, but it is not yet known whether its increased presence in CCLD is as an effect or a causal agent (Boland *et al*., 2014). Lubricin levels in SF of CCLD affected dogs have been found to be significantly increased (Wang *et al*., 2020), as have SF levels of albumin and apoprotein A-I, although further studies are needed to validate these as biomarkers (Shahid *et al*., 2018).

Biomarkers of meniscal injury have been investigated in humans, however, in dogs the only studies relating to biomarkers in joints with meniscal injuries have been related to examining biomarkers of OA secondary to experimental meniscectomy (Lindhorst *et al*., 2000). In humans, IL-6, monocyte chemoattractant protein-1 (MCP-1), macrophage inflammatory protein-1β (MIP-1β) and MMP-3 have been found to be increased in the SF of humans with meniscal injuries compared to healthy controls (Clair *et al*., 2019). MMP activity as well as prostaglandin E2 levels have been found to be increased in knee joint SF from humans with meniscal tears compared to healthy controls (Liu *et al*., 2017). The proteome of SF from human subjects with meniscal injuries and knee OA has been studied, with one study finding 13 proteins significantly altered in the disease group (Roller *et al*., 2016). In studies examining tissue explants from human torn meniscus, IL-6 and TNFα levels to be increased compared to healthy tissue (Ogura *et al*., 2016). At the gene transcript level, an increase in the expression of adiponectin and leptin in torn meniscal tissue was found by Brophy *et al*. (2017a), suggesting adipokines may play a role in meniscal degeneration. In another study, genetic expression of chemokines IL8 and C-X-C Motif Chemokine Ligand 6 (CXCL6), as well as MMP-1 and MMP-3 were found to be upregulated in meniscal tissue from human traumatic meniscal tears compared to degenerative tears (Brophy *et al*., 2017b). An outline of studies examining biomarkers of meniscal injury is shown in Table 1.

One technology that has been used to investigate biomarkers of joint diseases such as OA, rheumatoid arthritis (RA) and septic joint diseases in both humans and dogs is metabolomics (Anderson *et al*., 2018a, Damyanovich *et al*., 1999a). However, as yet, this technology has not been used to study alterations in the metabolome of SF that occurs with meniscal injuries in any species.

Table 1.1. Overview of studies examining biomarkers of meniscal injury in humans

Meniscal tissue or SF	**Sample size**	**Biomarker**	**Author**
SF	41 meniscal injury 41 controls	Increased: IL-6, MCP-1, MIP-1β, MMP-3	(Clair *et al*., 2019)
SF	16 meniscal injury 6 controls	Increased: Total MMP activity, PGE2 Decreased: MMP-10, s-GAG	(Liu *et al*., 2017)
SF	69 meniscal injury	Increased: IL-10, IL-6, TNFα, IL-8 Decreased: IL-1rs, IL-1β	(Bigoni *et al*., 2017)
SF	21 meniscal injury	Increased: aggrecan	(Roller *et al*., 2016)
SF	61 PTOA 62 controls	Decreased: ghrelin	(Zou *et al*., 2016)
SF	15 painful knee injuries, 5 meniscal injury	Increased: Fibronectin-aggrecan G3 complex	(Scuderi *et al*., 2010)
Meniscal tissue	19 (near to tear and furthest from tear)	Increased: IL-6, TNFα	(Ogura *et al*., 2016)
Meniscal tissue	68	Increased: IL-8, CXCL6. MMP-1, MMP-3	(Brophy *et al*., 2017b)
Meniscal tissue	48	Increased: Adiponectin, leptin	(Brophy *et al*., 2017a)

Abbreviations: SF=synovial fluid, IL=interleukin, MCP-1= monocyte chemoattractant protein-1, MIP-1β=macrophage inflammatory protein-1β, MMP=matrix metalloproteinase, PTOA=post-traumatic osteoarthritis, PGE2=prostaglandin E2, TNFα=tumour necrosis alpha, IL8=interleukin 8, CXCL6= C-X-C Motif Chemokine Ligand 6.

1.6. Metabolomics

1.6.1. Overview of metabolomics

Metabolomics is the study of metabolic pathways and the identification and quantification of small molecule metabolites present in biological systems including cells, tissues, organs and biological fluids (Bujak *et al*., 2015). It is a growing field of study, and part of the "-omics"

technologies that also includes genomics, transcriptomics and proteomics (Hasin *et al*., 2017). The metabolome is the sum of all the small biochemicals, including reactants, pathway intermediates and products as well as stable structural molecules within a biological sample at a specific moment (Kennedy *et al*., 2018). Metabolomics has been used to identify metabolites in a variety of biofluids, including serum, saliva, SF, bile, cerebrospinal fluid and urine (Bujak *et al*., 2015, Kennedy *et al*., 2018). The knowledge of these metabolites has massive implications for furthering our understanding of disease processes and holds the potential to aid with the development of diagnostic tests and targeted treatments (Kennedy *et al*., 2018). Metabolomics has been used to identify biomarkers of disease for a wide variety of diseases including neoplasia, immune-mediated diseases, degenerative diseases and infectious diseases (Graham *et al*., 2014, Anderson *et al*., 2018a, Ranjan and Sinha, 2019, Costa dos Santos Junior *et al*., 2020).

There are two main platforms used to identify metabolites. These are mass spectroscopy (often coupled with gas chromatography or liquid chromatography), and nuclear magnetic resonance (NMR) spectroscopy (Zhang *et al*., 2016, Emwas *et al*., 2019). Whilst mass spectroscopy is a more sensitive at identifying metabolites, the benefits of NMR spectroscopy is that it is a non-destructive, non-invasive method that allows for rapid and reproducible results with minimal sample preparation (Emwas *et al*., 2019).

1.6.2. NMR Spectroscopy

Nuclear magnetic resonance (NMR) spectroscopy is a technique used to identify and quantify metabolites within a given sample (Emwas *et al*., 2019). The physical theory of NMR relies on the principle that most atomic nuclei have an intrinsic angular momentum, known as spin (Hore, 1999). Different nuclei have different magnitudes of nuclear spin, with ^{1}H nuclei exhibiting a nuclear spin of ½, without an applied external magnetic field, these spins are randomly orientated in space. When an external magnetic field (B_o) is applied, these nuclear spins will become orientated in two different spin states, -½ or +½ (denoted by the magnetic quantum number [m]), depending on whether they are orientated against or with this applied field (Lambert and Mazzola, 2004).

Using the vector model of NMR, the magnetic moments of all the many nuclei in a sample have a net magnetic field along the direction of the applied magnetic field B_o (Figure 1.5). The nuclei will exhibit a precessional motion about the *z* axis parallel or antiparallel to B_o,

with the number of precesses about the axis per second being termed the Lamor frequency (ω_L). When a pulse of radio frequency is applied in the *x* axis, perpendicular to the external magnetic field, the nuclei spins will move to the direction of the *xy* axis, and will precess about the *xy* plane (Lambert and Mazzola, 2004, Keeler, 2011). When the radio frequency pulse is stopped, the spins will move back to the equilibrium state in the *z* axis. A wire coil detects this precession by a change in the magnetic field, inducing an alternating current in the coil. This current is amplified, before being digitised. The recording signal is called a free induction decay (FID), which appears as a decaying sine wave. A Fourier Transform is applied to the FID, which produces a spectrum (Bodenhausen *et al*., 1977). The precession frequency determines the position of a peak on the spectrum (Keeler, 2011).

Hydrogen nuclei in different molecules will precess at slightly different frequencies due to the effect of electron shielding. This results in a chemical shift frequency (in Hertz [Hz] or parts per million [ppm]), which determines the position of different hydrogen nuclei in different molecules on the NMR (Wishart *et al*., 1995).

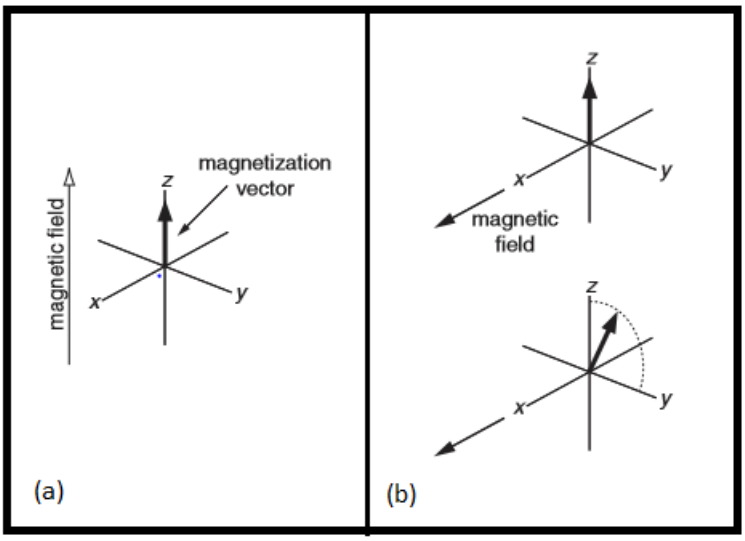

Figure 1.5. Illustration to represent the vector model of nuclear magnetic resonance (NMR). *a) At equilibrium, the sample has a net magnetisation aligned with the applied magnetic field on the z axis. The nuclei will precess around this axis. B) when a pulse of electromagnetic frequency is applied in the x plane, the nuclei will move to precess about the xy plane. Adapted from Keeler (2011).*

1.6.3. Metabolomics studies using synovial fluid

Current research in the metabolomics field analysing SF is outlined in Table 1.2. The majority of metabolomics studies using SF are in humans, and the most common area of research focuses on investigating OA (Anderson *et al*., 2018a, Carlson *et al*., 2018, Akhbari *et al*., 2019), rheumatoid arthritis (Ahn *et al*., 2015, Yang *et al*., 2015, Anderson *et al*., 2018a) and reactive arthritis (Ahmed *et al*., 2019, Dubey *et al*., 2019). Other species with published metabolomics studies using SF included horses (Anderson *et al*., 2018b, Graham *et al*., 2020), mice (Wu *et al.,* 2017), rats (De Visser *et al.*, 2018; Zhan *et al.*, 2020), rabbits (Hu *et al.,* 2020), sheep (Mickiewicz *et al.,* 2015), cows (Alarcon *et al.,* 2019) and dogs (Damyanovich *et al*., 1999a, Marshall *et al*., 2000).

Table 1.2. Outline of published metabolomics studies involving synovial fluid, listed in order of species studied.

Species	Clinical or experimental disease	Samples	Application/ disease studied	Number of samples	Analytical method	Findings	Authors
Human	Clinical	SF	PTAA	40 (20 PTAA, 20 control)	LC-MS GC-MS ELISA	107 metabolites in the PTAA group were significantly altered, including derangement in amino acid, carbohydrate, lipid, and energy metabolism, extracellular matrix turnover, and collagen degradation.	(Adams *et al*., 2014)
Human	Clinical	SF Plasma	pSpA, ReA	50 (13 pSpA, 19 ReA, 18 controls)	^{1}H-NMR	SF had higher levels of pyruvate and acetoacetate and lower levels of aspartate and ornithine.	(Ahmed *et al*., 2019)
Human	Clinical	SF	BD with arthritis/ seronegative arthritis (SNA)	24 (6 BD, 18 SNA)	GC/TOF MS	Glutamate, citramalate, and valine were selected and validated as putative biomarkers for BD with arthritis.	(Ahn *et al*., 2015)
Humans	Clinical	SF	RA	48	GC/TOF MS	Glycocyamine and indol-3-lactate increased with increasing disease severity. β-alanine, asparagine, citrate, cyano-L-alanine, leucine, nicotinamide, citrulline, methionine, oxoproline, and salicylaldehyde decreased with increasing disease severity.	(Ahn *et al*., 2020)
Human	Clinical	SF	Hip and knee OA	24 (12 hip, 12 knee)	^{1}H-NMR	N-acetylated molecules, glycosaminoglycans, citrate and glutamine were found in significantly greater quantities in the knee group compared to the hip group.	(Akhbari *et al*., 2019)
Human	Clinical	SF	OA, RA	10 OA 14RA	^{1}H-NMR	Metabolites of glycolysis and the tricarboxylic acid cycle were lower in RA compared to OA. Elevated taurine in OA.	(Anderson *et al*., 2018a)
Human	Clinical	SF	OA	13 (5 OA, 3 RA, 5 Normal)	LC-MS	35 metabolites as potential biomarkers of OA, including phosphatidylcholines, lysophoshatidylcholines, ceramides, myristate derivatives, and carnitine derivatives.	(Carlson *et al*., 2018)
Human	Clinical	SF	RA	8 (3 RA, 5 Normal)	LC-MS	162 metabolites identified as significantly different between diseased and control. 30 metabolites as putative RA biomarkers including various phospholipids, diol and its derivatives, arsonoacetate, oleananoic acid acetate, docosahexaenoic acid methyl ester, and linolenic acid .	(Carlson *et al*., 2019a)
Human	Clinical	SF	OA	75 (7 normal, 55 early OA, 17 late OA)	LC-MS	Metabolic pathways analysed. Pathways differentially activated among these groups included structural deterioration, glycerophospholipid metabolism, inflammation, central energy metabolism, oxidative stress, and vitamin metabolism.	(Carlson *et al*., 2019b)

Table 1.2. Outline of published metabolomics studies involving synovial fluid, listed in order of species studied (continued)

Human	clinical	SF	OA	93 patients (29 non-OA and 64 OA)	^{1}H-NMR ELISA	Glucose and glycerol concentrations higher in OA patients.	(de Sousa *et al*., 2019)
Human	Clinical	SF	ReA	8	^{1}H-NMR	53 metabolites in normal filtered SF and 64 metabolites in filtered pooled SF sample compared with nonfiltered SF samples for which only 48 metabolites (including lipid/membrane metabolites as well) have been identified.	(Dubey *et al*., 2019)
Human	Clinical	SF	RA, OA	10 RA, 10 OA	UPLC-QTOF-MS	The metabolic pathways for carnitine, tryptophan, phenylalanine, arachidonic acid, and glycophospholipid were significantly upregulated in OA SF. The metabolic pathways for taurine, cholesterol ester, and the β-oxidation of pristine acid, linolenic acid, and sphingolipid were activated more in RA SF than in OA SF.	(Kang *et al*., 2015)
Human	Clinical	SF	RA and non-RA	38 (13 RA, 25 nonRA)	GC/TOF-MS	20 metabolites, including citrulline, succinate, glutamine, octadecanol, isopalmitic acid, and glycerol, were identified as potential biomarkers for RA	(Kim *et al*., 2014)
Human	Clinical	SF	Early and late OA	15 OA	GC/TOF-MS	28 metabolites, including malate, ethanolamine, squalene, glycerol, myristic acid, oleic acid, lanosterol, heptadecanoic acid, and capric acid, were identified as discriminating between the early- and late-OA groups	(Kim *et al*., 2017b)
Human	Clinical	SF	OA	55 OA 13 control	^{1}H-NMR GC-MS	Fructose and citrate increased in OA. O-acetylcarnitine, N-phenylacetylglycine, methionine, ethanol, creatine, malate, ethanolamine, 3-hydroxybutyrate and hexanoylcarnitine were decreased in OA.	(Mickiewicz *et al*., 2015)
Human	Clinical	SF Serum	ReA/uSpA, RA and OA	30 ReA, 25 RA, 21 OA	^{1}H-NMR	Phe/Tyr ratio elevated in ReA/uSpA.	(Muhammed *et al*., 2019)
Human	Clinical	SF	RA	25 RA 10 normal	GC/TOF-MS	Glucose and lactic acid are reliable biomarkers for RA.	(Yang *et al*., 2015)
Human	Clinical	SF	OA	80	UPLC-MS	2 distinct groups of OA patients identified due to difference in concentrations of acylcarnitines.	(Zhang *et al*., 2014)
Human	Clinical	SF	OA	35 (10 normal, 25 OA)	GC/TOF-MS	Glutamine, 1,5-anhydroglucitol, gluconic lactone, tyramine, threonine, and 8-aminocaprylic acid strongly associated with OA.	(Zheng et al., 2017a)

Table 1.2. Outline of published metabolomics studies involving synovial fluid, listed in order of species studied (continued)

Canine	Clinical	SF	CCLR	10 dogs (5 chondroprotector tx post sx)	^{1}H-NMR	Lactate, alanine, acetyl groups of N-acetylated sugars on glycoproteins and alpha-anomers of glucose were found to differ to a statistically significant extent between the two groups.	(Crovace *et al*., 2006)
Canine	Experimental	SF	ACL transection	28 (14 normal, 14 OA)	^{1}H-NMR	In OA joints- increased concentrations of lactate, pyruvate, lipoprotein associated fatty acids, and glycerol as well as the ketones hydroxybutyrate and hydroxyisobutyrate, reduced levels of glucose, and elevated levels of N-acetylglycoproteins, acetate, and acetainide compared with healthy normal canine synovial fluid.	(Damyanovich *et al*., 1999a)
Canine	Experimental	SF	ACL transection and Nerve denervation	14	^{1}H-NMR	Significant increases in glycerol, hydroxybutyrate, glutamine/glutamate, creatinine/creatine, acetate and N-acetyl-glycoprotein concentrations, and trend towards elevated lactate, alanine and pyruvate levels in synovial fluids from denervated with respect to control knees.	(Damyanovich *et al*., 1999c)
Canine	Experimental	SF	OA secondary to ACL transection and nerve denervation,	24 (6x2 HA tx groups, 12 controls)	^{1}H-NMR	Late treatment group had decreased beta-glucose and sugars, and increased isoleucine. Acetate and hydroxybutyrate decreased in HA tx stifles.	(Marshall *et al*., 2000)
Canine	Clinical	SF	CCLR	13(6 treated with joint supplement)	^{1}H-NMR	Lactate and creatine levels significantly dropped in treated compared to control dogs.	(Martini *et al*., 2017)
Canine	Clinical	SF Serum	CCLR	4 CCLR, 4 OA of both SF and Serum	GC-MS LC-MS	65 metabolites and 349 lipids identified. Ceramides were significantly lower in ACL-rupture synovial fluid than OA synovial fluid.	(Overmyer *et al*., 2018)
Horse	Clinical	SF	Septic vs Non-septic joint pathologies	19 (7 septic, 12 non-septic)	^{1}H-NMR	Acetate, alanine, citrate, creatine phosphate, creatinine, glucose, glutamate, glutamine, glycine, phenylalanine, pyruvate, and valine were higher in the nonseptic group, while glycylproline was higher in sepsis.	(Anderson *et al*., 2018b)
Horses	Clinical	SF	OCD	10 (5 OCD, 5 control)	^{1}H-NMR	Reduced levels of glucose, pyruvate and lactate, and an increase in ketone bodies including hydroxybutyrate in OCD.	(Desjardin *et al*., 2014)

Table 1.2. Outline of published metabolomics studies involving synovial fluid, listed in order of species studied (continued)

Horse	Clinical	SF	Palmar osteochondral disease	51 (26 control, 25 cases)	^{1}H-NMR	Glucose and lactate decreased in palmar osteochondral disease.	(Graham *et al*., 2020)
Rabbit	Experimental	SF	ACL transection	33 (21 ACL transection, 12 control)	LC-MS	N1-acetylspermidine, 2-amino-1,3,4-octadecanetriol, l-phenylalanine, 5-hydroxy-l-tryptophan, and l-tryptophan were identified as potential biomarkers.	(Hu *et al*., 2020)
Rabbits	Experimental	SF	ACL injury	15 normal 15 ACL	LC-MS	Glycerophospholipid metabolism related compounds could serve as potential biomarkers for early degenerative changes of cartilage and meniscus after ACL injury.	(Tao *et al*., 2019)
Rats	Experimental	SF	Adjuvant arthritis (AA) and geniposide treatment	6 (2 control, 2 AA, 2 GE treatment)	HILIC-HRMS	20 metabolites significantly altered between AA rats and normal rate. GE tx reduced this to 13.	(Zhan *et al*., 2020)
Mice	Experimental	SF Serum	Obesity, OA, wound repair	28 (6 control, 6x3 different diet groups)	GC	Diet affected metabolic pathways in SF post injury.	(Wu *et al*., 2017)
Ovine	Experimental	SF	Early onset OA post ACL reconstruction	36 SF samples	^{1}H-NMR	Possible OA biomarkers: isobutyrate, glucose, hydroxyproline, asparagine, serine, and uridine.	(Mickiewicz *et al*., 2015)

Abbreviations: SF= synovial fluid, OA= osteoarthritis, RA= rheumatoid arthritis, ACL= anterior cruciate ligament, CCLR= cranial cruciate ligament rupture, OCD= osteochondritis dissecans, BD= Bechet's disease, SNA= seronegative arthritis, ReA= reactive arthritis, uSpA= unspecified arthritis, pSpA= peripheral spondyloarthritis, IA= intra-articular, AA= adjuvant arthritis, PTAA= post-traumatic ankle arthritis, tx= treatment, sx= surgery, HA=hyaluronic acid, LC-MS= light chromatography- mass spectrometry, GC-MS= gas chromatography- mass spectrometry, NMR= nuclear magnetic resonance, GC/TOF-MS= gas chromatography/time of flight mass spectrometry, UPLC-QTOF-MS= ultra-performance liquid chromatography to quadrupole time-of-flight mass spectrometry, GC= gas chromatography, HILIC-HRMS= hydrophilic interaction liquid chromatography coupled to high-resolution mass spectrometry, Phe/Tyr= Phenylalanine/Tyrosine ratio.

1.6.4. Metabolomic studies using canine synovial fluid

There have been only a few published studies investigating the metabolomic profile of canine stifle joint synovial fluid. Five studies have used NMR spectroscopy to examine metabolomic profiles of canine stifle joint synovial fluid (Damyanovich *et al*., 1999a, Damyanovich *et al*., 1999c, Marshall *et al*., 2000, Crovace *et al*., 2006, Martini *et al*., 2017). Damyanovich *et al*. (1999a) investigated the metabolite profile of stifle joint synovial fluid in 14 dogs using ^{1}H-NMR metabolomics, following experimental induction of OA by transection of the CCL. The study found that the levels of lactate, pyruvate, lipoprotein associated fatty acids, and glycerol as well as the ketones hydroxybutyrate and hydroxyisobutyrate were increased in those joints with experimentally induced OA, and that there were reduced levels of glucose, and elevated levels of N-acetylglycoproteins, acetate, and acetainide compared with the synovial fluid from the control group. These results suggested that, in canine OA, the intra-articular environment is more hypoxic and acidotic than a normal joint and that lipolysis may play an important role as an energy source in OA (Damyanovich *et al*., 1999a). Also, the authors concluded that the *N*-acetylglycoprotein polymer constituent of synovial fluid (mostly hyaluronan) seems to be increasingly fragmented and degraded into acetate by way of an acetamide intermediate with progressive OA, accounting for the increase in acetate in the affected joints. Two studies have used ^{1}H-NMR metabolomics to identify changes in the metabolome of canine synovial fluid with the use of a chondroprotector joint supplement after surgery for CCLR stabilisation (Crovace *et al*., 2006, Martini *et al*., 2017), highlighting the use of NMR metabolomics in the study of drug treatment outcomes. The numbers of participants in these studies were small (n=10 and n=13 respectively), but there was some indication of decreases in SF lactate concentrations in treated dogs, potentially showing a reduction in inflammatory responses. Another study investigating treatment effects on the metabolome of OA affected canine stifles involved using ^{1}H-NMR spectroscopy to compare the metabolome of joints treated with intra-articular hyaluronic acid injections at different time points after experimental induction of OA by transection of the CCL (Marshall *et al.,* 2000). The study found that decreased glucose, increased isoleucine levels and decreased acetate and hydroxybutyrate were found in a group of six dogs treated with three weekly injections of intra-articular hyaluronic acid two months after surgery, compared to a placebo group, suggesting an improvement in the joint environment. In one published abstract, Overmyer *et al*. (2018) used mass spectrometry (MS) coupled with gas chromatography (GC) and light chromatography (LC) to investigate the metabolite and lipid profile of serum and synovial fluid from four naturally occurring CCLR affected canine stifle joints, and four OA

affected joints (although the abstract does not mention if these were also stifle joints). Significantly increased concentrations of fatty acid hydroxy-fatty acids and sphingomyelins, and significantly decreased concentrations of ceramides in the CCLR synovial fluid than the OA synovial fluid respectively (Overmyer *et al*., 2018). Although the sample sizes were small, the study showed that metabolomics and lipidomics of synovial fluid hold a source for biomarker discovery for canine joint pathologies (Overmyer *et al*., 2018).

As far as could be found in the related literature, no studies investigating the metabolomic profiles of any species in relation specifically to meniscal injuries have been published, and none of the above papers mention meniscal injuries in those dogs with CCL rupture or transection.

1.7. Hypothesis and aims of the study

There is currently a gap in knowledge in terms of the study of metabolomic biomarkers of meniscal injury using synovial fluid from any species. In dogs, current non-surgical methods of diagnosis of meniscal injury can be either expensive, require specialist equipment and technical skills, and/or are relatively insensitive (Mahn *et al*., 2005, Samii *et al*., 2009, Neal *et al*., 2015). There is a need for a minimally invasive, highly sensitive diagnostic test for meniscal injuries, and late meniscal injuries, in dogs with CCLR.

It is hypothesised that the NMR metabolomic profile of canine stifle joint synovial fluid will differ depending on the presence of meniscal injuries in dogs with CCLR. This could then identify potential metabolite biomarker(s) that could be used to develop a simple, minimally invasive diagnostic test for meniscal injuries in dogs.

To answer this hypothesis, the aims of this study were:

1) To determine the NMR metabolite profile of synovial fluid derived from healthy canine stifle joints and those with CCLR, with and without meniscal injuries.
2) To undertake statistical and mathematical analysis of these datasets to identify specific disease groupings and determine effects of clinical variables on CCLR and meniscal injuries.

3) To undertake preliminary clinical validation studies to determine if the metabolites identified in Objectives 1 and 2 can be used to predict meniscal injuries.

2. Changes in the ^{1}H Nuclear Magnetic Resonance Metabolomic Profile of Equine and Canine Synovial Fluid with Regard to Increased Refrigerated Storage Time

2.1. Background

Metabolomics is a rapidly expanding field, involving the quantification of small molecule metabolites and the analysis of metabolic pathways in a variety of biofluids and tissues (Emwas *et al*., 2019). One analytical tool used in metabolomic studies is ^{1}H NMR spectroscopy (Clarke *et al*., 2020). This is a relatively inexpensive, highly reproducible, non-destructive and rapid technique that has been successfully used to identify alterations in the metabolome in different disease states, sample types and species (Clarke *et al*., 2020, Song *et al*., 2019). Synovial fluid has been found to hold a source of biochemical and metabolomic markers of joint disease, due to it being in close contact with joint structures (Boffa *et al*., 2020). Previous studies have used ^{1}H NMR spectroscopy to analyse changes in the metabolomic profile of synovial fluid of different species, including humans, horses and dogs and from different joint diseases, such as RA, OA, and septic joint pathologies (Anderson *et al*., 2018b, Anderson *et al*., 2018a, Damyanovich *et al*., 1999a).

As the number of metabolomic studies using SF increase, it is important that protocols involved in the collection, storage and processing of samples are optimised to increase the reproducibility and reliability of results (Anderson *et al*., 2020). Previous studies have examined the effects of different freezing protocols, centrifugation of samples, the number of freeze-thaw cycles, and long-term low temperature storage before processing SF samples for NMR spectroscopy (Anderson *et al*., 2020, Damyanovich *et al*., 2000). To date, no studies have examined the changes in the synovial fluid metabolome with increasing length of storage at four degrees Celsius before centrifugation and freezing prior to processing for NMR spectroscopy. As metabolomics studies hold promise in identifying changes in the metabolome that could be used as diagnostic or prognostic indicators, recognising how refrigeration time prior to processing samples can alter the metabolome is important for clinical studies where there is often some variation in storage time prior to laboratory analysis (Bernini *et al*., 2011).

This study aims to investigate the effects of increasing the length of time of storage at four degrees Celsius after collection and prior to processing, on the NMR metabolomic profiles of equine and canine SF. It is our hypothesis is that the SF metabolome will alter as the length of refrigerated storage time increases pre-processing.

2.2. Methods

2.2.1. Ethical approval

Equine synovial fluid sample was collected as a by-product of the agricultural industry, and therefore in conjunction with the Animals (Scientific Procedures) Act 1986, Schedule 2, ethical approval was not required for the use of this fluid.

Collection of canine synovial fluid for use in this study was authorised by the University of Liverpool Ethics committee (VREC634) as surplus clinical waste under the generic approval RETH00000553.

2.2.2. Synovial fluid collection

2.2.2.1. Equine synovial fluid collection

Synovial fluid was collected from the metacarpophalangeal joint of a horse euthanised at an abattoir less than eight hours prior to collection. The joint was aseptically opened, and SF aspirated using a 10ml syringe and kept on ice until processed.

2.2.2.2. Canine synovial fluid collection

Synovial fluid was collected from a dog admitted to the University of Liverpool Small Animal Teaching Hospital for surgery to treat CCLR. Synovial fluid was collected under general anaesthesia from the stifle joint to be operated on via aseptic arthrocentesis prior to the first surgical incision (Bexfield and Lee, 2014). The owner of the dog had given informed consent for the collection of SF prior to arthrotomy as part of their consent form, and ethical approval for use in this study had been granted (VREC634). The sample was transferred on ice to the laboratories at the Leahurst campus, University of Liverpool.

2.2.3. Sample preparation

2.2.3.1. Equine synovial fluid preparation

150µl of SF was aliquoted into 32 sterile plain 1.5ml microcentrifuge tubes (Eppendorf UK Ltd, Stevenage, UK). These were then kept refrigerated at 4°C. At each time point, four

aliquots were centrifuged at 2540*g* at 4°C for 5 minutes, the supernatant collected into a new sterile plain 1.5ml microcentrifuge tube, then snap frozen in liquid nitrogen and stored at -80°C (Anderson *et al*., 2020). The time points were immediately post collection (zero hours), six hours, 12 hours, 18 hours, 24 hours, 48 hours, one-week and four-weeks post sample collection. Time points were selected to examine changes up to 48 hours in more detail, as these are more likely to be the timepoints relevant to clinical tests involving synovial fluid. Time points one week and four weeks were included to investigate changes over a longer time frame.

2.2.3.2. Canine synovial fluid preparation

150µl of SF was aliquoted into 17 sterile plain 1.5ml microcentrifuge tube (Eppendorf UK Ltd, Stevenage, UK). These aliquots were then kept refrigerated at 4°C. At each time point, three to four aliquots were processed via centrifugation and freezing as above. The time points were four hours, 12 hours, 24 hours, 48 hours and one-week post sample collection.

2.2.4. NMR spectroscopy

2.2.4.1. Synovial fluid sample preparation for NMR

Samples were transferred on dry ice to the University of Liverpool NMR Centre. Immediately prior to processing for NMR spectroscopy, samples were thawed at room temperature for 20-30 minutes. 100µl of SF was then diluted with 100µl of a buffer master mix containing 200mM sodium phosphate (NaH_2PO_4, POSigmaAldrich, Gillingham, UK) pH 7.4 in 20% deuterium oxide (^2H_2O, SigmaAldrich) and 2.4mM sodium azide (NaN_3, SigmaAldrich). Samples were vortexed for 30 seconds, centrifuged at 12000*g* at 4°C for 5 minutes, and the supernatant transferred into a 3mm outer diameter NMR tubes using a glass Pasteur pipette.

2.2.4.2. ^{1}H NMR spectral acquisition

1D ^{1}H NMR spectroscopy was carried out using a 700 MHz NMR Bruker Avance III HD spectrometer, with associated TCI cryoprobe and chilled Sample-Jet autosampler. All synovial fluid prepared samples were placed in the spectrometer and analysed individually. Water suppression was obtained by presaturation, and a Carr–Purcell–Meiboom–Gill (CPMG) pulse sequence was used allowing the filtering of small molecules via a cpmgpr1d

filter. The CPMG spectra were acquired at 37 °C with a 15ppm spectral width, a four second interscan delay and 32 transients. Topspin 3.1 (Bruker Corporation, Billerica, Massachusetts, USA) and IconNMR 4.6.7 (Bruker Corporation) were the software used for carrying out spectral acquisition and processing (Anderson et al., 2020).

2.2.4.3. Spectra Quality Control

All spectra underwent quality control to ensure that they met recognised minimum reporting standards (Sumner *et al*., 2007). Spectra underwent assessment for quality control (QC) using Bruker Topspin version 3.1 (Bruker Corporation, Billerica, Massachusetts, USA). The spectra were first assessed for baseline errors, ensuring baselines had minimal curvature or deviations. The spectra were also assessed to ensure adequate water suppression had occurred, with the water peak being between 0.2 and 0.4ppm. Spectra were aligned to a glucose beta anomeric doublet at 5.24ppm, as the use of sodium trimethylsilyl propionate (TSP), commonly added to samples to act as a reference peak, is not indicated for use in synovial fluid due to the interference it can cause by binding to proteins such as albumin (Kriat et al., 1992). Lastly, the line-width half height (LWHH) of the glucose beta anomeric doublet at 5.24ppm was measured on all spectra, and any measurements that exceeded one standard deviation from the mean of all spectral line width at half heights were deemed to have failed QC.

2.2.4.4. Metabolite annotation and identification

Metabolites were identified using Chenomx NMR Suite Profiler version 7.1 (Chenomx, Edmonton, Canada). The spectra were divided into 430 spectral regions termed “bins” for the equine synovial fluid, and 405 bins for the canine synovial fluid spectra. Bins represented either single metabolite peaks, or multiple metabolites where metabolite peaks overlapped (Wishart, 2008).

This pattern file of bins and all spectra that passed QC were input into a software for metabolomics, TameNMR (hosted by galaxy.liv.ac.uk). Using TameNMR, the pattern files were assessed, and any bins were altered if needed to ensure the area under the peak was represented by the bin. Metabolites annotated using Chenomx were confirmed by downstream unique peak identification if present. The equine synovial fluid pattern file was

compared to previous pattern files for equine synovial fluid, where internal ^{1}H 1D NMR standards and ^{1}H ^{13}C 2D NMR had been used for confirmation of metabolite identity where possible. TameNMR was then used to create a spreadsheet of binned spectra, which was subsequently inputted into statistical software R studio (R Core Team, 2020).

2.2.5. Statistical Analysis

- Binned spectra were normalised using Probabilistic Quotient Normalisation (PQN) (Dieterle *et al*., 2006), and Pareto scaled prior to analysis.
- Multivariate analysis was carried out with Principal Component Analysis (PCA), using a script for metabolomic data analysis on R Studio (R Studio, Boston, Massachusetts, USA) (R Core Team, 2020). This was carried out on the normalised and scaled dataset.
- Univariate analysis using one-way analysis of variance (ANOVA) was undertaken using a script for metabolomic data analysis on R Studio. The significance level (p) was set for less than 0.05, and Benjamini–Hochberg (BH) correction method was used for the data. Tukey *post-hoc* analysis was carried out on all variables.
- Boxplots were performed on R studio using a script for metabolomics data.

2.3. Results

2.3.1. Metabolites annotated to synovial fluid spectra

Equine SF- The spectra were divided into 430 bins. Of these, 123 remained with an unknown metabolite identification, and 307 bins were assigned to a total of 62 metabolites. A list of metabolites annotated using the software Chenomx version 7.1, along with their identification number from the Human Metabolome Database (HMDB) (Wishart *et al*., 2018) is shown in Table 2.1. As ethanol is considered to be a contaminant in NMR (van der Sar *et al*., 2015), any bins containing ethanol were removed from the pattern file prior to statistical analysis.

Canine SF- The spectra were divided into 405 bins. Of these, 202 bins remained with an unknown metabolite identification, and 203 bins were assigned to a total of 52 metabolites (Table 2.1).

Table 2.1. List of metabolites annotated to ^{1}H NMR spectra of equine synovial fluid and canine synovial fluid. HMDB ID= Human metabolite database identification number.

Metabolite	HMDB ID	Equine	Canine
2-Aminoadipate	HMDB0000510	NO	YES
2- Phenylpropionate	HMDB0011743	YES	YES
2-Hydroxyisobutyrate	HMDB0000729	YES	NO
3-Hydroxybutyrate	HMDB0000011	YES	NO
3-Phenylpropionate	HMDB0000764	YES	YES
4-Pyridoxate	HMDB0000017	NO	YES
5-Aminolevulinate	HMDB0001149	YES	NO
5-Hydroxyindole-3-Acetate	HMDB0000763	NO	YES
Acetaminophen	HMDB0001859	NO	YES
Acetate	HMDB0000042	YES	YES
Acetoacetate	HMDB0000060	YES	NO
Acetone	HMDB0001659	NO	YES
Agmatine	HMDB0001432	YES	NO
Alanine	HMDB0000161	YES	YES
Alloisoleucine	HMDB0000557	YES	YES
Anserine	HMDB0000194	YES	NO
Arabinose	HMDB0000646	YES	NO
Arginine	HMDB0000517	YES	NO
Betaine	HMDB0000043	YES	YES
Carnitine	HMDB0000062	NO	YES
Citrate	HMDB0000094	YES	YES
Creatine	HMDB0000064	YES	YES
Creatine Phosphate	HMDB0001511	YES	YES
Creatinine	HMDB0000562	YES	YES
Cystine	HMDB0000192	YES	NO
Dimethyl sulfone	HMDB0004983	NO	YES
dTTP	HMDB0001342	YES	NO
Ethanol	HMDB0000108	YES	NO
Formate	HMDB0000142	YES	YES
Fucose	HMDB0000174	YES	NO

Table 2.1. List of metabolites annotated to ^{1}H NMR spectra of equine synovial fluid and canine synovial fluid (continued)

Galactarate	HMDB0000639	YES	YES
Galactitol	HMDB0000107	YES	NO
Galactose	HMDB0000143	YES	NO
Glucose	HMDB0000122	YES	YES
Glutamate	HMDB0060475	YES	YES
Glutamine	HMDB0000641	YES	YES
Glycerol	HMDB0000131	YES	NO
Glycine	HMDB0000123	NO	YES
Glycylproline	HMDB0000721	YES	YES
Glycolate	HMDB0000115	NO	YES
Histamine	HMDB0000870	YES	YES
Histidine	HMDB0000177	YES	YES
Isobutyrate	HMDB0001873	YES	NO
Isoleucine	HMDB0000172	YES	YES
Lactate	HMDB0000190	YES	YES
Leucine	HMDB0000687	YES	YES
Levulinate	HMDB0000720	YES	YES
Mannitol	HMDB0000765	YES	YES
Mannose	HMDB0000169	YES	YES
Methanol	HMDB0001875	YES	YES
Methionine	HMDB0000696	NO	YES
Methylglutarate	HMDB0000752	YES	YES
Methylsuccinate	HMDB0001844	YES	YES
N-acetylglutamate	HMDB0001138	YES	NO
N-acetylglycine	HMDB0000532	YES	NO
N-Isovaleroylglycine	HMDB0000678	YES	NO
O-Cresol	HMDB0002055	NO	YES
P-Cresol	HMDB0001858	NO	YES
Pantothenate	HMDB0000210	NO	YES
Phenylalanine	HMDB0000159	YES	YES
Pi-Methylhistidine	HMDB0000001	YES	YES

Table 2.1. List of metabolites annotated to ^{1}H NMR spectra of equine synovial fluid and canine synovial fluid (continued)

Proline	HMDB0000162	YES	NO
Pyridoxine	HMDB0000239	YES	NO
Pyruvate	HMDB0000243	YES	YES
Serine	HMDB0000187	YES	NO
sn-glycero-3-phosphocholine	HMDB0000086	YES	YES
Succinate	HMDB0000254	NO	YES
Succinylacetone	HMDB0000635	NO	YES
Tau-Methylhistidine	HMDB0000479	YES	YES
Threonine	HMDB0000167	YES	YES
Thymine	HMDB0000262	YES	NO
Thymol	HMDB0001878	NO	YES
Tyramine	HMBD0000306	NO	YES
Tyrosine	HMDB0000158	YES	YES
Uridine	HMDB0000194	YES	NO
Valine	HMDB0000883	YES	YES

2.3.2. Multivariate and univariate analysis of changes in the metabolome of equine synovial fluid with increased refrigerated storage time

Of the 32 samples ran, one sample failed to run and three spectra failed quality control, and were excluded from the rest of the analysis. The reasons for failure included poor baseline (for two samples) and excessive line width half height (for one sample).

Multivariate analysis using PCA showed clustering of samples in groups from zero hours to one week of storage at 4°C before centrifugation and freezing, and clear separation of the time point of four weeks (Figure 2.1). The separation of the group of samples at four weeks compared to other groups was determined primarily by the second principle component. 95% variance was accounted for by 14 principle components. The PCA was repeated removing the group at four weeks of storage, in order to examine changes between groups at zero hours to one week in more detail (Figure 2.2).

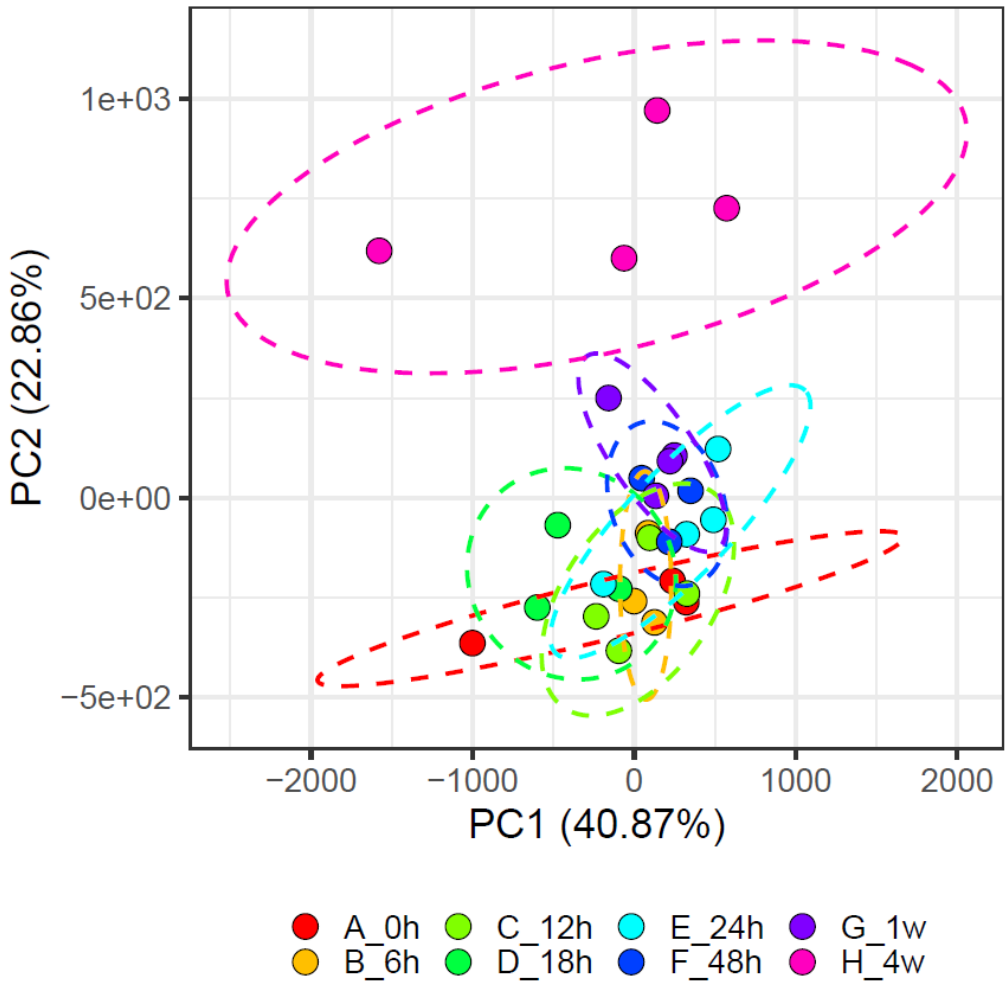

Figure 2.1. Principle component analysis two-dimensional scores plot showing changes in the metabolomic profile of equine synovial fluid with increased length of time of storage at four degrees celsius prior to centrifugation and freezing prior to processing for nuclear magnetic resonance spectroscopy. *Samples from zero hours to one week show clustering, whereas samples stored for four weeks show separation indicating distinct changes in the overall metabolomic profile.*

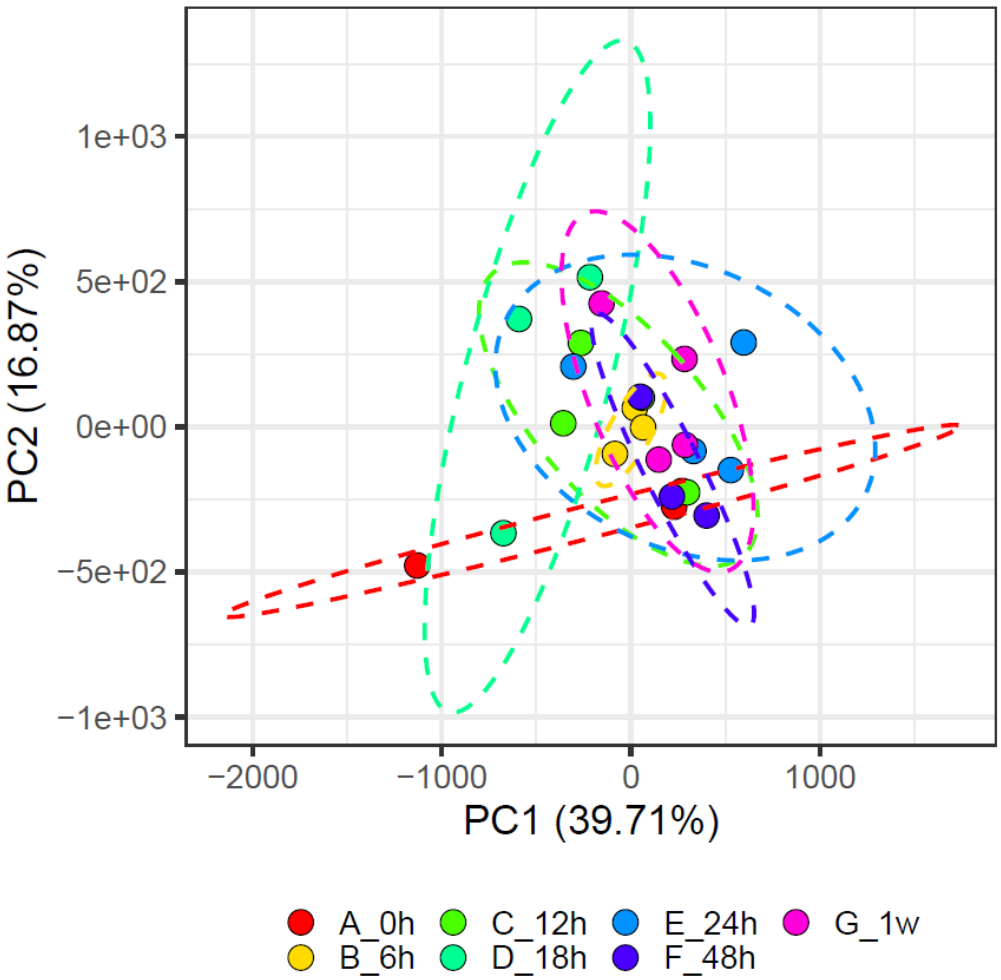

Figure 2.2. Principle component analysis two-dimensional scores plot showing changes in the metabolomic profile of equine synovial fluid with increased length of time of storage at 4 degrees celsius prior to centrifugation and freezing prior to processing for nuclear magnetic resonance spectroscopy. *Samples from zero hours to one week show clustering, indicating no overall change to the metabolome.*

Univariate analysis using one-way ANOVAs examined changes in spectral bins between groups. The results are shown in Table 2.2. Between the groups zero hours to six hours of storage, and six hours to twelve hours of storage, none of the 422 spectral bins were significantly altered (significance set as $p \leq 0.05$). One spectral bin became significantly changed between time points 12 hours and 18 hours. Zero bins became significantly altered between 18 hours and 24 hours, and between 24 hours and 48 hours. From 48 hours to one week four metabolite peaks became significantly different, and between one week and four-week groups, 43 out of 421 bins became significantly changed. The most significant changes

were between the specific time points at zero hours and four weeks, over which time 91/421 spectral bins, assigned to 26 metabolites, became significantly changed, including a decrease in glucose concentration. Boxplots showing the changes in significant metabolites over time are shown in Figure 2.3.

Table 2.2. Table showing number of spectral regions (termed "bins"), and their associated metabolites, found to be significantly altered in equine synovial fluid with increased length of refrigerated storage prior to nuclear magnetic resonance spectroscopy. Time points indicate length of time of storage of equine synovial fluid at four degrees Celsius prior to processing for nuclear magnetic resonance (NMR) spectroscopy. P values are after Benjamini-Hochberg false discovery rate correction.

Time points being compared	**Number of significantly altered bins out of 422 bins (p≤0.05)**	**Metabolites identified as significantly changing between time points (p≤0.05)**
0 hours to 6 hours	0	
6 hours to 12 hours	0	
12 hours to 18 hours	1	Unknown
18 hours to 24 hours	0	
24 hours to 48 hours	0	
48 hours to 1 week	4	Increased: Pyruvate. Decreased: 5-Aminolevulinate.
1 week to 4 weeks	43	Increased: Pyruvate, 3-hydroxybutyrate, leucine, O-acetylcarnitine. Decreased: Glutamine.

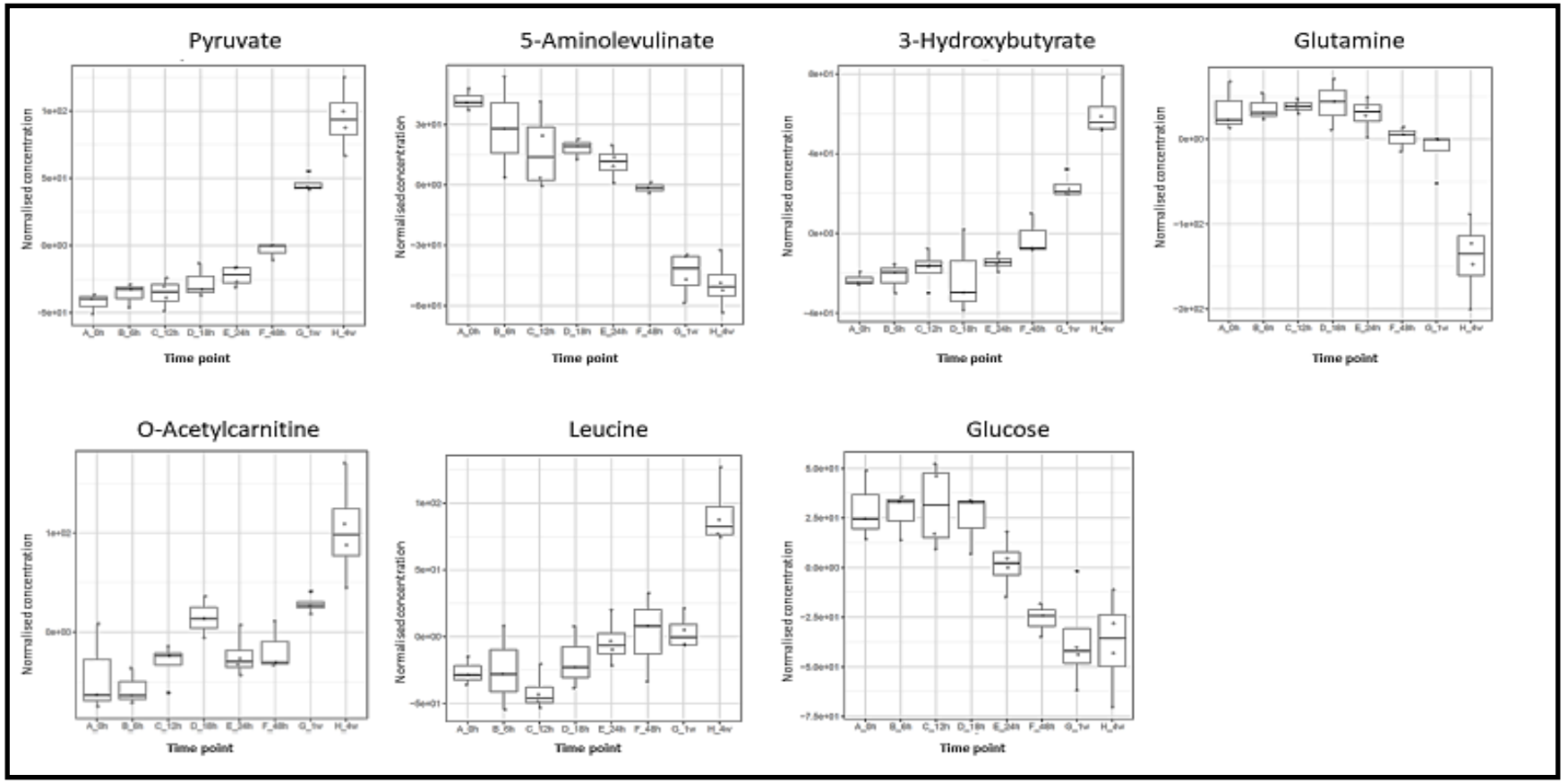

Figure 2.3. Boxplots showing changes in normalised concentrations of certain metabolite peaks in equine synovial fluid with increased length of storage at 4°C before centrifugation and freezing. *The x axis represents the time point, and the y axis represents normalised peak intensity following probabilistic quotient normalisation and pareto scaling. Time points on the x axis are zero, six, twelve, eighteen, twenty-four and forty-eight hours then one week and four weeks post collection.*

2.3.3. Multivariate and univariate analysis of changes in the metabolome of canine synovial fluid with increased refrigerated storage time

Of the 17 samples of canine synovial fluid, six failed quality control. Reasons for failure included poor baseline (for two samples) and poor water suppression (for four samples). These samples were re-run and again failed quality control and so were excluded from statistical analysis. Due to the failure of these spectra to meet minimum reporting standards (Sumner *et al*., 2007), to continue with statistical analysis of the remaining samples, time points of four hours, 12 hours and 24 hours were amalgamated into a single group.

Multivariate analysis by way of PCA showed separation of the grouped samples at time points 4-24hours, 48 hours, and one week, primarily through the second principal component (Figure 2.4). At one week of storage at four degrees Celsius prior to centrifugation and freezing, the PCA shows a wider separation between samples, indicating the metabolomic profile increasingly changing at this time point. 95% of variance was accounted for by six principal components.

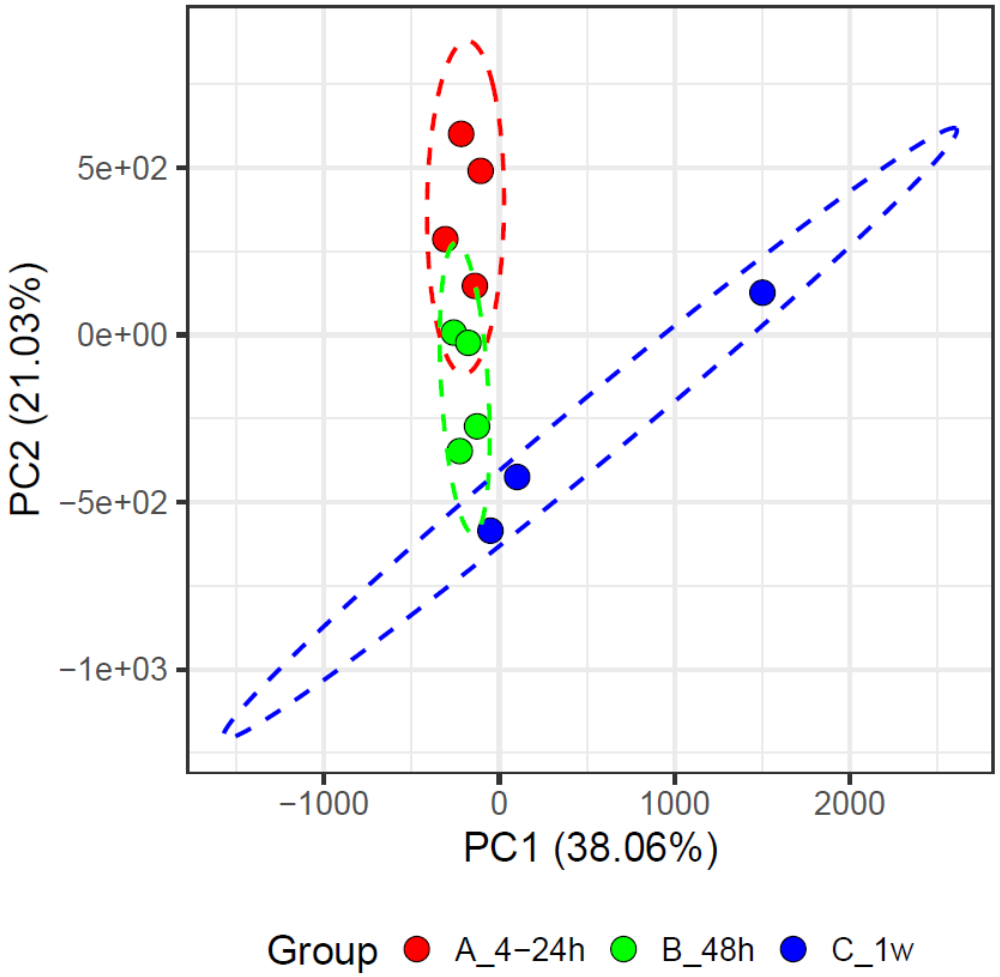

Figure 2.4. Principle component analysis two-dimensional scores plot showing changes in the metabolomic profile of canine synovial fluid with increased length of time of storage at four degrees celsius prior to centrifugation and freezing prior to processing for nuclear magnetic resonance spectroscopy.

Univariate analysis by way of one-way ANOVAs showed that there were four bins that became significantly changed between time points at less than or equal to 24 hours and 48 hours, nine significant bins between timepoints of 48 hours and one week, and 10 significant changes between time points of less than or equal to 24 hours and one week (Table 2.3). Significance was set as $p \leq 0.05$. Boxplots showing the changes in metabolite concentrations over time of storage are shown in Figure 5. Although not significant, there was a trend towards decreasing glucose concentration over time.

Table 2.3. Table showing number of spectral regions (termed "bins"), and their associated metabolites, found to be significantly altered in canine synovial fluid with increased length of refrigerated storage prior to nuclear magnetic resonance spectroscopy. Time points indicate length of time of storage of canine synovial fluid at four degrees Celsius prior to processing for nuclear magnetic resonance (NMR) spectroscopy. P values are after Benjamini-Hochberg false discovery rate correction.

Time points being compared	**Number of significantly altered bins out of 405 bins (p≤0.05)**	**Metabolites identified as significantly changing over time (p≤0.05)**
≤24hours and 48 hours	4	Increased: Lactate, unknown
48 hours and 1 week	9	Increased: Lactate, valine, unknown.

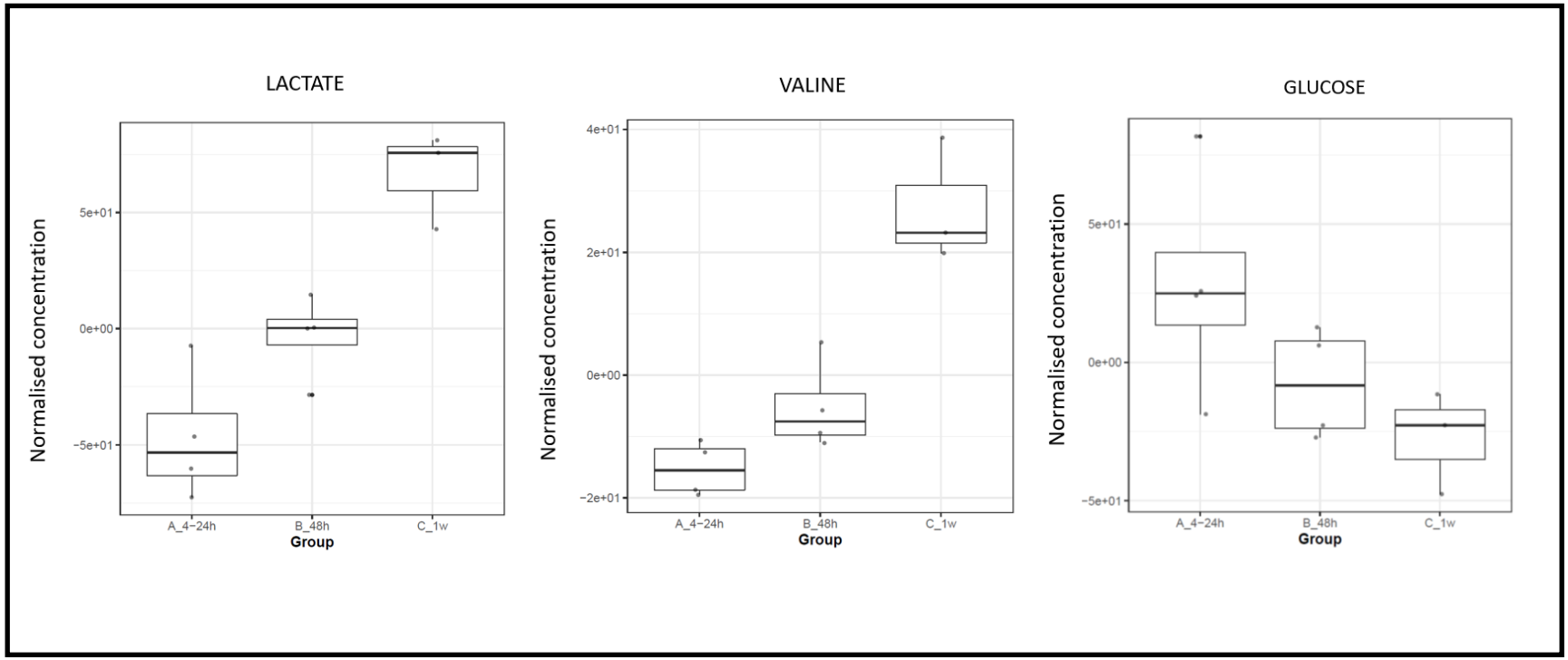

Figure 2.5. Boxplots showing changes in normalised concentrations of certain metabolites in canine synovial fluid with increased length of storage at 4°C before centrifugation and freezing. *The x axis represents the time point, and the y axis represents normalised peak intensity following probabilistic quotient normalisation and pareto scaling. The time points on the x axis are four to 24 hours, 48 hours and one-week post collection.*

2.4. Discussion

To our knowledge, this is the first study examining changes in the metabolome of equine and canine SF over a defined time period following storage at four degrees Celsius prior to centrifugation, freezing and subsequent processing for NMR spectroscopy. Overall, the results show that the metabolome of both equine and canine SF remains relatively stable for at least 48 hours of storage at 4°C prior to centrifugation and freezing, with few significant changes in metabolite concentrations. When the synovial fluid underwent NMR spectroscopy after storage times of one week or more, greater changes in the metabolome are evident.

For the equine SF analysis, the inclusion of a time point at four weeks shows the greatest metabolomic changes compared to time points of zero hours to one week. It is interesting to note that no metabolites were significantly differentially abundant in the equine synovial fluid between the consecutive time points of zero hours to six hours, six hours to 12 hours, 18 hours to 24 hours or between 24 hours and 48 hours of storage.

In the canine synovial fluid, there appears to be a greater separation of groups less than and including 24 hours of storage, and 48 hours of storage on multivariate analysis. However, the loss of some spectra to meet minimum reporting standards and the subsequent inability to include these in statistical analysis meant that the sample size per time point is lower than the equine synovial fluid analysis, with the amalgamation of time points at four hours, 12 hours and 24 hours into a single group. It is therefore difficult to draw firm conclusions as to the changes up to 24 hours of storage time.

Metabolites that appear to be changing over time from 0 hours to four weeks of storage in the equine synovial fluid included an increase in pyruvate, 3-hydroxybutyrate, leucine and O-acetylcarnitine, and a decrease in glutamine, 5-aminolevulinate, and glucose. For the canine synovial fluid, the main drivers of change over the one week of storage time appear to be an increase in lactate and valine. Glucose appears to be also decreasing over time in the canine synovial fluid, although not reaching significance over the one week analysed.

These changes in the metabolomic profile over time are likely due to ongoing cellular processes and cellular degradation within the SF samples prior to centrifugation. A significant increase in pyruvate and general trend to reduction in glucose concentration evident after one week in the equine synovial fluid could indicate ongoing glycolysis in cellular material. Likewise, in the canine synovial fluid, lactate concentrations were found to increase, whilst

glucose concentrations trended toward decreasing over time, again indicating glycolysis in the remaining cellular contents (Akram, 2013). Previous studies examining changes over time pre-processing with serum samples have also found pyruvate, lactate, and glucose to be amongst the metabolites most affected by pre-processing delays in centrifugation and storage time (Stevens *et al*., 2019, Fliniaux *et al*., 2011, Bernini *et al*., 2011).

The amino-acids leucine and valine were found to have increased in the equine and canine synovial fluid respectively with increased storage time. This finding correlates with previous studies evaluating changes in amino-acids with varying pre-processing protocols, and is hypothesised to be due to protein degradation in the samples over time (An *et al*., 2021).

The canine and equine SF samples were collected under different experimental conditions, which could have an impact on the differences in the observed rate of changes of the metabolome. The equine synovial fluid was taken from a horse approximately eight hours post mortem. Some changes to the metabolome of this fluid could have already occurred in those eight hours that have not been accounted for in this study. Although no existing peer-reviewed studies examining changes specifically to SF post-mortem could be found in the literature, it has been found that the metabolome of serum samples changes post-mortem due to several factors, including an absence of circulating oxygen, degradation of cells, changed enzymatic reactions, and a termination of anabolic production of metabolites (Donaldson and Lamont, 2015).

There was also a difference in the pathology of the joints from which the synovial fluid samples were obtained from the two different species. The equine synovial fluid was obtained from a metacarpophalangeal joint with no gross pathological changes. The canine synovial fluid was obtained *in vivo* from a dog undergoing surgery for CCLR, with OA in the affected stifle joint. Total nucleated cell counts have been found to be increased in synovial fluid obtained from OA joints compared to normal joints (Hollander *et al*., 1966) and in dogs with CCLR compared to normal canine stifle joints (Wood and Gibson, 2020). This increased cellularity could cause a more rapid change in the metabolomic profile compared to the equine synovial fluid.

There are some limitations to this study. Firstly, there is a low sample size, with three to four samples per group. Secondly, time points between 48 hours and one week were not investigated. This was due to the volume of synovial fluid able to be obtained from a single donor limiting the number of aliquots. With the canine synovial fluid study, failure of six spectra to meet minimum reporting standards limited the number of spectra per time point,

eliminating the ability to statistically compare time points of four hours, 12 hours and 24 hours. Future work could use pooled synovial fluid to increase volume to enable more time points with a higher sample size to be used, however this could prove difficult for samples taken directly from clinical cases, such as the canine synovial fluid, as there would likely be differences between times of sampling. Repeating the experiment using synovial fluid obtained from a dog with a larger volume of synovial fluid would also be of benefit, enabling a larger sample size per time point.

2.5. Conclusion

In clinical scenarios, there is often some differences between time of sampling and time of laboratory processing. Determining how significant the effect of prolonged pre-processing refrigerated storage time is on the metabolome of SF has relevance for future metabolomic studies, and also for future development of any diagnostic test using SF. During this study, the effects of increasing the length of time of refrigerated storage pre-processing on both equine and canine synovial fluid have been examined. For the first 48 hours of storage at four degrees Celsius prior to centrifugation and freezing, there are relatively few significant changes to metabolites within equine and canine synovial fluid, meaning that there can be some confidence in including samples up to this time point in future studies and in future diagnostic tests using SF.

3. ^{1}H NMR metabolomic and lipidomic analysis of canine stifle joint synovial fluid from dogs with cranial cruciate ligament rupture, with or without meniscal injury.

3.1. Introduction

Cranial cruciate ligament rupture is one of the most common causes of pelvic limb lameness in dogs (Witsberger *et al*., 2008). It presents a significant cause of morbidity amongst the canine population, with a recent study finding that dogs with CCLR accounted for 0.56% of all cases presented to primary care veterinary practices in the UK (Taylor-Brown *et al*., 2015).

One sequelae of the instability in the stifle joint caused by loss of function of the CCL can be tears to the menisci, which has been found to occur in approximately 50% of cases at time of surgery for CCLR (Bennett and May, 1991). The menisci are a pair of C shaped fibrocartilaginous structures within the stifle joint that are located in between the tibial plateau and femoral condyles (Kambic and McDevitt, 2005). The menisci have several important functions in the canine stifle joint. They are involved in load bearing, load distribution and shock absorption, as well as contributing to joint stability, proprioception and joint lubrication (Arnoczky *et al*., 1980, Pozzi *et al*., 2010b, Pozzi and Cook, 2017). Meniscal injuries as a result of CCLR most commonly affect the medial meniscus, due to its firmer attachment to the tibia caudally making it more prone to becoming trapped between the tibia and femur during cranial translocation of the tibia in stifle joints without a functioning CCL (Pozzi *et al*., 2006). Currently, treatment of meniscal injuries in dogs most commonly involves removal of part, or all, of the affected meniscus via an arthrotomy or arthroscopy (Franklin *et al*., 2017b). The resultant loss of the normal meniscal structure leading to alterations in pressure distribution across the articular cartilage that could perpetuate the development of osteoarthritis (OA) (Pozzi *et al*., 2008b).

Meniscal injuries can occur post-operatively after surgery for CCLR has been performed, likely due to either residual instability in the joint, or failure to diagnose at time of surgery (Metelman *et al*., 1995a). The reported prevalence of these late meniscal injuries varies, depending on the study, from 2.8% to 13.8% (Metelman *et al*., 1995a, Fitzpatrick and Solano, 2010, Stein and Schmoekel, 2008). Late meniscal injuries can be a cause of recurring stifle joint pain and lameness in the affected dogs, and can be challenging for the veterinary practitioner to diagnose (Dillon *et al*., 2014). Affected dogs often present with a recurring lameness on the operated limb weeks or months after CCLR surgery, with clinical examination potentially revealing pain on stifle flexion, and/or a “click” on stifle flexion (Dillon *et al*., 2014, Case *et al*., 2008). The presence of this so-called meniscal click has been

found to be an unreliable diagnostic sign, with one recent systematic review finding it to have a reported sensitivity of 26.6% to 66.6% (McCready and Ness, 2016b). Radiographs can be useful in ruling out other causes of recurring lameness post-operatively, such as implant related problems, but cannot show meniscal injuries directly. Won *et al.* (2020) recently investigated using radiographic joint space width as an indicator of meniscal injuries in lateral projections of the canine stifle, although this was only 40.5% sensitive. Further diagnostic imaging techniques for these late meniscal injuries can involve low field or high field magnetic resonance imaging (MRI), computed tomography (CT) with arthrography, or ultrasound examination (McCready and Ness, 2016b). Depending on the study, the sensitivity of these techniques in diagnosing meniscal injuries in dogs has been found to be 64-100% for low field MRI (Böttcher *et al*., 2010, Gonzalo-Orden *et al*., 2001) and 75-100% (Olive *et al*., 2014, Blond *et al*., 2008) for high field MRI. CT with arthrography and ultrasonography have been found to have a sensitivity of 71% (Samii *et al*., 2009) and 90% (Mahn *et al*., 2005) respectively. All of these imaging techniques require either expensive specialised equipment, and/or advanced technical expertise, both of which can limit the availability of these diagnostics in veterinary practice, and amount to a considerable cost for the owner, caregiver, or pet insurance provider (Arnault *et al*., 2009, Böttcher *et al*., 2010). Surgical methods of diagnosis include either stifle joint arthroscopy (Van Gestel, 1985) or arthrotomy (Miller and Presnell, 1985). These surgical diagnostic techniques are more invasive than imaging and hold inherent risk, although they also allow for treatment of any meniscal injuries at time of diagnosis (Ritzo *et al*., 2014). Furthermore, using surgery as a means of diagnosis holds the risk of having the animal go through a potentially unnecessary surgical procedure if no meniscal injury is found (Blond *et al*., 2008).

Currently, there are no biomarkers of meniscal injury that can be used as a diagnostic aid. Also, no biomarkers of CCLR exist that could lead to earlier intervention or target preventative treatment in “at risk” stifles, such as the contralateral stifles of high-risk breeds. One potential source of biomarkers of stifle joint pathologies is synovial fluid (SF) (Boffa *et al*., 2020, Fox and Cook, 2001). SF is a viscous fluid, that is a dialysate of plasma (Ropes *et al*., 1940), and functions as a joint lubricant. It contains a high level of the high molecular weight glycosaminoglycan hyaluronic acid (HA), which is secreted by synoviocytes and forms complexes with proteins within the SF (Ghosh, 1994). Another function of SF involves permitting the transport of nutrients from the synovial membrane to other joint structures such as the articular cartilage, and the transport of waste products to the lymphatic system (Gibson and Rooney, 2007). SF has been found to contain a unique source of biomarkers of

joint disease, due to its close proximity to structures within joints that become altered with different joint pathologies, as well as containing markers of systemic disease due to it being a derivative of plasma (Fox and Cook, 2001, de Bakker *et al*., 2017, Anderson *et al*., 2018b). Previous studies have investigated potential cytokine and protein biomarkers of CCLD within canine stifle joint SF, including interleukin-8 (IL-8) (de Bruin *et al*., 2007c), anti-collagen type 1 antibodies (de Bruin et al., 2007b) and matrix metalloproteinases (MMP) 2 and MMP9 (Boland et al., 2014, Murakami et al., 2016) and lubricin (Wang *et al*., 2020). There are relatively few studies in the literature examining biomarkers specific to meniscal injury within SF in dogs. Studies have examined biomarkers of OA in canine stifle joint SF using experimental models of meniscectomy in dogs to induce OA (Lindhorst *et al*., 2000). In humans, a recent study by Clair *et al.* (2019) found IL-6, monocyte chemoattractant protein-1 (MCP-1), macrophage inflammatory protein-1β (MIP-1β) and MMP-3 to be increased in the SF of humans with meniscal injuries compared to healthy controls. Proteomic analysis of synovial fluid in humans with meniscal injuries compared to healthy controls has also been examined (Roller *et al*., 2016).

Metabolomics is an -omics technology that allows the identification and quantification of small molecule metabolites and analysis of metabolic pathways within a variety of biofluids, cells and tissues (Bujak *et al*., 2015). Proton nuclear magnetic resonance (^{1}H NMR) is a tool for metabolomics studies, having the benefits of being rapid, non-destructive and relatively inexpensive compared to other metabolomics tools such as mass spectrometry (Clarke *et al*., 2020). ^{1}H NMR has been used successfully to investigate changes in the SF metabolomic profile in humans and horses with joint pathologies such as OA, rheumatoid arthritis and septic arthritis (Anderson *et al*., 2018a, Anderson *et al*., 2018b, Clarke *et al*., 2020). Therefore, there is promise for using NMR spectroscopy to investigate biomarkers of joint pathology within canine stifle joint SF. To date, four published peer-reviewed studies have used NMR spectroscopy as a tool for metabolomic studies of canine stifle joint SF (Damyanovich *et al*., 1999b, Damyanovich *et al*., 1999c, Marshall *et al*., 2000, Crovace *et al*., 2006). These involved examining metabolome changes after experimental induction of OA by transection of the CCL (Damyanovich *et al*., 1999b, Damyanovich *et al*., 1999c, Marshall *et al*., 2000), and changes in the SF metabolome in dogs with OA after treatment with chondroprotectants (Crovace *et al*., 2006). However, these studies typically involved a small sample size, and were mainly focused on biomarkers of OA rather than CCLR and meniscal injuries. NMR metabolomics could be used as a tool to study metabolites that could

potentially act as biomarkers of meniscal injuries in CCLR affected stifle joints. This information could then potentially allow for the development of a simple, minimally invasive diagnostic test more reliable at detecting meniscal injuries, and late meniscal injuries, than pre-existing non-surgical diagnostic techniques.

We therefore hypothesise that the metabolomic profile of canine stifle joint SF will alter depending on the presence of CCLR, and depending on the presence of concurrent meniscal injuries and in order to prove this, the objectives of this study are:

1) to investigate the ^{1}H NMR metabolomic profile of canine stifle joint SF in dogs without CCLR and those with CCLR;

2) to investigate whether the metabolome of canine CCLR affected stifle joint SF changes depending on the presence of meniscal injuries;

3) to examine the effects of various clinical variables on the canine stifle joint SF; and

4) to investigate whether any metabolite identified could be used as a biomarker for the diagnosis of meniscal injuries in canine CCLR affected stifle joint SF.

3.2. Materials and methods:

3.2.1. Ethical approval

Ethical approval for the collection of canine SF for use in this study was granted by the University of Liverpool Veterinary Research Ethics Committee (VREC634) as surplus clinical waste under the generic approval RETH00000553.

3.2.2. Synovial fluid collection

Canine SF was collected from dogs undergoing surgery for CCLR or patella luxation, or as excess clinical waste from dogs undergoing arthrocentesis as part of lameness investigations from March 2018 to June 2021. Cases were recruited from three veterinary practices in the north-west of England, namely the University of Liverpool Small Animal Teaching Hospital, Leahurst, and the Animal Trust CIC Veterinary Practices at Bolton and Blackburn. Owners of

the dogs were approached at time of admission for the procedure, and informed consent was obtained from the owners of the animals for the collection of the SF and participation in the project (veterinary surgeon and owner information and consent forms are included in the supplementary material S1-4). SF was collected by stifle joint arthrocentesis as per the BSAVA guide to procedures in small animal practice (Bexfield and Lee, 2014). A 21 gauge to 23-gauge needle attached to a two to five millilitre sterile syringe (depending on the size of the dog) was inserted into the stifle joint space either medially or laterally to the patella ligament after sterile preparation of the skin, prior to first surgical incision. After aspiration of the SF, samples were placed in sterile 1.5ml Eppendorf tubes (Eppendorf UK Ltd, Stevenage, UK), and immediately refrigerated at 4^{o}C.

3.2.3. Clinical information on the canine participants

Clinical information regarding the dogs was also collected. This included:

- Breed
- Age
- Sex and neuter status
- Body weight (kilograms)
- Body condition score 0-9 (Laflamme, 1997)
- Presence of CCLR, and whether partial or complete CCLR
- Presence of meniscal injury, location and type (Bennett and May, 1991)
- Presence of patella luxation
- Length of time of lameness
- Co-morbidities
- Medication being received by the dog
- Radiographic level of OA in the stifle joint: Two scales for OA were used. A scale of 0-10, including a global assessment of OA (0-3), level of joint effusion (0-2), osteophytosis (0-3) and intra-articular mineralisation (0-2) (Innes *et al*., 2004), and a 45 point scale examining 15 separate areas on mediolateral and craniocaudal radiographic views developed by Mager and Matis and Colleagues (Wessely *et al*., 2017) (Supplementary material 5).

3.2.4. Synovial fluid processing

SF samples were transported on ice from the veterinary practices to the laboratory at the University of Liverpool, Leahurst Campus within 48 hours of collection. Samples stored for longer than 48 hours before processing were excluded from the study based on previous unpublished data examining changes in the synovial fluid with elongated refrigerated storage time (Chapter 2). Samples were centrifuged at 2540*g* at four °C for five minutes. The supernatant was pipetted into 200 µl aliquots, and snap frozen in liquid nitrogen before storing at -80°C (Anderson *et al*., 2020).

3.2.5. NMR Metabolomics

3.2.5.1. Sample preparation for NMR metabolomics

SF samples were thawed on ice immediately prior to sample preparation for NMR spectroscopy. 100µl of synovial fluid was then diluted with 100µl of a buffer master mix containing 200mM sodium phosphate (NaH_2PO_4, SigmaAldrich, Gillingham, UK) pH 7.4 in 20% deuterium oxide (^2H_2O, SigmaAldrich) and 2.4mM sodium azide (NaN_3, SigmaAldrich). Samples were vortexed using Vortex-Genie® 2 Shaker (Scientific Industries, New York, USA) for 30 seconds, centrifuged at 12000*g* at 4°C for 5 minutes, and the supernatant transferred into a 3mm outer diameter NMR tubes using a glass Pasteur pipette.

3.2.5.2. NMR metabolomics spectral acquisition

Spectra were acquired using a 700MHz Bruker Avance III spectrometer (Bruker Corporation, Billerica, Massachusetts, USA) with associated triple resonance inverse (TCI) cryoprobe and chilled Sample Jet auto-sampler. Software used for spectral acquisition and processing were Topspin 3.1 (Bruker Corporation, Billerica, Massachusetts, USA) and IconNMR 4.6.7 (Bruker Corporation).

1D ^1H NMR spectra were acquired using a Carr-Purcell-Meiboom-Gill (CPMG) filter to suppress background signal disturbances from proteins and other endogenous constituents, and allow acquisition of small molecule metabolite signals (Carr and Purcell, 1954, Meiboom

and Gill, 1958). A CPMG-1r vendor pulse sequence was used to achieve this. Water suppression was carried out by pre-saturation (Hoult, 1976). The CPMG spectra were acquired at 37 °C with a 15ppm spectral width, a four second interscan delay and 32 transients (Anderson *et al*., 2020).

Samples were ran in the NMR spectrometer over two batches, with the buffer master-mix used to prepare samples for NMR being the same for both batches (stored at -20°C between batches), and the same spectrometer and experimental conditions used for both batches to minimise any batch effect.

3.2.5.3. NMR metabolomics spectral quality control

1D ^{1}H NMR spectra were individually assessed to ensure minimum reporting standards were met (Sumner *et al*., 2007). These steps for quality control included:

- Assessment of the baseline, ensuring minimal curvatures or deviations in the baseline.
- Assessing quality of water suppression, with water peak at 4.7ppm being no more than 0.4ppm wide.
- Alignment of spectra to glucose beta anomeric doublet at 5.24.
- Measurement of the line-width half height (LWHH) of reference peak, in this case glucose peak at 5.24 ppm. Any spectrum where the width of this peak measured at the half height of the peak exceeded more than one standard deviation from the mean was regarded as failing quality control. Glucose was used as a reference peak in this case as sodium trimethylsilyl propionate (TSP), commonly added to samples to act as a reference peak, is not indicated for use in SF due to the interference it can cause by binding to proteins such as albumin (Kriat *et al*., 1992).

Any samples that were deemed to have failed quality control were re-ran on the spectrometer up to a maximum of three spectral acquisitions. Any that failed after the third spectral acquisition were totally excluded from the study.

3.2.5.4. Metabolite annotation and identification

The NMR spectra were divided into spectral regions (termed "bins") using Topspin 3.1 (Bruker Corporation, Massachusetts, USA), with each bin represented either single metabolite peaks or multiple metabolite peaks where peaks overlapped on the spectra. These bins were also examined using TameNMR (hosted by www.galaxy.liv.ac.uk), a software for NMR spectral processing. Bins were altered accordingly upon visualising the fit to the overlaid spectra to ensure the area under the peak was represented by the bin.

Metabolites were annotated to the spectra using Chenomx NMR Suite Profiler version 7.1 (Chenomx, Edmonton, Canada), a reference library of 302 mammalian metabolite NMR spectra. When metabolite peaks overlapped, multiple metabolites were annotated to the bin.

When peaks were unable to be annotated to a metabolite, they were classed as being an "unknown" metabolite. Previous literature specifying metabolite chemical shifts and spectral appearance were examined to aid with annotating any unknown areas. Downstream unique peak metabolite identification and in-house NMR metabolite standards were examined to confirm metabolite identities where possible.

A pattern file was created of the spectral bins and metabolite annotated to that bin. This is a spreadsheet outlining the bin boundaries in ppm, and the metabolites annotated to that bin (Pattern file included in supplementary material S.6). The pattern file and the Bruker spectra files were input into TameNMR (galaxy.liv.ac.uk), in order to create a spreadsheet of binned spectra, with the relative intensities of each bin for each sample, which could then be used for statistical analysis of the spectra.

3.2.6. NMR Lipidomics

3.2.6.1. Sample preparation for NMR lipidomics

Canine SF samples were thawed on ice, and separated into 100 µl aliquots. Aliquots were snap frozen in liquid nitrogen, and lyophilised overnight until completion. Lyophilised samples were then reconstituted in 200µl deuterated chloroform ($CDCl_3$, SigmaAldrich), and incubated on ice for five minutes. Samples were then vortexed for 30 seconds and centrifuged at 21,500 x *g* and 4°C for five minutes. Using a glad Pasteur pipette, 200µl was then transferred to a 3mm outer diameter clean NMR tube.

3.2.6.2. NMR lipidomics spectral acquisition

Spectra were acquired using the same spectrometer and software as previously stated above. 1D ^{1}H NMR spectra were acquired using a Nuclear Overhauser Effect Spectroscopy (NOESY) (Kaiser, 1963) pulse sequence at 37 °C with a 15ppm spectral width, a four second interscan delay and 32 transients.

3.2.6.3. NMR lipidomics spectral quality control

Spectra were aligned to a chloroform peak at 7.26ppm, and underwent quality control, ensuring flat baseline, and a LWHH of the chloroform peak at 7.26ppm not exceeding one SD of the mean (Sumner *et al*., 2007).

3.2.6.4. Lipid annotation and identification

Lipid spectra were divided into bins in the same manner as the metabolite spectra above. Lipid annotation was completed using previous literature and theses (Cheung and Olson, 1990, Ulrich *et al*., 2007, Kosinska *et al*., 2013, Morgan, 2019) as well as an online lipid spectra library (https://lipidlibrary.aocs.org/lipid-analysis/nmr).

3.2.7. Statistical analysis

3.2.7.1. Sample size power calculation

Sample size power calculations were completed using a previous unpublished small cohort study (n=5 with CCLR and meniscal injury and n=7 with CCLR without meniscal injury), with a specified FDR or 0.05. These calculations were completed using MetaboAnalyst 5.0 (https://www.metaboanalyst.ca), a software based on a metabolomics data analysis package written in R (the MetaboAnalystR package) (Pang *et al*., 2021).

3.2.7.2. Differences in clinical features of the canine participants

Analysis of the differences in clinical features between the groups in terms of age, sex and neuter status, body condition score, and radiographic OA score was carried out using one-way analysis of variance (ANOVA) with Benjamini-Hochberg false discovery rate (FDR) adjustment, and significance set at $p<0.05$. Where any variable did not fit to ANOVA

assumptions of having a common variance, Brown-Forsythe and Welch ANOVA tests with Benjamini-Hochberg FDR adjustment was carried out. These analyses and creation of graphs to visualise this data was carried out using GraphPad Prism 9.1.0 (GraphPad Software, San Diego, CA, USA).

3.2.7.3. Metabolomics data analysis

- Metabolomics data was normalised using probabilistic quotient normalisation (PQN) (Dieterle *et al*., 2006), and pareto scaled using R prior to statistical analysis.
- Unsupervised multivariate analysis was carried out using principle component analysis (PCA) on the normalised and scaled data using R (R Core Team, 2020).
- The variance between canine phenotypes was investigated through analysis of principal components 1 through 10 using One-Way ANOVAs or linear models depending on the data type. Briefly, CCLR, sex, neuter status, BCS, radiographic OA score and batch were numerically encoded and assessed against each principal component using a One-Way ANOVA. Age, Length of time of lameness, weight, length of time of storage pre-processing which were already numeric variables were assessed against each principal component using a linear model. All p values were corrected using FDR (Bejamini Hochberg) correction. The function written to perform the assessment of variance between phenotypes and principal components is included in supplementary material (S.7). Correlation matrices between phenotypes were computed using the spearmans correlation using the *cor* function in R and visualised using a heatmap generated with the *pheatmap* function in R (Kolde, 2012).
- Univariate analysis was carried out using One-Way ANOVAs and One-Way ANCOVAs. To account for multiple testing across all 236 metabolite bins FDR correction was applied to the F-Test p value of each metabolite, significance was accepted at $p < 0.05$. For metabolites with an FDR < 0.05 Tukey's honest significant difference post-hoc test was applied to assess between group variances. Age adjusted One-Way ANCOVAs were applied to each metabolite to assess differences between meniscal and no meniscal injury, FDR adjustment was applied as a above. Univariate analysis was undertaken on R. Boxplots to visualise the changes in metabolite abundances were created in MetaboAnalyst 5.0 (https://www.metaboanalyst.ca), a software based on a metabolomics data analysis package written in R (the MetaboAnalystR package) (Pang *et al*., 2021).

3.2.7.4. Lipidomics data analysis

- Lipid spectra were normalised to the chloroform peak at 7.26ppm, and pareto scaled prior to analysis.
- Multivariate analysis was performed using PCA, and heirarchical clustering using Euclidean distancing and Ward's Linkage clustering algorithm, shown as a heatmap.
- Univariate analysis was performed by students *t*-test, with FDR adjusted p-values and significance set to $p<0.05$. Volcano plots were used to examine fold changes alongside p-values.
- All these analyses were completed using Metaboanalyst 5.0 (Pang *et al*., 2021).

3.3. Results

3.3.1. Sample size power calculations

Results of the power calculations revealed a sample size of 60 per group would give a predictive power of 0.83 when plotted on a predictive power curve (Figure 3.1).

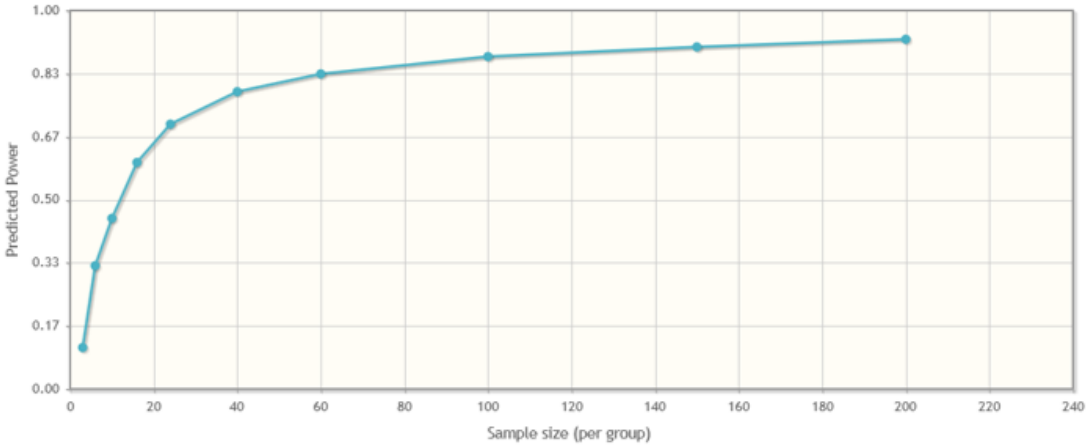

Figure 3.1. Plot of the predictive power curve use to calculate sample size for the nuclear magnetic resonance metabolomic study of biomarkers of meniscal injury in canine stifle joint synovial fluid with cranial cruciate ligament rupture. *Maximum sample size of 200 samples is shown. n=60 per group gives a predictive power of 83%.*

3.3.2. Clinical features of the canine participants

For the metabolomic study, 191 samples of canine stifle joint synovial fluid were collected and submitted for NMR spectroscopy. Of these, 14 samples had been stored for longer than 48 hours prior to collection for processing, and so were excluded from the study. Four samples were from cases in which the meniscal injury status was unknown, and so were excluded from the study. Nineteen samples were excluded as they failed to meet minimum reporting standards (Sumner *et al*., 2007) after three spectral acquisitions.

In total, 154 canine stifle joint synovial fluid samples were included in the statistical analysis. These were divided into three groups, namely CCLR without meniscal injury (n=72), CCLR with meniscal injury (n=65), and control group with neither CCLR or meniscal injury present (n=17). The control group consisted of 13 cases of patella luxation, three cases from arthrocentesis of the stifle joints during lameness investigations which subsequently were found to have no pathology, and one sample from a case with fraying of the caudal cruciate ligament. Information regarding the signalment of the dogs in each group is shown in Table 3.1.

There was a significant difference between the control group and the CCLR groups with or without meniscal injury in terms of age, weight, and radiographic OA score, but not with BCS (Figure 3.2).

Table 3.2: Table to show clinical features of the canine participants included in the nuclear magnetic resonance metabolomic study of biomarkers of meniscal injury in canine stifle joint synovial fluid with cranial cruciate ligament rupture.

	Group		
	Control (no CCLR, no meniscal injury)	**CCLR without meniscal injury**	**CCLR with meniscal injury**
Sample size (*n*)	17	72	65
Age, years (mean [SD])	3.8 (2.9)	5.9 (2.9)	6.8(2.8)
Weight, kg (mean [SD])	17.5(12.0)	30.4(15.1)	27.1(13.7)
Sex, n (%)	FE=2 (12%) FN=3 (18%) ME=7 (41%) MN=5 (29%)	FE= 8 (11%) FN=28 (29%) ME=5 (7%) MN=30 (42%)	FE= 7 (11%) FN=26 (40%) ME=12 (19%) MN=18 (28%)
BCS, 1-9 (mean [SD])	5.5 (1.4)	5.9(1.4)	6.0(1.4)
Radiographic OA score (0-10) (Innes *et al*., 2004) (mean [SD])	2.8 (1.0)	4.4 (1.8)	4.6(1.7)
Radiographic OA score (0-45, mean [SD])(Wessely *et al*., 2017)	2(2.2)	6.7(6.1)	7.3(5.1)
Length of time of lameness, months (mean [SD])	4.0 (5.2)	2.8(2.7)	2.8(3.0)
Partial vs complete CCLR, *n*	N/A	Partial =29 Complete=42 Unknown=1	Partial =9 Complete=55 Unknown=1

Abbreviations= Cranial cruciate ligament rupture (CCLR), female entire (FE), female neutered (FN), male entire (ME), male neutered (MN), body condition score (BCS), kilograms (kg) standard deviation (SD), osteoarthritis (OA), not applicable (N/A)

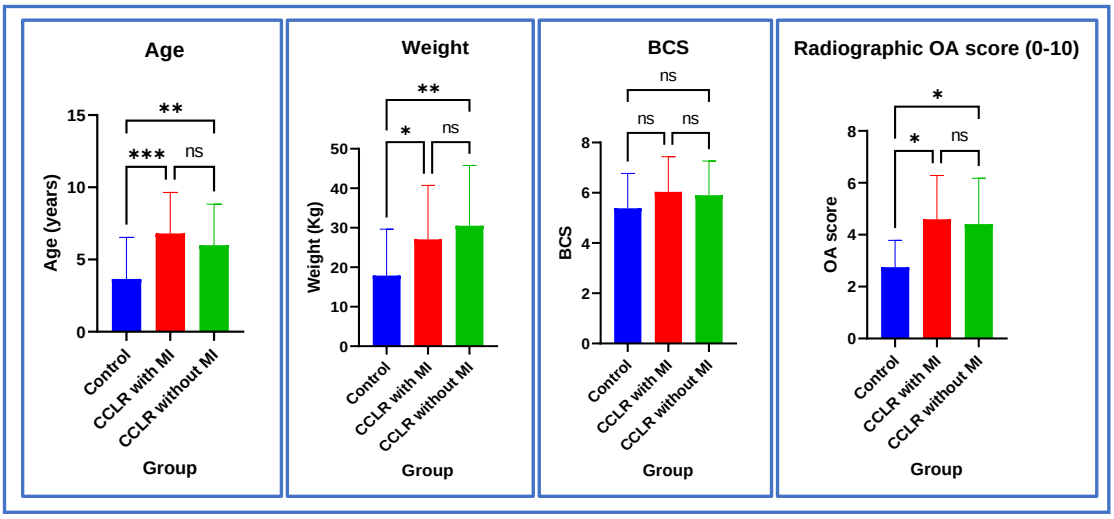

Figure 3.2. Column Bar graphs (mean and standard deviation) to show differences in clinical features of the canine participants between groups in the nuclear magnetic resonance metabolomic study of biomarkers of meniscal injury in canine stifle joint synovial fluid with cranial cruciate ligament rupture. *(CCLR=cranial cruciate ligament disease, MI=meniscal injury, OA= osteoarthritis, *=p<0.05, **=p<0.01, ***=p<0.0001)*

3.3.3. Metabolite annotation and identification.

Spectra were divided into 246 bins. Of these, 84 remained with an unknown metabolite identification, and 162 (66% of bins) were annotated to one or more metabolites. In total, 64 metabolites were annotated to the spectra (Table 3.2). The pattern file of these bins and metabolite annotations is included in the supplementary information (S6). Any bins containing ethanol peaks were excluded from the statistical analysis, due to ethanol being considered a contaminant in NMR, usually either during the collection of the synovial fluid from the sterilisation of skin with surgical spirit, or during the processing steps (van der Sar *et al*., 2015). Propylene glycol, a metabolite found in solvents used in pharmaceuticals (Zar *et al*., 2007) was found in one spectrum, and so those bins were excluded so as to not bias the statistical analysis.

Table 3.3. Metabolites annotated to canine stifle joint synovial fluid nuclear magnetic resonance spectra, including HMDB identification number where possible.

AMINO ACIDS		**FATTY ACIDS AND ORGANIC ACIDS**	
2-AMINOADIPATE	HMDB0000510	2-HYDROXYVALERATE	HMDB0001863
ALANINE	HMDB00161	2-METHYLGLUTARATE	HMDB0000422
ALLOISOLEUCINE	HMDB0000557	2-PHENYLPROPIONATE	HMDB0011743
BETAINE	HMDB0000043	3 HYDROXYISOVALERIC ACID	HMDB0000754
CREATINE	HMDB00064	4-PYRIDOXATE	HMDB0000017
CREATINE PHOSPHATE	HMDB0001511	AZELATE	HMDB0000784
CREATININE	HMDB00562	CARNITINE	HMDB00062
CREATININE PHOSPHATE	HMDB0041624	CITRATE	HMDB00094
GLUTAMINE	HMDB0000641	FORMATE	HMDB0000142
GLUTAMINE	HMDB00641	GLUTAMATE	HMDB0060475
HISTIDINE	HMDB0000177	GLYCOCHOLATE	HMDB0000138
ISOLEUCINE	HMDB00172	GLYCOLATE	HMDB0000115
LEUCINE	HMDB00687	GLYCYLPROLINE	HMDB0000721
LYSINE	HMDB00182	ISOBUTYRIC ACID	HMDB0001873
METHIONINE	HMDB00696	LACTATE	HMDB00190
PHENYLALANINE	HMDB0000159	METHYLSUCCINATE	HMDB0001844
THREONINE	HMDB00167	MOBILE LIPIDS	
TYROSINE	HMDB0000158	PYRUVATE	HMDB00243
VALINE	HMDB00883	SEBACATE	HMDB0000792
		THYMOL	HMDB0001878
SUGARS		**OTHERS**	
FRUCTOSE	HMDB0000660	3-HYDROXY-3-METHYLGLUTARATE	HMDB0041199
GALACTOSE	HMDB0000143	ACETAMINOPHEN	HMDB0001859
GLUCITOL	HMDB0000247	ACETONE	HMDB0001659
GLUCOSE	HMDB0000122	ACETYLCHOLINE	HMDB0000895
MANNITOL	HMDB0000765	CHOLINE	HMDB0000097
MANNOSE	HMDB0000169	DIMETHYL SULFONE	HMDB0004983
MYOINOSITOL	HMDB00211	DTTP	HMDB0001342
		ETHANOL	HMDB0000108
		HISTAMINE	HMDB0000870
		IBUPROFEN	HMDB0001925
		O-CRESOL	HMDB0002055
		P-CRESOL	HMDB0001858
		PI-METHYLHISTIDINE	HMDB00001
		PROPYLENE GLYCOL	HMDB0001881
		SN-GLYCERO-3-PHOSPHOCHOLINE	HMDB00086
		TAU-METHYLHISTIDINE	HMDB0000479
		TRIGONELLINE	HMDB0000875
		XANTHINE	HMDB0000292

HMDB=Human metabolome database

3.3.4. Metabolomic statistical analysis results

3.3.4.1. Multivariate analysis of canine synovial fluid with respect to CCLR and meniscal injury status

Firstly, multivariate PCA was undertaken exploring all samples depending on CCLR and meniscal injury status, divided into the following groups: partial CCLR with meniscal injury, complete CCLR with meniscal injury, partial CCLR without meniscal injury, complete CCLR without meniscal injury and no CCLR or meniscal injury (control group) (Figure 3.3).

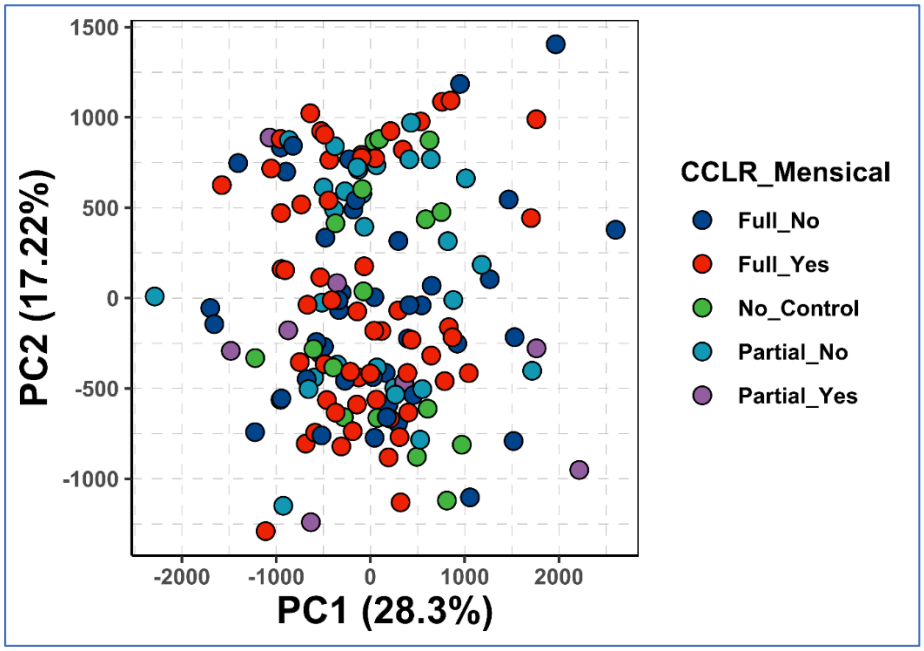

Figure 3.3. Principle component analysis 2D scores plot of samples of canine stifle joint synovial fluid after nuclear magnetic resonance spectroscopy, divided into groups dependant on cranial cruciate ligament rupture and meniscal injury. *Clustering of samples is evident between groups with full cranial cruciate ligament rupture (CCLR) or partial CCLR with or without meniscal injury, and groups with neither CCLR or meniscal injury (control group).*

Principle component analysis was then also undertaken examining differences in the overall metabolomic profiles when just considering the presence of either complete CCLR, partial CCLR or no CCLR (Figure 3.4a) and considering CCLR and meniscal injury status against the control group (Figure 3.4b). Again, when examining the data over the first two principal

components, there is clustering of these groups suggesting little overall difference in the metabolomic profiles.

From these PCA plots, it can be inferred that principal components one and two are relatively uninformative when investigating metabolomic changes in the dataset based on CCLR and meniscal injury status within the dataset.

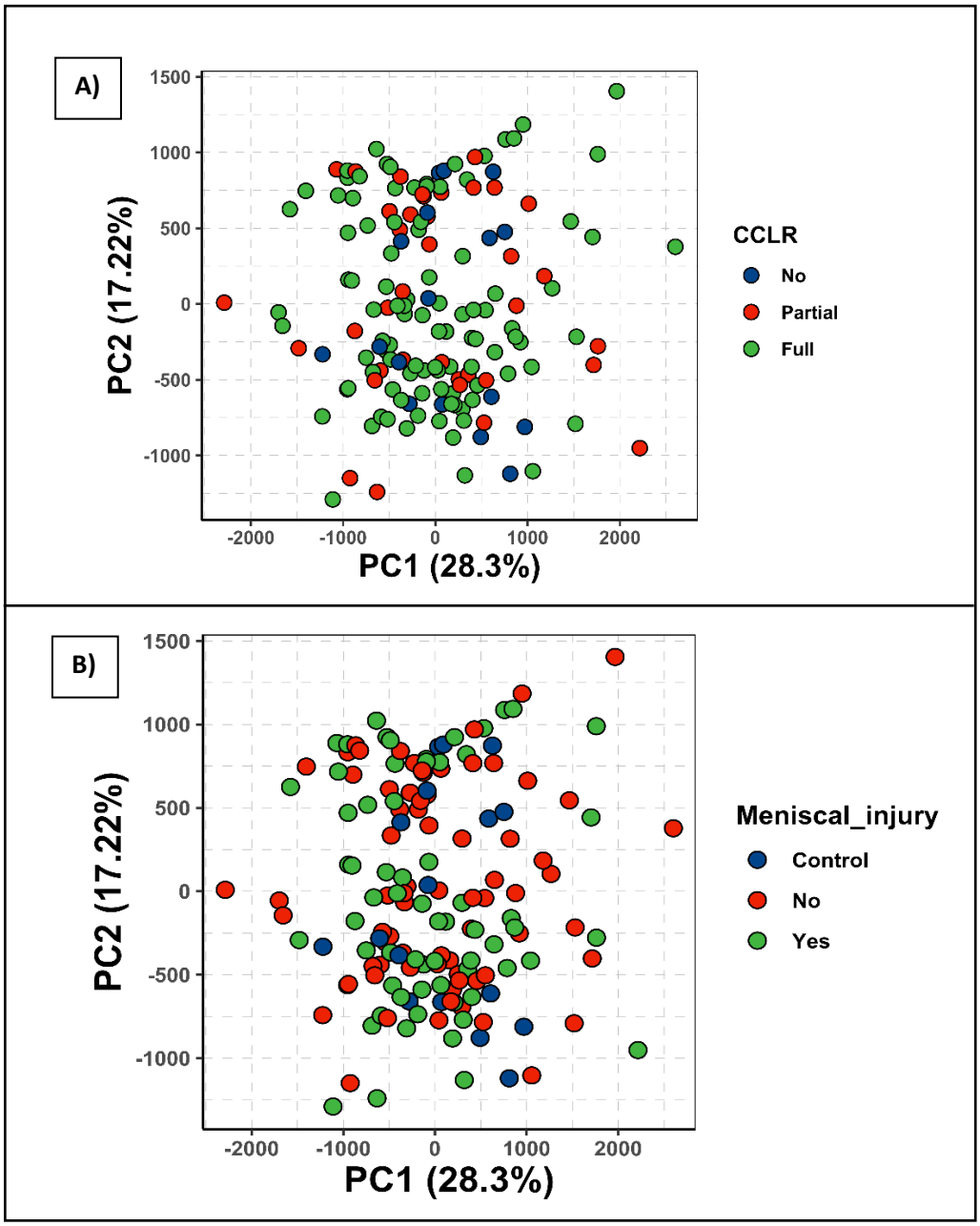

Figure 3.4. Principle component analysis 2D scores plot of samples of canine stifle joint synovial fluid after nuclear magnetic resonance spectroscopy depending on A) cranial cruciate ligament rupture (CCLR) status (either full, partial or none), and B) meniscal injury status. *(control=no CCLR, no meniscal injury, No=CCLR without meniscal injury, Yes=CCLR with meniscal injury).*

Due to the amount of confounding clinical variables between groups, the association between phenotype and principal components (PC) within the PCA was investigated. Figure 3.5 shows a heatmap visualising associations between different phenotypes and PC one to ten. From this heatmap, we can infer that PC three and four are primarily associated with CCLR and meniscal injury. Figure 3.6b shows PCA examining changes in the metabolomic profiles between groups with CCLR, with and without meniscal injury, and the control group (no CCLR and no meniscal injury), when plotted against PC three and four. The level of CCLR (partial, complete or none) was also investigated using PCA over PC three and four (Figure 3.6a). Here, we start to see some separation of the control group (with is homologous to the no CCLR group) compared to the other groups with CCLR with or without meniscal injury over these PCs.

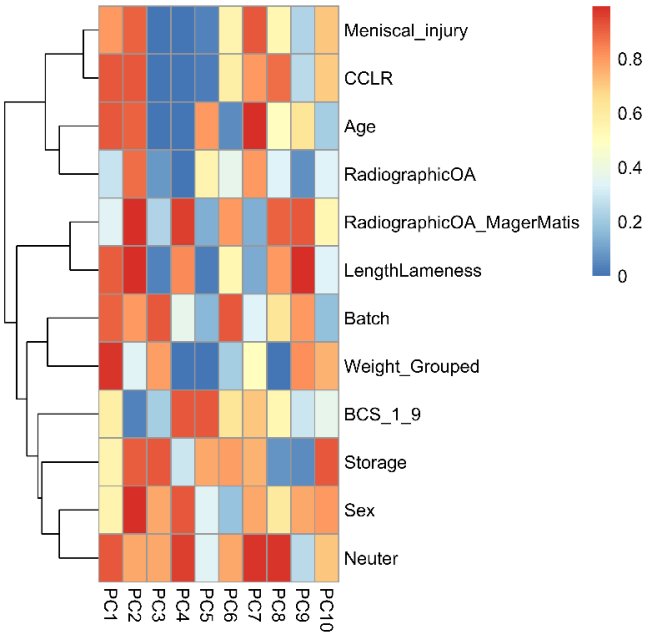

Figure 3.5. Heat map showing association of clinical features of dogs whose synovial fluid was submitted for metabolomic analysis in the study with the first ten principal components in a principal component analysis. *The key on the right denotes FDR corrected p-values from 0 (blue) to 1 (red). Meniscal injury and cranial cruciate ligament rupture (CCLR) appear to be associated primarily with principal components (PC) three to five. (OA= osteoarthritis, BCS= body condition score, Radiographic OA= global assessment of radiographic OA score (0-3), RadiographicOA_MagerMatis= Mager and Matiss et al. radiographic osteoarthritis score (0-45), LengthLameness= length of time of lameness, Storage= time stored at four degrees Celsius prior to processing and freezing).*

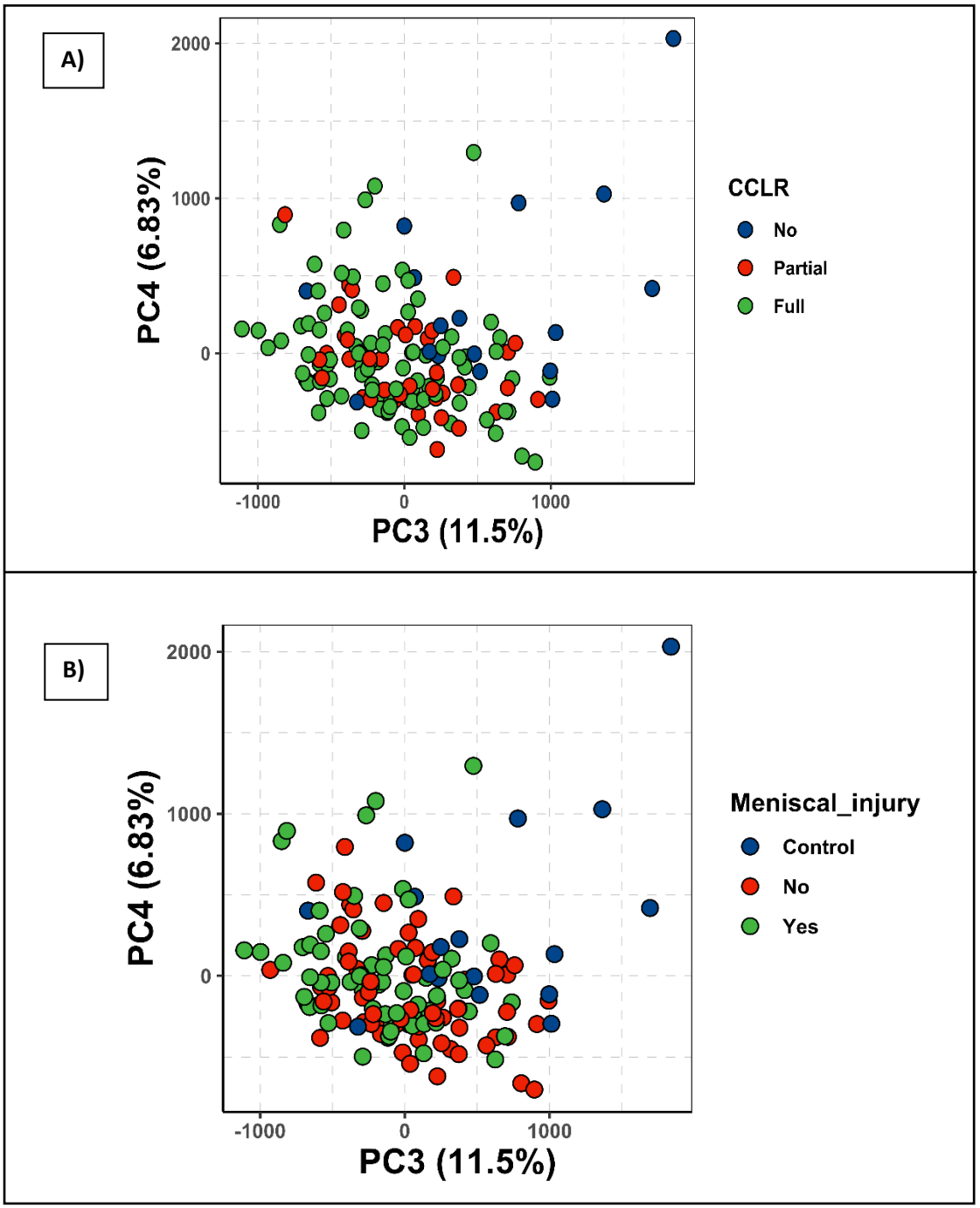

Figure 3.6. Principal component analysis 2D scores plot showing changes in the metabolomic profiles of canine stifle joint synovial fluid depending on A) the presence and type of cranial cruciate ligament rupture (CCLR Full, Partial, No), and B) the presence of meniscal injury *(Yes= CCLR with meniscal injury, No=CCLR without meniscal injury, Control = No CCLR and no meniscal injury) over principal components three and four. There is a separation of control group samples (no CCLR, no mensical injury) from the other groups indicating a difference in the overall metabolome in these samples.*

These findings using multivariate analysis correlated with findings of univariate analysis using ANOVA with Tukey's HSD *post-hoc* analysis to examine significant differences between the type of CCLR (partial, full or none). No significant difference was found between partial and full CCLR groups, but a significant difference between both partial or full CCLR, and the no CCLR group. This was also the case when examining CCLR with meniscal injury, CCLR without meniscal injury and no CCLR or meniscal injury. Therefore, the control group appears to have a differing metabolome from the other two groups.

3.3.4.2. Metabolomic analysis of canine synovial fluid with respect to CCLR status

Univariate analysis using a one-way ANOVA with FDR adjusted p-values and Tukey's HSD *post-hoc* test was carried out on all spectral bins against groups partial CCLR, full CCLR and no CCLR, to examine whether any differences existed in the metabolome depending on type or level of CCLR. No significant metabolites were found to exist between complete or partial CCLR groups. Due to both multivariate and univariate analysis demonstrating no significant changes depending on whether the CCLR was partial or complete, the examination of groups with CCLR was not subdivided further into partial or complete CCLR.

A limitation of the confounding clinical variables that are statistically significantly different between the control group and other groups, is that it is not possible to accurately state whether the changes seen between the control group and others is related to the presence of CCLR, or due to the confounding clinical variables. There were 45 spectral bins, relating to 15 metabolites that were found to be significantly altered with the presence of CCLR compared to the control group. Metabolites significantly ($p<0.05$) increasing or decreasing between groups with CCLR vs control were:

- Increased with CCLR: Glutamine, pi-methylhistidine, mobile lipids, lysine, isoleucine, sn-glycero-3-phosphocholine
- Decreased with CCLR: Glutamate, betaine, glycerol, lactate, formate, tyrosine, phenylalanine, methanol, unknown.

However, analysis of metabolite changes with respect to clinical variables also found significantly altered metabolites with differing age, weight and OA score. It is therefore not possible to accurately assess the changes with regard to CCLR versus the control group, due

to the differences between the clinical variables in the control group versus the other groups and the small sample size in the control group compared to the other groups.

3.3.4.3. Metabolomic analysis of canine synovial fluid with respect to clinical features of the canine participants

With multivariate and univariate analysis revealing changes in the metabolomic profile of SF when grouping by CCLR status, changes in the metabolome based on differing clinical variables was examined. As the group without CCLR or meniscal injuries was found to be statistically different in terms of weight, age and OA level as well as in terms of CCLR and meniscal injury status, the ability to analyse the control group when comparing CCLR and meniscal injury status alone without confounding variables was explored. Although medications the dogs were receiving was recorded at the time of surgery, these were too sparse to be able to effectively group for analysis, with the majority of dogs receiving meloxicam with or without paracetamol and codeine, and others receiving carprofen, robenacoxib, tramadol, amantadine and/or gabapentin. The breed of dog was not analysed due to their being too many breed types to analyse effectively, although dogs were grouped by weight bracket. All samples with CCLR with or without meniscal injury were analysed against clinical variables of the dogs. Control group samples were removed to control for CCLR status due to findings of multiple metabolite differences in the SF between dogs with CCLR and those without CCLR (section 3.3.3.2.). Correlation between the clinical variables is shown in Figure 3.7. Amongst the correlations include a positive relationship with both OA scoring methods, showing a good agreement with these methods in the study.

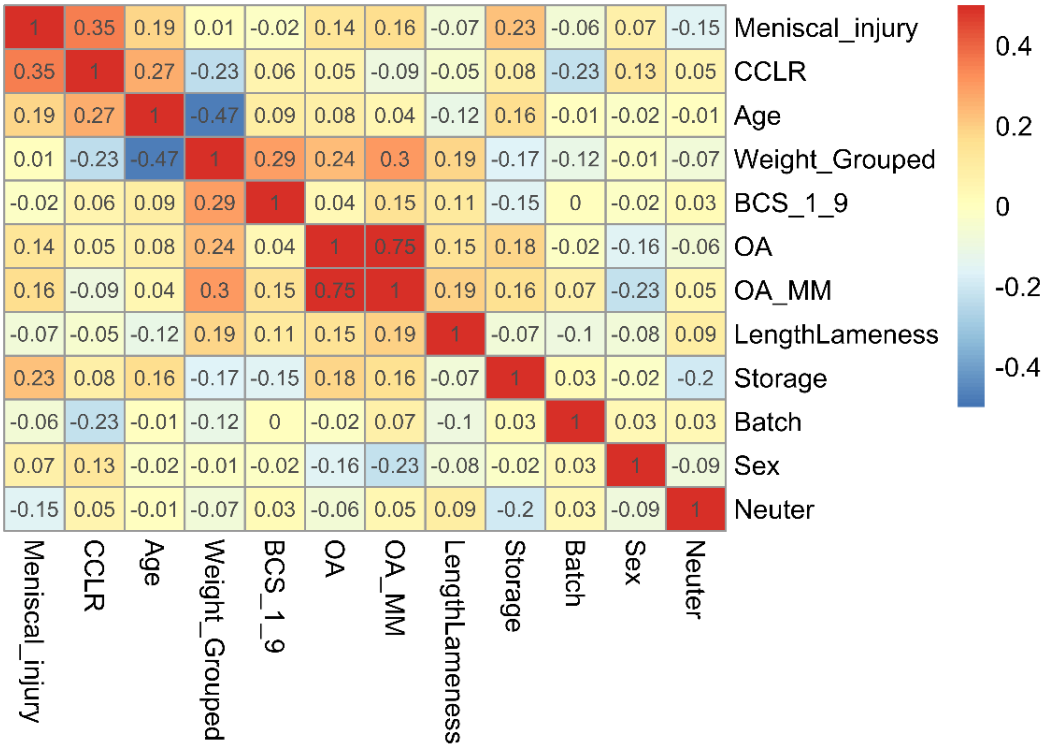

Figure 3.7. Correlation matrix showing relationship between clinical variables analysed from samples of canine stifle joint synovial fluid. *Key on the right shows colour scale from minus 0.5 to plus 0.5 relating to positive or negative relationships where one is completely related and minus one is completely unrelated. CCLR=Cranial cruciate ligament rupture, BCS= body condition score, OA= global assessment of radiographic osteoarthritis score (0-3), OA_MM= Mager and Matiss and colleague's radiographic osteoarthritis score (0-45), LengthLameness= length of time of lameness, Storage= time stored at four degrees Celsius prior to processing and freezing.*

3.3.4.3.1. Bodyweight

Univariate analysis examining changes in metabolite concentrations revealed 33 significantly altered spectral bins over all groups, with the majority of changes being between the group of dogs less than 10kg and other groups. Glutamine, sn-glycero-3-phosphocholine, threonine, formate, creatine, dimethyl sulfone, acetate and unknown metabolites were found to be significantly altered with increasing bodyweight. Boxplots of these changes are shown in Figure 3.8.

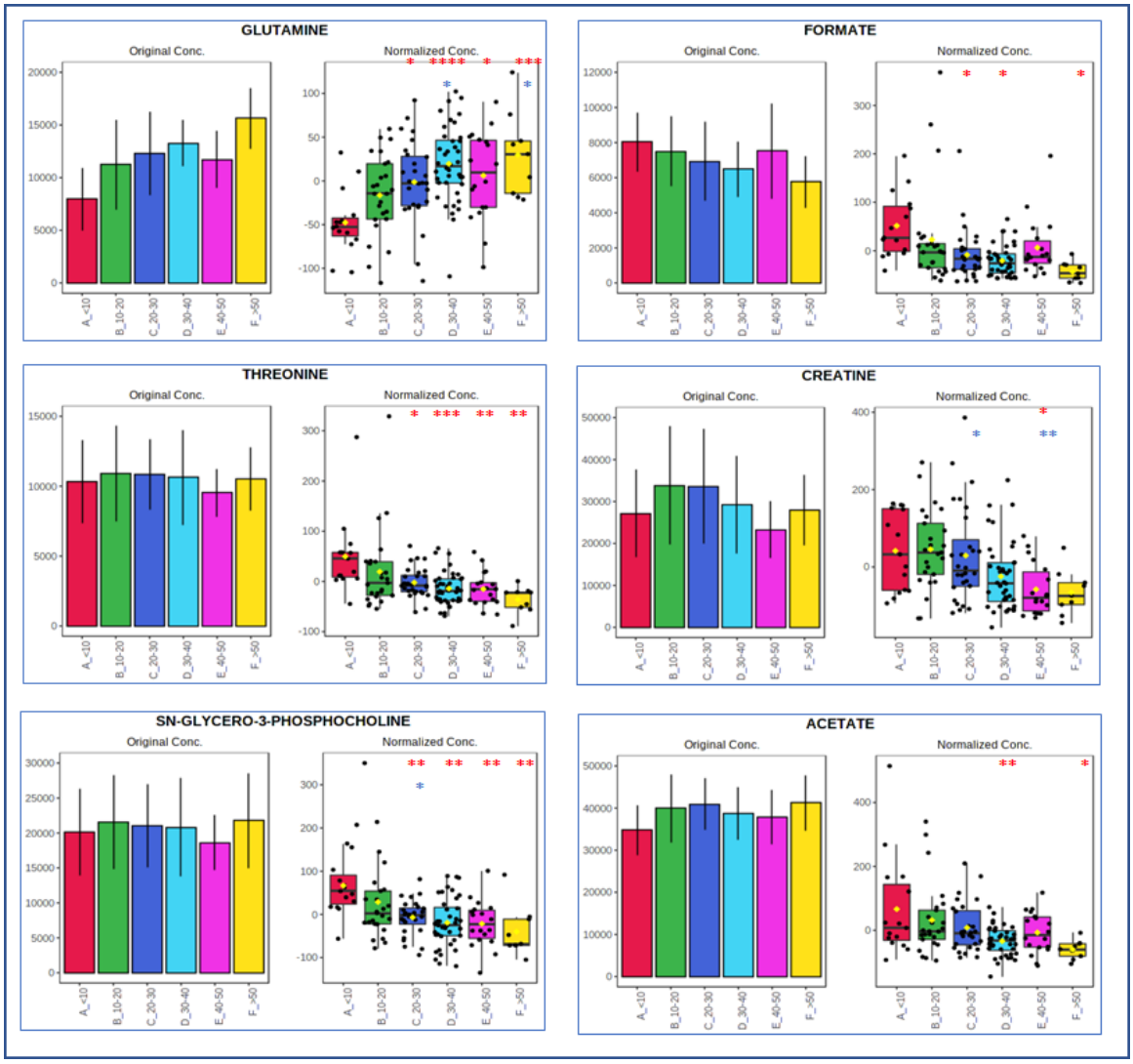

Figure 3.8. Bar plots and box and whisker plots showing changes in metabolites with increasing body weight in canine stifle joint synovial fluid from dogs with cranial cruciate ligament rupture. *Bar plots on the left show the original values (mean +/- SD), and box and whisker plots on the right show the normalised values. The x axis shows the weight groups in Kg. Key to colours of bar charts: Red= <10kg, Green = 10-20kg, Navy blue= 20-30kg, Light blue= 30-40kg, Pink=40-50kg, Yellow= >50kg. Red stars above the boxplots denote significance in comparison with the <10kg group, blue stars above the box plots denote significance in comparison with the 10-20kg group; *=p<0.05, **=p<0.01, ***=p<0.001, ****=p<0.0001.*

3.3.4.3.2. Age

Age groups were divided into young adult (one up to two years), mature adult (two to six years), early senior (seven to nine years), late senior (ten to eleven years) and geriatric (twelve years and over), as per the division of age ranges used by Harvey (2021). 38 bins overall were significantly altered over all age ranges with 20 of these having no known metabolite identification. Metabolites annotated to the remaining 18 bins included four regions of mobile lipid resonances, which increased with increasing age, mannose, glycolate, and glutamine. Boxplots of metabolites significantly altering with different age groups are shown in Figure 3.9.

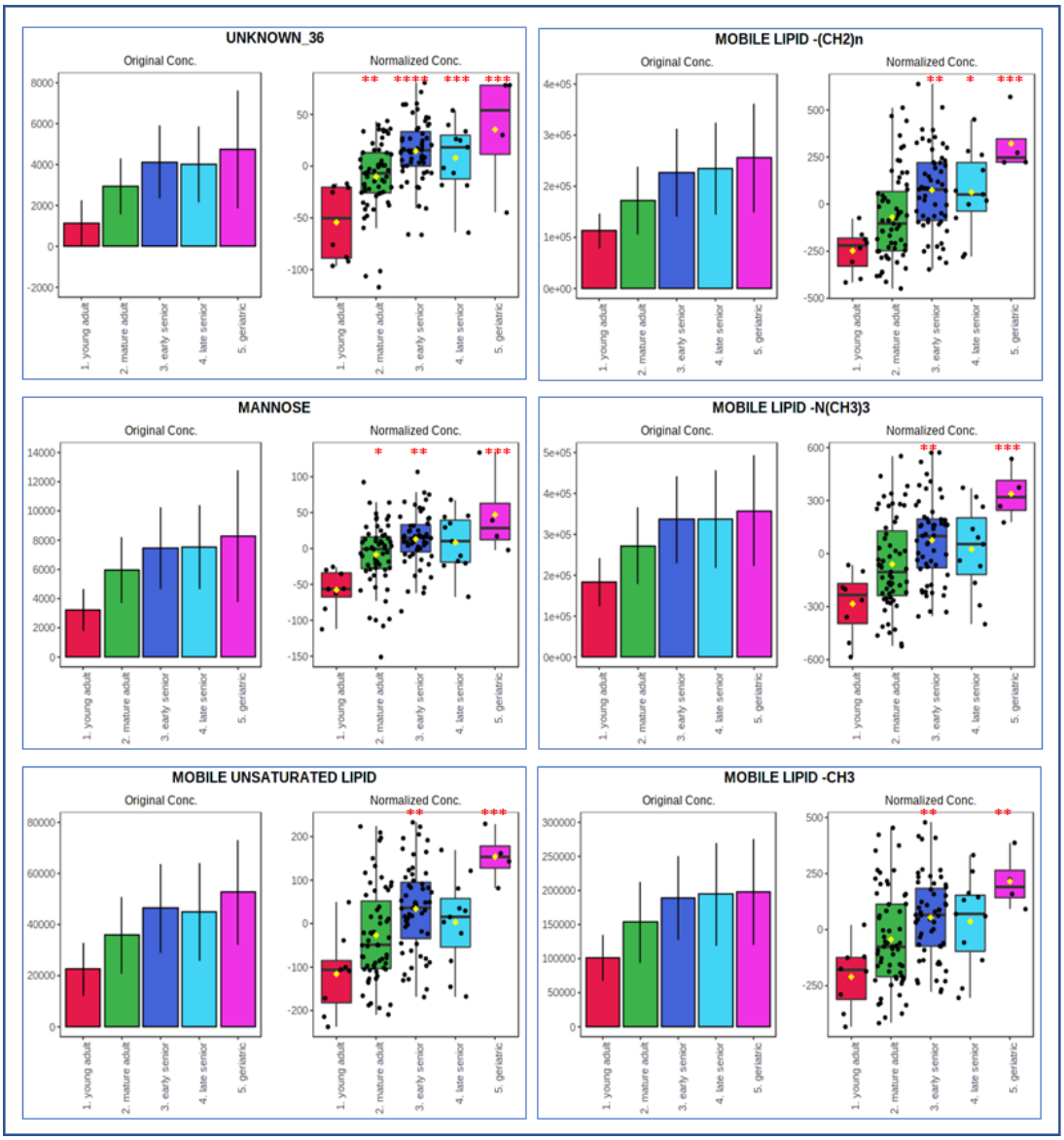

Figure 3.9. Bar plots and box and whisker plots showing changes in metabolites with increasing age of the dog in canine stifle joint synovial fluid from dogs with cranial cruciate

ligament rupture. *Bar plots on the left show the original values (mean +/- SD), and box and whisker plots on the right show the normalised values. The x axis shows the age groups from young adult to geriatric. Key to colours of bar charts: Red=young adult, Green =mature adult, Navy blue=early senior, Light blue=late senior, Pink=geriatric. Red stars above boxplots denote significance in comparison with group 1 (young adult); *=p<0.05, **=p<0.01, ***=p<0.001, ****=p<0.0001.*

3.3.4.3.3. Sex and neuter status

Samples were divided into male entire, male neutered, female entire and female neutered. There were no significantly altered metabolite concentrations when analysed against sex and neuter status, although betaine was trending towards significance with an FDR adjusted p-value of 0.18, due to an increase in male entire dog SF (Figure 3.10).

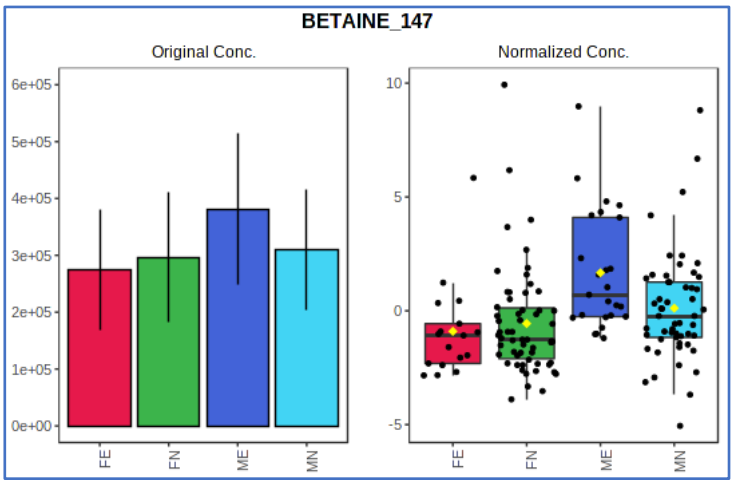

Figure 3.10. Bar plots and box and whisker plots showing changes in betaine levels dependant on sex and neuter status in the canine stifle joint synovial fluid from dogs with cranial cruciate ligament rupture. *Bar plots on the left show the original values (mean +/- SD), and box and whisker plots on the right show the normalised values. The x axis shows sex and neuter status (FE=female entire [red], FN=female neutered [green], ME=male entire [navy blue], MN=male neutered [light blue]).*

3.3.4.3.4. OA score

Samples were divided based on the global assessment of radiographic OA score (0-3), with 0 being no OA, 1=mild OA, 2=moderate OA and 3=severe OA (Innes *et al*., 2004). Another more recent scoring system was also examined based on a 0-45 point scale examining 15 areas on mediolateral and craniocaudal radiographic projections (Wessely *et al*., 2017), however, for statistical analysis with multiple comparisons, the 0-3 scale was chosen as an overall assessment of radiographic OA in the joint. In total 14 bins were significantly altered with OA score. The OA scores zero to one had the most changes with 10 significant bins. Significantly altered metabolites annotated to these areas included threonine, glycerol, citrate, leucine and unknown metabolites. Figure 3.11 shows the changes in metabolite abundances.

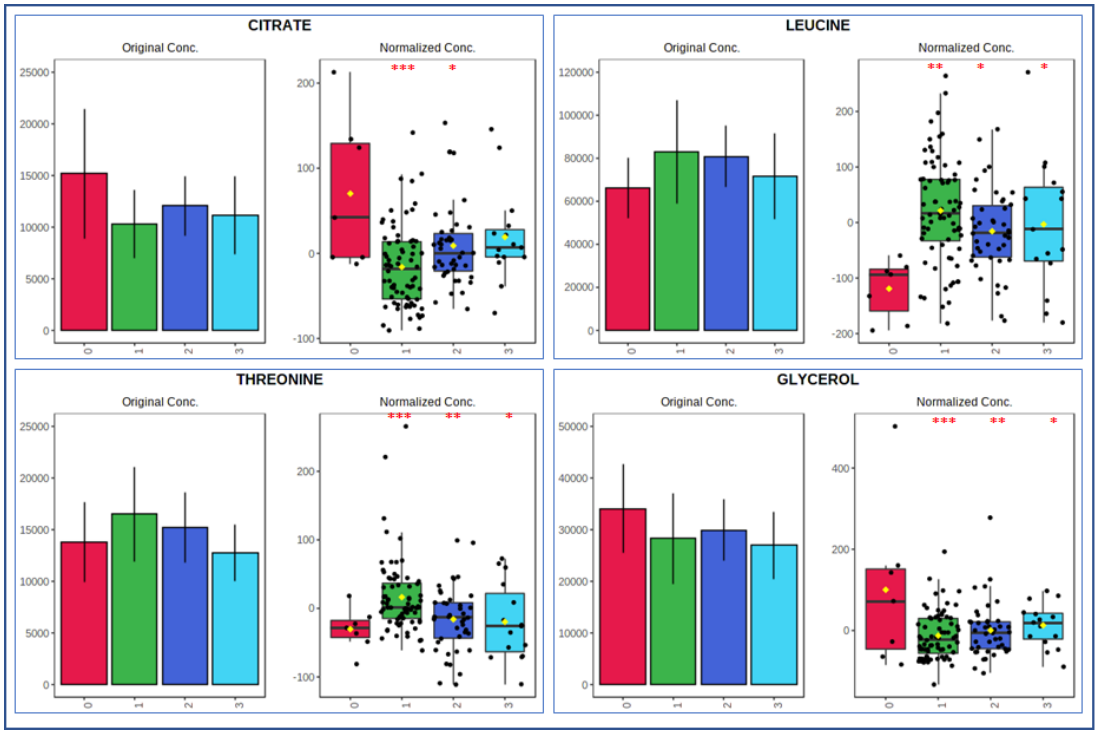

Figure 3.11. Bar plots and box and whisker plots showing changes in metabolites with increasing radiographic osteoarthritis score of the dog in canine stifle joint synovial fluid from dogs with cranial cruciate ligament rupture. *Bar plots on the left show the original values (mean +/- SD), and box and whisker plots on the right show the normalised values. The x axis shows OA scores from 0-3 (Red=0, Green=1, Navy blue=2, Light blue=3). Stars above boxplots denote significance against OA score 0 (*=p<0.05, **=p<0.01, ***=p<0.001).*

3.3.4.3.5. Duration of lameness

Duration of lameness was divided into groups less than one month, one to three months, three to 6 months and 6-12 months. No significantly altered metabolites were found to significantly alter with increasing duration of lameness.

3.3.4.3.6. Body condition score

Changes in metabolite abundances was examined against body condition score (BCS) of the dogs examined using a scale from 1-9 (Laflamme, 1997). Only two dogs had a BCS of three, so these were combined with BCS four, to form a group with a score of three to four. No metabolites were found to significantly alter in the SF with changes in BCS. This was also examined in dogs of each weight group (less than ten kilograms[kg], 20-30kg, 30-40kg, 40-50kg), and no significantly differentially abundant metabolites were found with increasing BCS in each weight group.

3.3.4.3.7. Site of SF sample collection

Samples of canine stifle joint SF were collected from three veterinary hospitals. No significant difference was found with multivariate or univariate analysis when metabolites were compared with site of collection.

3.3.4.4. Metabolomic analysis of canine synovial fluid with respect to meniscal injury status.

When examining clinical variables, none of the variables analysed (age, weight, BCS, sex and neuter status, radiographic OA score) were significantly different between the groups CCLR with meniscal injury and CCLR without meniscal injury.

Multivariate analysis with regards to meniscal injury status was completed using PCA (Figure 3.3b). Samples belonging to groups CCLR with meniscal injury and CCLR without meniscal injury show clustering over the first 10 PCs, showing similarities of the metabolomic profiles in these groups.

Univariate analysis was completed using one-way ANOVA with FDR adjusted p-values and Tukey's HSD *post-hoc* test between the three groups. There were six spectral bins that were below the threshold of significance ($p<0.05$), and two others that neared the threshold ($p<0.06$). Table 3.3 shows these spectral bins, their number on the pattern file, the metabolites annotated to these peaks and the FDR adjusted p-value.

Table 3.3. Table to show nuclear magnetic resonance spectral bins, their chemical shifts and their annotated metabolites that were found to be significantly altered dependent on the presence of meniscal injury in canine stifle joint synovial fluid with cranial cruciate ligament rupture using analysis of variance (ANOVA). False discovery rate (FDR) adjusted p values are shown.

Bin number	Chemical shift (ppm)	Metabolite(s) annotated to bin	FDR adj p-value
145	3.268-3.272	UNKNOWN	0.003991
230	1.071-1.080	METHYLSUCCINATE and 2-METHYLGLUTARATE	0.004215
129	3.362-3.371	METHANOL	0.017345
210	1.936-2.020	GLYCYLPROLINE, ISOLEUCINE and UNKNOWN	0.030997
152	3.203-3.238	MOBILE LIPID -N(CH3)3	0.037435
246	0.789-0.891	MOBILE LIPID -CH3	0.038808
37	5.212-5.353	MOBILE UNSATURATED LIPID	0.050414
224	1.199-1.312	MOBILE LIPID –(CH2)n	0.058996

Figure 3.12 shows these areas on a plot of the NMR spectra, and the identification of mobile lipid peaks based on previous literature (Soininen *et al*., 2009). Figure 3.13 shows boxplots of the abundances of mobile lipids between control, CCLR with and CCLR without meniscal injury.

As it was noted that mobile lipids were also significantly altered with increasing age of the canine participants, ANCOVAs were then also carried out to control for age within the samples. The significance of the metabolites identified using ANOVA retained significance except for the methylsuccinate and/or 2-methylglutarate peak (bin number 230).

As it was not possible to identify whether the peak annotated to methylsuccinate, and/or 2-methylglutarate was correlating with either one or both of these metabolites, ^{1}H ^{13}C 2D NMR spectra was obtained (supplementary material S.8). Unfortunately, the signal of these peaks was too small to distinguish between the two metabolites on this experiment.

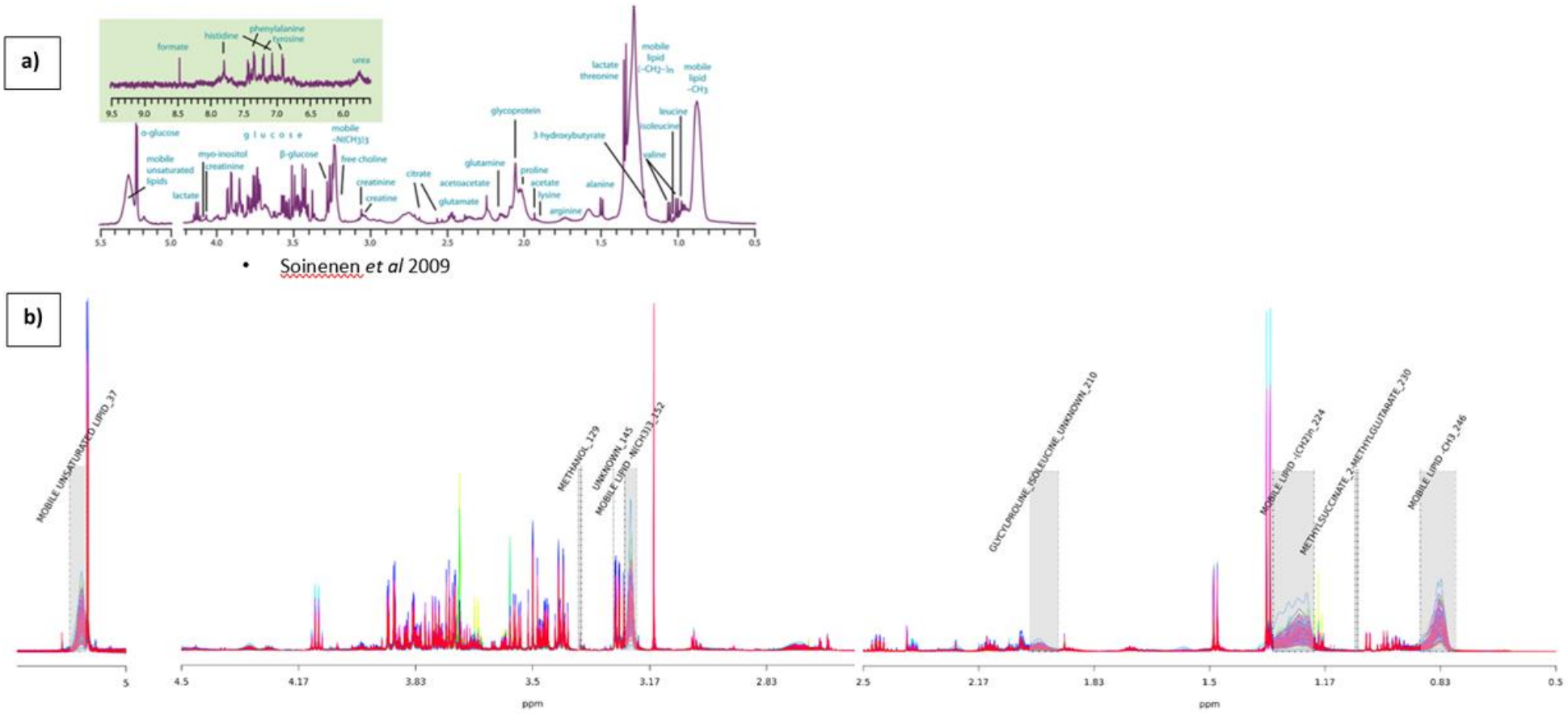

Figure 3.12. Nuclear magnetic resonance spectra highlighting differentially abundant metabolites depending on meniscal injury presence between areas 5.5 to 0.5ppm. *a) ^{1}H NMR spectra of human serum showing regions of mobile lipids (taken from Soininen et al., 2009), and b) combination of 154 spectra of canine stifle joint synovial fluid from the study showing spectral bins with differentially abundant metabolites depending on meniscal injury presence between areas 5.5 to 0.5ppm.*

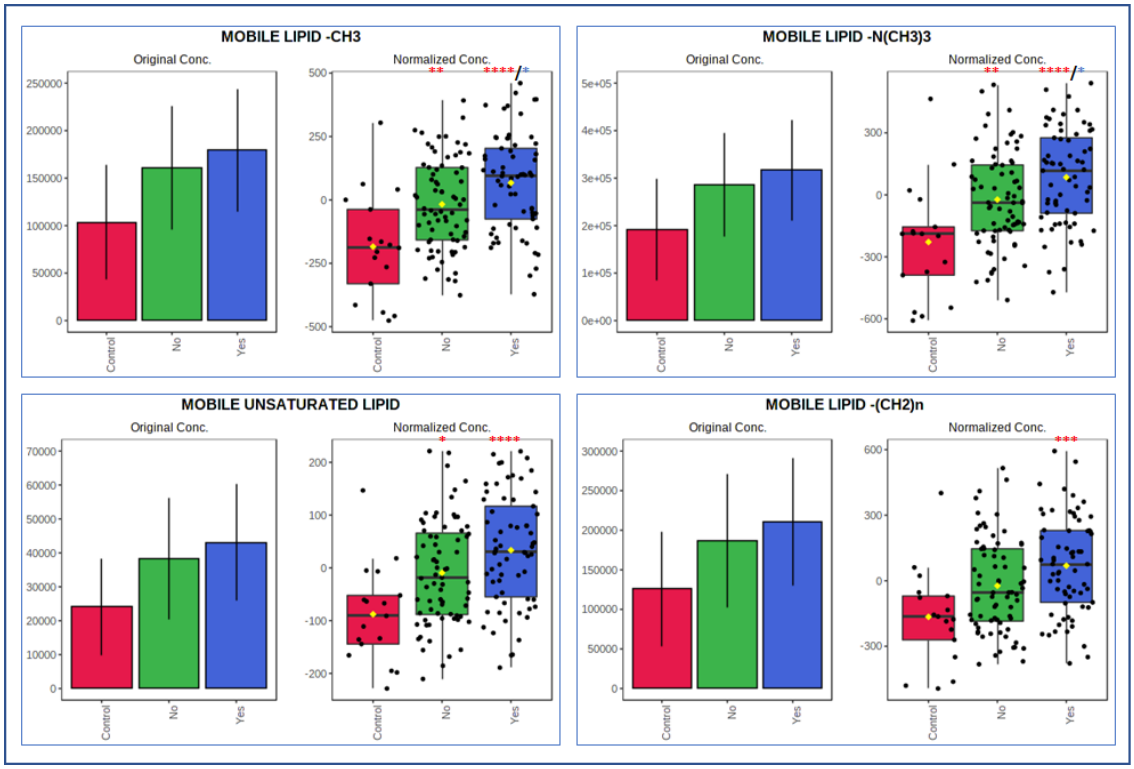

Figure 3.13. Bar plots and box and whisker plots showing changes in 1H NMR identified mobile lipids with respect to meniscal injury status in canine stifle joint synovial fluid from dogs*. Bar plots on the left show the original abundances (mean +/- SD), and box and whisker plots on the right show the normalised abundances. Control (red)= no CCLR or meniscal injury. No (green)= CCLR without meniscal injury. Yes (blue)= CCLR with meniscal injury. Red stars above boxplots denote significance against control group. Blue stars above boxplots denote significance against 'No' group (*=p<0.05, **=p<0.01, ***=p<0.0001, ****=p<0.00001).*

3.3.5.Lipidomic statistical analysis results

3.3.5.1. Clinical features of canine participants included in lipidomic study

A subset of 40 SF samples underwent lipid extraction, with 26 samples passing quality control after spectral acquisition and being submitted for analysis (13 samples CCLR with meniscal injury, 13 samples CCLR without meniscal injury). There was no significant difference between groups in terms of age, sex, weight, OA, BCS or duration of lameness. The clinical features of the canine participants in the NMR lipidomic experiment are outlined in Table 3.4.

Table 3.4. The clinical features of the canine participants included in the nuclear magnetic resonance lipidomic study of biomarkers of meniscal injury in canine stifle joint synovial fluid with cranial cruciate ligament rupture.

	Group	
	CCLR without meniscal injury	**CCLR with meniscal injury**
Sample size (*n*)	13	13
Age, years (mean [SD])	6.8 (2.9)	6.5(3)
Weight, kg (mean [SD])	32.8 (14)	33 (17)
Sex, FE/FN/ME/MN (*n*)	2/4/2/5	1/4/4/4
BCS, 1-9 (mean [SD])	5.6(1.4)	6.2(1.6)
Radiographic OA score (0-10) (Innes *et al*., 2004) (mean [SD])	4.3(1.1)	5.3(1.6)
Radiographic OA score (0-45, mean [SD])(Wessely *et al*., 2017)	8.1(4.4)	9.4(5.1)
Length of time of lameness, months (mean [SD])	2.2(1.6)	2.7(2.7)

Abbreviations= Cranial cruciate ligament rupture (CCLR), female entire (FE), female neutered (FN), male entire (ME), male neutered (MN), body condition score (BCS), kilograms (kg) standard deviation (SD), osteoarthritis (OA), not applicable (N/A)

3.3.5.2. Lipid NMR spectra pattern file creation

A pattern file was created by dividing the lipid spectra into 198 bins using the same technique as above for the metabolite spectra (supplementary material S9).

Annotation of features of interest in the lipid spectra was by use of reference spectra in previous literature (Ulrich *et al*., 2007, Tynkkynen, 2012, Morgan, 2019) as well as an online lipid spectra library (https://lipidlibrary.aocs.org/lipid-analysis/nmr).

3.3.5.3. Multivariate analysis of lipidomic data

Principle component analysis revealed the two groups largely clustered, indicating a similar lipidome (Figure 3.14). 95% of the variance between groups was accounted for by the first two principle components.

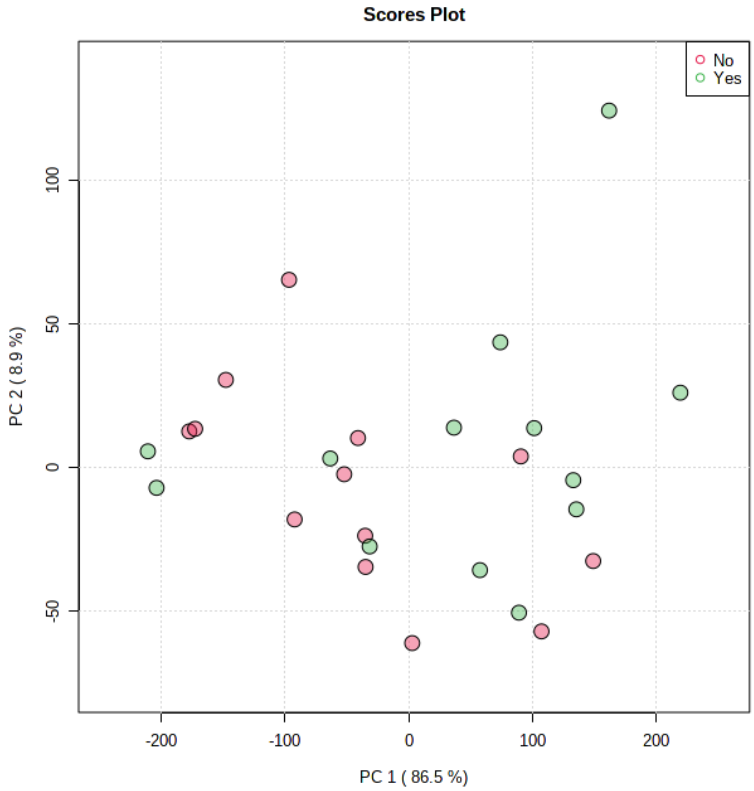

Figure 3.14. Principle component analysis 2D scores plot showing samples analysed in the lipidomic study of canine SF from stifle joints of dogs with CCLR with meniscal injury (group Yes [green dots]), and CCLR without meniscal injury (group No [red dots])

A heatmap to visualise the outline of hierarchical clustering of samples is shown in Figure 3.15. The general trend towards lower concentrations in those samples with CCLR but no meniscal injury compared to those with CCLR and meniscal injury can be seen.

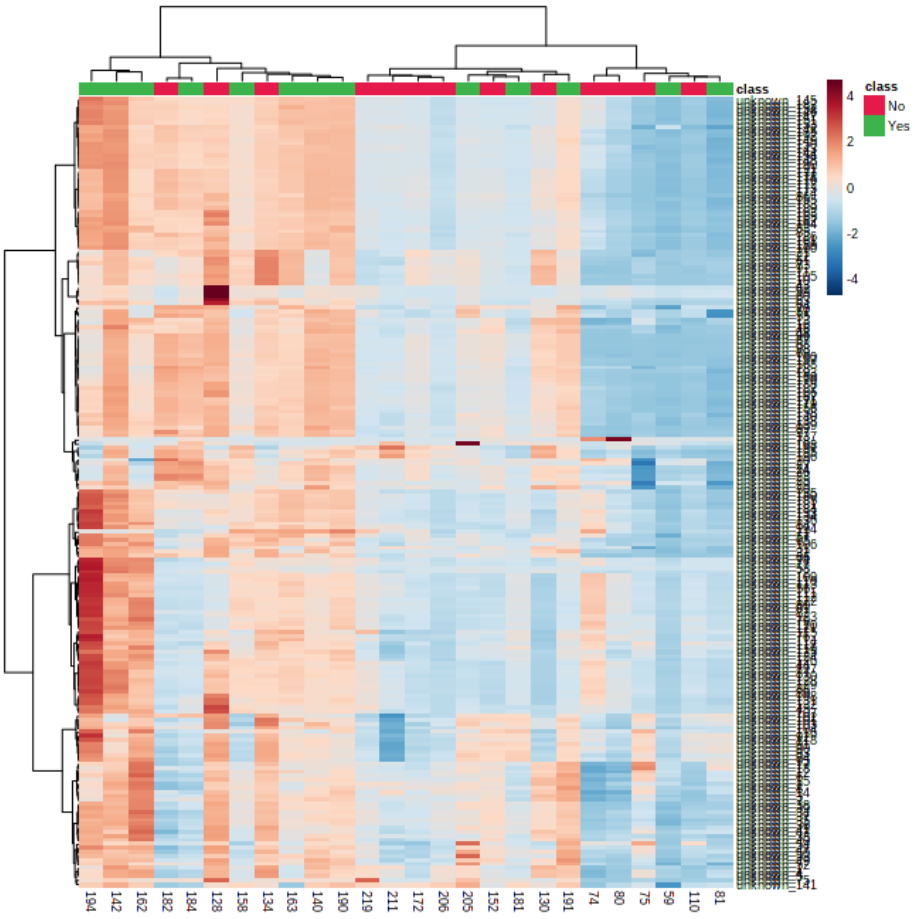

Figure 3.15. Heatmap and dendrogram to visualise hierarchical clustering of samples of canine SF with CCLR and with meniscal injury (group Yes) canine SF with CCLR without meniscal injury (group No), based on the spectral bins representing lipids. *Sample numbers are shown along the bottom of the heat map, and spectral bins are shown along the vertical aspect. Positive changes (in this case an increase in relative intensity of lipid species) are shown by red colouring, whereas negative changes (indicating a decrease in relative intensity of lipid species) are shown by blue colouring. Only 3/13 samples in group "No" cluster with 8/13 samples in group "Yes", showing that the majority of samples of canine SF within groups cluster depending on the relative intensity of lipids in the sample.*

3.3.5.4. Univariate analysis of lipidomic data

Two-sample *t*-tests revealed no significantly altered lipids once p values were FDR corrected. However, it was generally observed that the relative intensity was increased with meniscal injury in 190/196 bins. A volcano plot was used to explore those features with the highest fold change and lowest p-value (Figure 3.16). Four features had a fold change greater than

one, and an FDR adjusted p-value of less than 0.3 (p=0.27). All four of these bins represented peaks consistent with phosphatidylcholine, including a peak between 4.31 to 4.36 ppm, two peaks at 3.7 and 4.0ppm, and a peak at 3.3ppm representing three methyl groups in phosphatidylcholine (Tynkkynen, 2012, Cheung and Olson, 1990). Figure 3.17 shows a boxplot of changes in relative intensity of the phosphatidylcholine peak at 3.3ppm, which is the characteristic singlet peak that can be used for the quantification of phosphatidylcholine in lipid mixtures (Tynkkynen, 2012). An image of a section of one of the canine SF lipid NMR spectrum showing these regions of interest against a reference standard ^{1}H 1D NMR for phosphatidylcholine spectrum obtained from the Biological Magnetic Resonance Data Bank (Ulrich *et al*., 2007) shown in Figure 3.18.

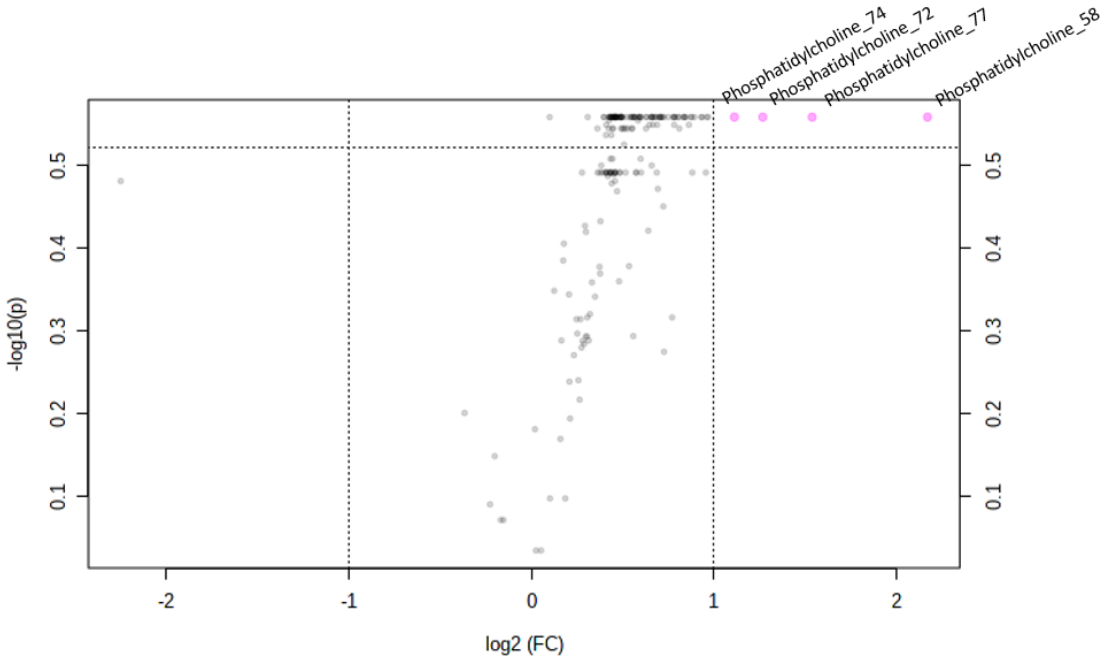

Figure 3.16. Volcano plot of NMR lipidomic study examining lipid changes in canine synovial fluid with cranial cruciate ligament rupture with or without meniscal injury. *Important features were selected with fold change threshold of 2.0 (x axis), and t-test threshold of FDR adjusted p-values 0.3, represented as -log^{10} of the p-value (y axis). The pink circles represent four spectral bins annotated to phosphatidylcholine that were above that threshold. Note both fold change and p values are log transformed. Positive fold changes are represented as samples of canine synovial fluid with meniscal injury compared to samples without meniscal injury.*

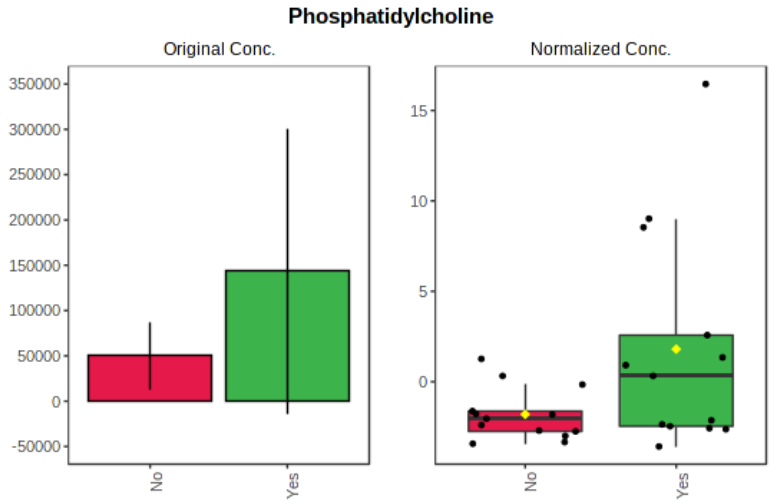

Figure 3.17. Bar plot and box and whisker plot showing changes in relative intensity of phosphatidylcholine in canine SF from dogs with meniscal injury and dogs without meniscal injury. *Bar plots on the left show the original values (mean +/- SD). The box and whisker plots on the right summarise the normalised values, with the notch representing the median and interquartile range and the yellow diamond representing the mean concentration*

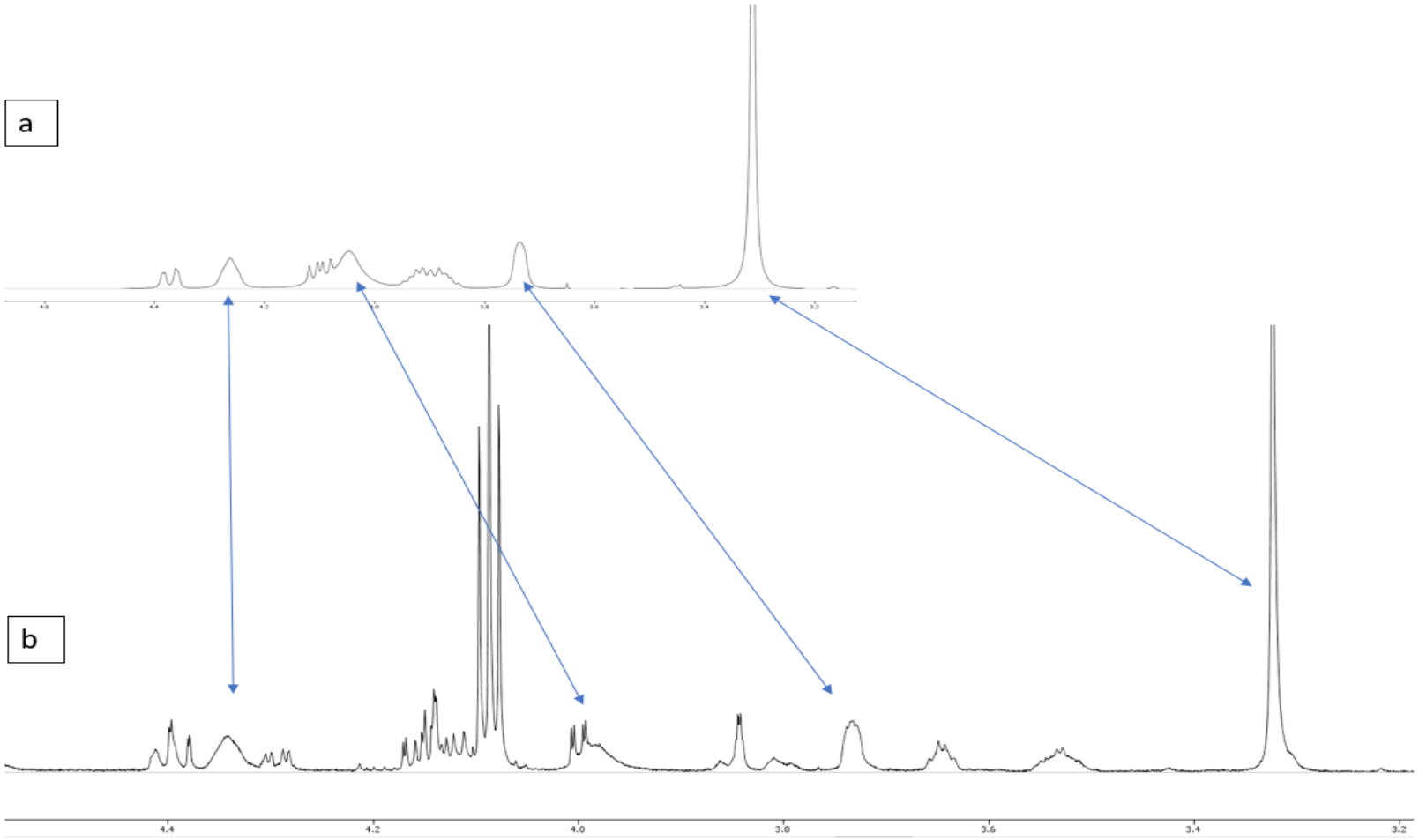

Figure 3.18. a) 1H 1D Nuclear Magnetic Resonance (NMR) reference standard for phosphatidylcholine between 3.2 and 4.5 ppm *(Ulrich et al., 2007).* ***b) A spectrum from one of the canine SF samples showing peaks visible between 3.2 and 4.5 ppm.*** *Arrows denote peaks differentially abundant (although not significantly as p=0.27) between canine SF from dogs with CCLR with meniscal injury and CCLR without meniscal injury samples. X axis shows chemical shift represented as parts per million (ppm).*

3.4. Discussion

As far as the author is aware, this is the first study to use NMR metabolomic and lipidomic analysis to examine biomarkers of meniscal injury in any species. The aims of the study were to examine changes in the metabolomic profile of canine stifle joint SF that occurred firstly in CCLR compared to "normal" canine stifles, and then in CCLR affected stifles that had concurrent meniscal injury, considering various clinical variables. Based on this, the next objective was to explore whether any metabolite could be identified as a biomarker for meniscal injury in CCLR affected canine stifle joints that could be a potential target for a diagnostic test.

3.4.1. Differences in the metabolome of canine SF based on clinical variables

Overall, the inclusion of clinical samples from dogs with a variety of signalments allowed for a well profiled sample set. It could be seen that when examining the profiles of the dogs, there was also a negative correlation between age and weight, which is in agreement with other studies finding smaller breeds tending to develop CCLR at a later age than larger dogs (Witsberger *et al*., 2008). Although this meant that there were many clinical variables to take into consideration, there are benefits to collecting samples from dogs with a variety of signalments in clinical scenarios when attempting to explore potential biomarkers compared to sampling from an experimental group of dogs where clinical variables are controlled. In clinical scenarios in veterinary practice, there is often a wide variety in breeds, ages and sexes of dogs affected by conditions like CCLR (Witsberger *et al*., 2008). This study was able to examine for the first time how the changes in body weight, age, sex, BCS and OA level affected the SF metabolome, which is of interest to future studies in the field of canine metabolomics. In particular, several metabolites were found to significantly alter with increasing weight of dogs, including glutamine, sn-glycero-3-phosphocholine, threonine, formate, creatine, dimethyl sulfone, acetate and unknown metabolites. Confounding factors could affect the conclusions drawn from this, as larger dogs also had a negative correlation with age, so therefore tended to be younger, however glutamine was also found to increase with increasing age of the dogs. Glutamine was also found to increase when analysing metabolite changes with CCLR, it may be that as dogs in the CCLR groups tended to be heavier than the control groups, that the increased weight was a confounding factor. Glutamine is one of twenty amino acids, and in humans, seventy percent of glutamine is stored in skeletal muscles (Mittendorfer *et al*., 1999). Degradation of muscle protein can lead to a release of

glutamine into the extracellular space (Soeters and Grecu, 2012). During lameness in dogs caused by CCLR muscle atrophy due to dis-use of the affected limb can occur (Hyytiäinen *et al*., 2013, Santarossa *et al*., 2020), and as larger dogs tend to have a larger muscle mass, it could be hypothesised that the increase in glutamine SF concentrations in larger dogs could be related to skeletal muscle composition. As a positive correlation between increasing OA score and increasing weight was also found between cases, it cannot be ruled out the OA was a confounding factor in the finding of increased glutamine with weight, as glutamine has been found to be increased with increasing levels of OA in metabolomic studies of human synovial fluid (Zheng et al., 2017b).

Glutamine is synthesised from the excitatory amino acid neurotransmitter glutamate (Cruzat *et al*., 2018), which was amongst the metabolites found to be significantly altered with the CCLR groups compared to control. Glutamate in synovial fluid in humans has been investigated with regards to osteoarthritic changes, and studies have varied in terms of their findings, with some finding an increased glutamate concentration in the synovial fluid of OA affected joints, and some finding a decreased level (Anderson *et al*., 2018a). There were no significant changes in glutamate concentrations with increasing level of OA in the CCLR affected joints in this study.

Other clinical variables that were analysed included age. With increasing age, it was found that lipid abundances within the SF also increased. Serum lipid concentrations have been found to be increased with age in humans (Feng *et al*., 2020), although data in the literature on canine SF lipid concentrations in respect to their correlation to age of dogs is lacking.

With increasing radiographic signs of OA we found few changes in metabolites compared to other studies (Kim *et al*., 2017b). This could be due to the limitations of a lack of healthy controls, with the control group also having a degree of joint pathology, and other confounding factors such as the variety in sizes of dogs in the study could affect results. A further limitation is that the radiographs were scored by veterinary students, and not experienced radiologists, although the students were supervised by experienced veterinary surgeons. Further analysis of OA groupings could prove more informative as to the alterations in the metabolome of dogs with CCLR with increasing OA levels which is outside the scope of this current study.

An interesting note is that no significant differences in the metabolomic profile of the canine SF was found with increasing BCS. Metabolomics studies using serum samples from humans have indicated changes in the serum metabolome with obesity (Moore *et al*., 2014).The BCS

is a subjective measurement of the degree of body fat composition in dogs, and can have some degree of variability between assessors, although low between experienced veterinary surgeons (Laflamme, 1997, German *et al*., 2006).

3.4.2. Differences in the metabolome of canine SF based on meniscal injury status

Although the confounding clinical variables made assessment of the metabolite changes with CCLR difficult, the groups with CCLR and meniscal injury and CCLR without meniscal injury were similar in terms of the variables analysed. There were no significant differences between these two groups in terms of age, weight, BCS, sex and neuter status, and OA score.

A consistent finding when analysing the difference in groups based on meniscal injury status was an increase in mobile lipids on the ^{1}H NMR spectra in stifle joints with meniscal injury. Mobile lipids are NMR lipid resonances that arise from isotropically tumbling, relatively non-restricted molecules such as methyl and methylene resonances belonging to lipid acyl chains (Hakumäki and Kauppinen, 2000, Delikatny *et al*., 2011). These arise primarily from triglycerides, fatty acids and cholesteryl esters in lipid droplets, and also from phospholipidic acyl chains if not embedded in lipid membrane bilayers (Mannechez *et al*., 2005). Lipids serve various important functions in biological systems, including being components of cell membranes and other cellular organelles, acting as an energy source, having a crucial role in signalling and regulation of cellular processes (Onal *et al*., 2017). Many biological processes have been associated with changes in NMR mobile lipids, including cell necrosis and apoptosis, malignancy, inflammation, proliferation and growth arrest (Hakumäki and Kauppinen, 2000). Lipid analysis of SF in humans have found differential abundance of lipids with different disease states, including OA, rheumatoid arthritis and trauma (Wise *et al*., 1987). A more recent NMR lipidomic study in SF from canine and human OA affected joints found an increase in numerous lipid species in OA compared to healthy controls in both species (Kosinska *et al*., 2016).

Amongst the other differentially abundant metabolites between groups, CCLR with and without meniscal injury, was methanol. Although methanol could be considered a contaminant in NMR (Fulmer *et al*., 2010), it has also been found to be a naturally occurring metabolite in humans, either through dietary consumption in various fruit and vegetables, the artificial sweetener aspartame, alcohol, or through actions of gut microbiota (Dorokhov *et al*., 2015). Some of these sources cannot be ruled out, and therefore the decision not to

remove methanol from analysis was made. However, its association with meniscal injury remains unclear. Unfortunately, the spectral bin that had the highest significance in differential abundance between CCLR with and without meniscal injury SF groups was unable to be identified using reference libraries and in-depth literature searches.

Another peak in the NMR spectra that was significantly different with meniscal injury status was annotated to either 2-methylglutarate, methylsuccinate, or a combination of both. 2-methylglutarate and methylsuccinate are methyl-branched fatty acids and are involved in lipid metabolism pathways and cell signalling (Wishart *et al*., 2018). Both methylsuccinate and 2-methylglutarate show as a doublet with a chemical shift of 1.06 to 1.08ppm on a 1H NMR spectrum. There is only a small signal associated with this peak on the spectra, and only one of two peaks of the doublet showed as significant, therefore the relevance of this finding is difficult to substantiate. 2D NMR was unable to elucidate the identity. A spiking experiment to attempt to identify this peak could be of use in the future (Le Gall, 2015).

The significant region including overlapping peaks of glycylproline, isoleucine, and an unknown metabolite also requires further work to identify. It is possible that in this region at 1.93 to 2.02 ppm there is also mobile lipid resonances, as fatty acyl chains have been noted to be attributed to this region (Delikatny *et al*., 2011). This would correlate with the findings of increases in mobile lipids with meniscal injury.

There are a number of possible hypotheses for the increase in lipid resonances found in the SF of dogs with CCLR and concurrent meniscal injury compared to CCLR without meniscal injury in this study. Injury to the meniscus could lead to damage to cellular phospholipid membranes, resulting in the release of lipids into the synovial fluid. Human menisci have also been found to contain lipid debris that could have an impact on SF lipid concentrations in meniscal injury (Ghadially and Lalonde, 1981). Also, lipid droplets could be released from the intracellular environment due to cell necrosis or apoptosis in the damaged meniscal tissue (Uysal *et al*., 2008), leading to an increased concentration of lipid droplets in the SF. Lipid droplets have been found to play a key role in inflammation, as such it may be that meniscal tears lead to a release of lipid droplets to facilitate in the inflammatory response within the joint (Melo *et al*., 2011). As lipid droplets contain mediators of inflammation such as pro-inflammatory cytokines, lipids could also potentiate inflammatory changes in meniscal injury affected joints (Ichinose *et al*., 1998). Alterations in SF lipid composition and lipid species can also have a role in affecting the lubricating ability of the SF (Antonacci *et al*., 2012). The concentration of phospholipid species in human SF have been found to be increased in OA

affected joints, therefore the observed increase in lipids could also be an attempt to improve lubrication of the SF after meniscal injury in order to have protective effects on the articular cartilage (Kosinska *et al*., 2015).

In order to validate these NMR metabolomic findings, an untargeted NMR lipidomic experiment was undertaken on a subset of 26 samples in order to elucidate the lipid species that were most differentially abundant. Although no lipid reached significance when p-values were adjusted for FDR, it was generally observed that the relative intensity of the majority of lipids were increased with in the CCLR group with meniscal injury compared to without meniscal injury.

Phosphatidylcholine (PC) was one lipid found to be most increased in canine SF with meniscal injury. PC is a phospholipid species with a choline head group, and is the most abundant phospholipid in animal cells (Vance, 2015). It is one of the major constituents of cell membrane phospholipid bilayers, as well as being the primary phospholipid species circulating in plasma, and it has a role in the creation of lipoproteins and in cell signalling (van der Veen *et al*., 2017). In SF, PC has a role in lubrication, interacting with hyaluronic acid to form the lubricating molecular layer in synovial joints (Siódmiak *et al*., 2017). In a lipidomic study examining lipid profiles of human SF with and without OA and rheumatoid arthritis (RA), phospholipid species including PC were found to be increased with OA and RA compared to control samples and PC was also found to be the predominant phospholipid in the human SF, accounting for 67% of phospholipids (Kosinska *et al*., 2013). The PC in SF may either originate from plasma, or be produced locally by fibroblast like synoviocytes (Schwarz and Hills, 1996a). Although the exact mechanisms for the increase in PC in the SF of OA affected joints is unknown, Sluzalska *et al*. (2017) found that the actions of tumour necrosis factor alpha (TNFα) may be involved in the increase in PC biosynthesis. The authors also speculated that other agents such as growth factors may play a role in relation to fibroblast-like synoviocytes production of PC. As yet, the cause of increase PC in meniscal injury can only be hypothesised and further work into the exact mechanisms are required.

3.4.3.Limitations

In terms of the first objective of examining changes in the SF metabolomic profile depending on the presence of CCLR compared to non-CCLR affected stifles, one of the major limitations of the study was the lack of a balanced control group to compare with the CCLR affected joints. There are several reasons for this. Firstly, collection of “normal” SF via arthrocentesis

from joints without pre-existing pathology involves a level of risk, including introducing infection into the joint, and the need for sedation or anaesthetic for the protocol (Bexfield and Lee, 2014). Therefore, this would have ethical implications, and was outside the ethical approval for this study. SF from dogs with no stifle joint pathology collected post-mortem would have been subjected to metabolite changes that would have compromised the comparison to the diseased groups (Donaldson and Lamont, 2015). Control samples in this study were collected from dogs undergoing surgery for patella luxation, or excess SF from dogs undergoing arthrocentesis from investigations of lameness. These were cases without CCLR or meniscal injuries, but also may not have been completely without pathological changes, as patella luxation can be cause of OA and synovitis (Roush, 1993). Patella luxation also tends to be more common in smaller breeds of dogs, and as primarily a congenital disease, cases often cases show clinical signs of lameness at a younger age than CCLR affected dogs (LaFond *et al*., 2002, Rudd Garces *et al*., 2021). Both these factors lent towards the control being on average younger and smaller than the CCLR groups, with less osteoarthritic changes. This, along with the fewer samples collected in the time constraints of this study affected the ability to infer conclusions from the metabolite changes between the control and other groups in terms of CCLR alone.

There were factors such as diet and level of exercise that have been found to affect the metabolome of human serum that had not been accounted for in this study (Esko *et al*., 2017, Sakaguchi *et al*., 2019). Medications were found to be too heterogeneous between the dogs in this study from which to make any statistical conclusions but are known to affect the metabolomic profile of biofluids (Um *et al*., 2009).

There were a number of metabolite peaks that are, as yet, unidentified on the canine SF spectra, including one that was found to be significantly altered with meniscal injury. Further work in identifying these regions, or using more sensitive methods of molecule identification, such as mass spectrometry, could prove useful.

For the lipidomics experiment, the sample sizes were limited. Repeating this experiment with a larger sample size could improve statistical significance in the findings.

3.5. Conclusions and further work

This study is the first of its kind in using ^{1}H NMR spectroscopy in identifying biomarkers of meniscal injury with SF. Both the metabolomic and lipidomic studies have identified that SF

lipid species appear to be of interest in the study of biomarkers of meniscal injury, and future work to increase the sample size for lipidomic analysis could prove useful in exploring the potential for a diagnostic marker.

The inclusion of a more donors in the control group of healthy, non-diseased canine stifle joint SF would be of value in future work to allow analysis of changes due to CCLR and OA in the canine stifle joint.

The work presented here is also of translational value into metabolomics studies in human and other mammalian species. No SF biomarker has been found to date in human SF with meniscal injury, therefore this research could also lead to the investigation of biomarkers of meniscal injury in human SF.

4. Investigation of protein, cytokine and endocrine biomarkers of meniscal injury in canine stifle joint synovial fluid with cranial cruciate ligament rupture

4.1. Introduction

Meniscal injuries are a relatively common occurrence in humans, with an estimated incidence of 60 to 70 cases per 100,000 people per year, with one third of these injuries being as a result of a sports injury (Manson and Cosgarea, 2004). In dogs, meniscal injuries are very rare in isolation, and tend to arise as a consequence of CCLR. Injuries to the canine menisci can also happen post-operatively after CCLR stabilisation surgery (Fitzpatrick and Solano, 2010). These late meniscal injuries can also go on to be a source of pain and lameness in the affected dog, and can be difficult to diagnose, with current methods of diagnosis relying on surgical means such as arthrotomy and arthroscopy (Dillon *et al*., 2014).

Currently, there are no reliable biomarkers of meniscal injury in humans or dogs that can be used as a diagnostic test, or for targeted treatment or prevention. Synovial fluid can be a unique source of biomarkers of joint pathologies, due to its presence within the intra-articular space next to various joint structures (Boffa *et al*., 2020). The presence of a biomarker of meniscal injury within synovial fluid could allow for the potential development of an inexpensive, minimally invasive diagnostic test for meniscal injuries. Previous studies have investigated synovial fluid biomarkers that could indicate alterations in biological pathways and processes in meniscal injuries (Rai *et al*., 2020). Timur *et al*. (2021) examined different proteins present in synovial fluid from human osteoarthritic knee joints and compared their abundance in the protein secretome of different joint structures. It was found that seven proteins in the knee synovial fluid were detected in higher concentrations in the meniscal protein secretome than other structures such as cartilage, Hoffa's fat pad and synovium. These included tenascin C, histidine-rich glycoprotein, inter-alpha-trypsin inhibitor heavy chain H1, cartilage acidic protein 1, N-acetylmuramoyl-L-alanine amidase, and complement component C7 and C8 gamma chain.

Other studies investigating sources of biomarkers of meniscal injury have found increased levels of cytokines interleukin (IL)-6 and tumour necrosis factor alpha (TNFα) in injured meniscal tissue compared to non-injured tissue (Ogura *et al*., 2016). Bigoni *et al*. (2017) examined concentrations of pro-inflammatory and anti-inflammatory cytokines in the synovial fluid of humans with meniscal tears, finding an increase in IL-10, IL-6, TNFα and IL-8 and a reduced level of IL-1ra and IL-1β.

Luciferase reporter assays are bioluminescent biological assays that can be used to examine whether a particular protein promotes or represses the transcription of a target gene in biological samples (Carter and Shieh, 2015). Use of luciferase reporter assays for studying cellular responses in biofluids such as serum and urine has been presented in relatively few studies (Ponnurangam *et al*., 2010, Kinoshita *et al*., 2019), and a recent study has examined the use of luciferase based bioluminescent reporter assays in SF (Neefjes *et al*., 2021). The use of these assays could give information on signalling pathways that become altered in different joint pathologies, and potentially aid with identifying biomarkers based on those proteins that activate these reporter genes (Carter and Shieh, 2015).

We hypothesise that there will alterations in signalling pathways depending on meniscal injury status, and that there will be an alteration in the composition of proteins that are expressed preferentially in meniscal tissue in the SF of dogs with meniscal injury. Therefore, the aim of this study was to investigate alterations in signalling pathways and their associated upstream signallers, in the synovial fluid of dogs with CCLR and meniscal injuries. Another aim was to investigate whether proteins, that have previously been found to be increased in meniscal tissue compared to other joint tissue types, were increased in the synovial fluid of dogs with meniscal injuries.

4.2. Materials and methods

4.2.1. Collection of canine stifle joint synovial fluid

Collection of canine stifle joint synovial fluid was as previously described in Chapters 2 and 3 (sections 2.2.2 and 3.2.2) of this thesis.

4.2.2. Examination of alterations in pathway activation in canine SF dependant on meniscal injury status

Twenty canine SF samples (ten with CCLR and meniscal injury, ten with CCLR and no meniscal injury) were transferred on dry ice to the Laboratory for Experimental Orthopaedics, Department of Orthopaedic Surgery, Maastricht University, Maastricht, The Netherlands. This number of samples were selected dependent on availability of samples with a large enough volume of SF, and with an equal variance of clinical features such as bodyweight, age, BCS and OA level. Luciferase reporter assays were carried out to examine the activity of 13 pathways, by determining the expression of 13 response element driven

Nano luciferase SW1353 reporter cells upon stimulation with either 10% phosphate buffer solution (PBS), or 10% canine SF. Reporter cell lines were generated by using lentiviral transduction to incorporate reporter sequence into the genome. Cells were puromycin selected. Cells were seeded for 24 hours prior to stimulation in 0.5% fetal calf serum (FCS) supplemented DMEM/F12 (Dulbecco's Modified Eagle Medium/Nutrient Mixture F12) + 1% antibiotic antimycotic penicillin/streptomycin (P/S) solution at a density of 60.000 cells/cm^2. Cells were stimulated with either 10% phosphate buffer solution (control) or 10% canine SF in DMEM/F12 HEPES (4-(2-hydroxyethyl)-1-piperazineethanesulfonic acid) + 1% P/S. A total volume of 30µl per well was used, and each sample was ran in quadruplets for each reporter gene. Cells were stimulated for six hours before the luminescence was read at 460nm.(Neefjes *et al*., 2021). The 13 response elements and their associated pathways are outlined in Table 4.1.

4.2.3. Investigation of differentially abundant proteins in canine SF dependant on meniscal injury status

SF samples were thawed on ice immediately prior to use. SF samples were treated with hyaluronidase (1mg/ml; Sigma-Aldrich, St. Louis, MO, USA) to SF at a dose of 1µg/ml, and incubated at 37°C for 1 hour before being centrifuged at 1000 x *g* for five minutes (Mateos *et al*., 2012) and supernatant collected. The following ELISA tests were performed according to the manufacturer ELISA protocols. All samples and standards were ran in duplicate as per the recommendations of each ELISA manufacturers' protocols.

- Histidine rich glycoprotein (Canine Histidine rich glycoprotein quantitative sandwich ELISA kit, My BioSource Inc., San Diego, California, USA)
- Tenascin C (Canine Tenascin C Competitive ELISA kit, My BioSource Inc., San Diego, California, USA)
- Cartilage acidic protein 1 (Cartilage acidic protein 1 competitive ELISA kit, My BioSource Inc., San Diego, California, USA)
- Tumour necrosis factor alpha (TNFα) (Tumour necrosis factor alpha canine solid phase sandwich ELISA kit, Invitrogen, Thermo Fisher Scientific, Massachusetts, USA)
- Epidermal growth factor (EGF) (Canine EGF ELISA kit, My BioSource Inc., San Diego, California, USA)
- Cortisol (Canine Cortisol ELISA kit, Assay Genie, Dublin, Ireland) – preliminary dilution factors test was carried out with samples diluted 1:2, 1:4, 1:7. Dilution 1:7 was found

to be most appropriate, so was used for the test comparing canine SF with and without meniscal injury.

Table 4.4. The thirteen response elements investigated in the study of canine synovial fluid with cranial cruciate ligament rupture depending on meniscal injury status, along with their transcription factor complexes, their signalling intermediates, upstream signallers, and associated gene receptors.

Response Element	Transcription factor Complex	Signalling intermediates	Upstream	Associated Receptor
Nuclear factor-kappa B response element **(NFkB-RE)**	p65/p50	IKK	Cytokine signalling	IL1R, TNFR1, TLR
Smad binding element **(SBE)**	Smad3/Smad4		TGFβ signalling	TGFβR2, ALK5
Nuclear factor of activated T-cells 5 response element (**NFAT5-RE)**	NFAT5		Osmotic stress	
T-cell specific transcription factor/lymphoid enhancer binding factor response element (**TCFLEF-RE)**	TCF/LEF	b-catenin	Canonical Wnt signalling	Frizzled family receptors
cAMP response element **(CRE)**	CREβ	cAMP/PKA	GPCR signalling	EP2, EP4, PTHR1, A2AR
Antioxidant response element (**ARE)**	NRF2	KEAP1	Reactive oxygen species	
Activator protein 1 response element (**AP1-RE)**	c-Fos/c-Jun/ATF2	p38/JNK	Cytokine/Growth factor signalling	TNFR1, EGFR, PDGFR
Serum response element (**SRE)**	Elk1/SRF dimer	MAPK/ERK	Growth factor signalling	EGFR, FGFR, IGFR, PDGFR
Serum response factor response element (**SRF-RE)**	SRF dimer	RhoA	Growth factor signalling	EGFR, FGFR, IGFR, PDGFR
Sis-inducible element (**SIE)**	STAT3 dimer	JAK1/2	IL6 signalling	IL6R
Interferon-sensitive response element (**ISRE)**	STAT1/STAT2	JAK1/TYK2	IFNα signalling	IFNAR1, IFNAR2
Glucocorticoids response element (**GRE)**	GR		Glucocorticoids signalling	GR
NKX3-2 Binding element (**NBE)**	NKX3-2		Anti-hypertrophic signalling	

Abbreviations: IL1R= Interleukin 1 Receptor; TNFR1= Tumour necrosis factor receptor 1 ; TLR= Toll-like receptor; TGFβ= transforming growth factor beta; TGFβR2= transforming growth factor beta receptor 2; ALK5= Activin-like kinase 5, TCF= T cell factor; LEF= Lymphoid enhancer factor; cAMP= cyclic adenosine monophosphate; CREβ= cAMP response element beta, PKA= protein kinase A; GPCR= G protein coupled receptors; EP2/4=Prostaglandin E2/4; PTHR1= parathyroid hormone receptor 1; A2AR= adenosine A2A receptor; NRF2= Nuclear factor-erythroid factor 2-related factor 2; KEAP1= Kelch-like ECH-associated protein 1; ATF2= activating transcription factor 2; JNK= c-JUN N terminal kinases; EGFR= epidermal growth factor receptor; PDGFR= platelet-derived growth factor receptor; SRF=serum response factor; MAPK/ERK= mitrogen-activated protein kinases/extracellular-signal related kinases; FGFR= fibroblast growth factor receptor; IGFR= insulin-like growth factor ; RhoA= Ras omolog family member A; STAT3= Signal transducer and activator of transcription 3; JAK= Janus kinase; IL6= interleukin 6; IL6R= interleukin 6 receptor; GR= Glucocorticoid receptor

4.2.4. Statistical analysis

Luciferase reporter assay readings were normalised to the mean of the unstimulated control conditions before statistical analysis. Two-tailed unpaired students *t*-tests were used for the luciferase reporter assay results (on the normalised readings) with significance set at $p \leq 0.05$. Where there was unequal variance between the groups, Welch's correction was applied to the *t*-tests. These analyses and creation of graphs to show results were carried out using GraphPad Prism (GraphPad Prism 9.1.0, San Diego, CA, USA).

Four parametric logistic curve fits were used to calculate ELISA concentrations from raw optical density (OD) values using standard curve of known concentrations (www.myassays.com online statistical tool was used for these four parametric logistic curves, MyAssays Ltd, UK). Normality was tested using Shapiro-Wilk normality test. Where data was normally distributed, the difference between groups was tested using two-tailed unpaired students *t*-tests were used with significance set at $p \leq 0.05$. Where there was unequal variance between the groups, Welch's correction was applied to the *t*-tests. If data was not normally distributed, Mann Whitney tests were used. These analyses and creation of graphs to show results were carried out using GraphPad Prism (GraphPad Prism 9.1.0, San Diego, CA, USA).

4.3. Results

4.3.1. Differences in pathway activation upon stimulation with canine synovial fluid with CCLR depending on meniscal injury status

Twenty samples of canine SF were included, with n=10 from dogs with CCLR and meniscal injury, and n=10 from dogs with CCLR but no meniscal injury. The signalment of these dogs was similar in terms of age, weight, body condition score (1-9) (Laflamme, 1997), and assessment of radiographic signs of OA in the stifle joint based on a global assessment of OA from zero to three with zero being no signs of OA, one being mild OA, two being moderate OA and three being severe OA (Innes *et al*., 2004). There were more female dogs in the group without meniscal injuries (seven out of ten, of which five were neutered) and more males in the meniscal injury group (eight out of ten, of which three were neutered). These results are shown Table 4.2.

Thirteen different response elements were examined by luciferase reporter assays (Table 4.1), which were associated with specific signalling pathways. Three response elements showed significant up regulation when stimulated by canine SF with meniscal injury compared to canine SF without meniscal injury. These were glucocorticoid response element (GRE)($p<0.0001$), activator protein 1 response element (AP1-RE) ($p=0.03$), and serum response element (SRE) ($p=0.01$). Figure 4.1 shows an overview of the results obtained from all 13 response elements.

Table 4.5. Clinical features of twenty canine participants included in the luciferase reporter assays examining changes in signalling pathways between canine stifle joint SF with cranial cruciate ligament rupture (CCLR) with meniscal injury and CCLR without meniscal injury. Osteoarthritis (OA) score represents 0-3 with 0 being no OA, 1 being mild OA, 2 being moderate OA and 3 being severe OA.

	CCLR with no meniscal injury (n=10)	**CCLR with meniscal injury (n=10)**
Age, years (mean [SD])	5.4 (3.0)	5.1 (3.7)
Sex (n)	FE=2 FN=5 ME=1 MN=2	FE=0 FN=2 ME=5 MN=3
Weight, kg (mean [SD])	32.3 (12.1)	35.3 (8.8)
BCS, 1-9 (mean [SD])	5.6 (1.5)	5.9 (1.2)
OA score, 0-3 (mean [SD])	1.6 (1.0)	1.5 (0.7)

Abbreviations: CCLR=cranial cruciate ligament rupture BCS= Body condition score, OA=osteoarthritis

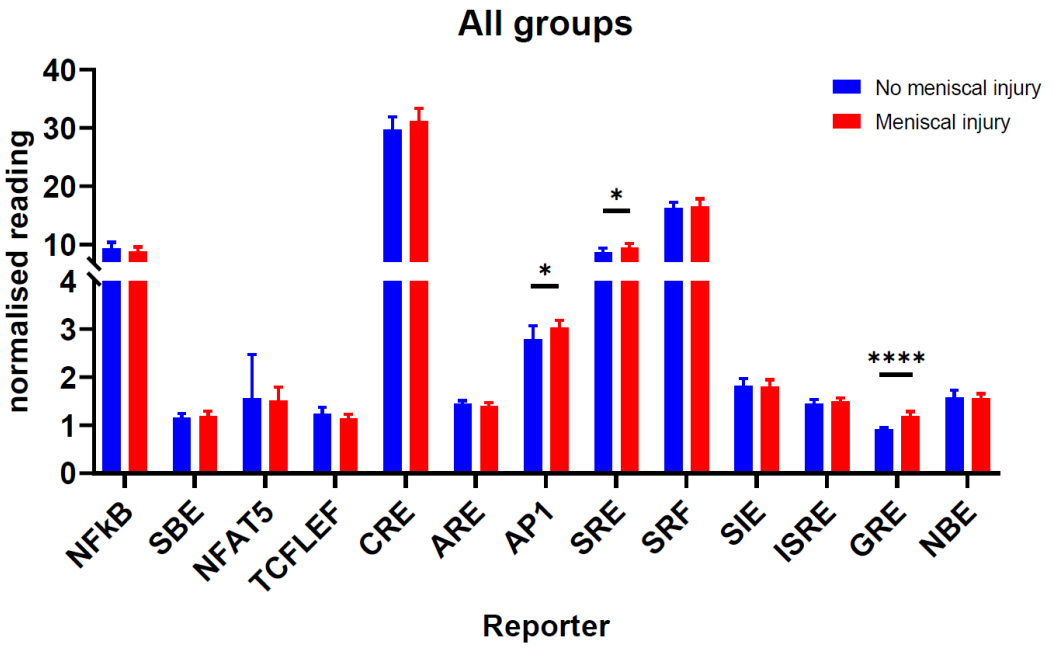

Figure 4.3. Bar charts to show results of luciferase reporter assays of 13 response elements when stimulated by canine synovial fluid from dogs with CCLR with meniscal injury (red group) and CCLR without meniscal injury (blue group). *Level of significance: ****=p<0.0001, ***=p<0.001, **=p<0.01, *=p<0.05. (Abbreviations: NFκB= Nuclear factor-kappa B response element; SBE=Smad binding element; NFAT5= Nuclear factor of activated T-cells 5 response element; TCFLEF: T-cell specific transcription factor/lymphoid enhancer binding factor response element; CRE= cAMP response element; ARE: antioxidant response element; AP1= Activator protein 1; SRE= Serum response element; SRF=Serum response factor; SIE= Sis-inducible element; ISRE= Interferon-sensitive response element; GRE= Glucocorticoid response element; NBE= NKX3-2 Binding element).*

4.3.2. Differences in concentrations of cortisol, TNFα, and EGF with canine synovial fluid with CCLR depending on meniscal injury status

As GRE was found to be upregulated, clinical records of the dogs included in the study were examined to ensure no animals were receiving exogenous glucocorticoid medication at the time of sample collection. No dogs had received glucocorticoids in the month before surgery and none were noted to have hyperadrenocorticism. Cortisol ELISA was carried out to examine whether canine SF from dogs with meniscal injury had a higher concentration of cortisol than from SF without meniscal injury. TNFα ELISAs were also carried out, as TNFα can upregulate the enzyme 11β-hydroxysteroid dehydrogenase 1 (11β-HSD1), which

converts inactive cortisone to active cortisol (Loerz and Maser, 2017). SRE and AP1-RE have common signallers of epidermal growth factor (EGF), and TNFα can also act as a signaller of AP1-RE (Li *et al*., 2003, Granet *et al*., 2004). Therefore, ELISAs for TNFα and EGF were also carried out on the canine SF, using separate aliquots of SF from the same donors as the luciferase reporter assays. For the cortisol ELISA, a total of n=32 samples were used, with an additional 12 donors on top of the 20 used for the luciferase reporter assays.

The concentrations of TNFα were below the threshold of the ELISA. Sixteen samples (eight samples of each group) were included for the EGF ELISA. Thirty-two samples (16 of each group) were included in the cortisol ELISA. There was no significant difference between the concentration of EGF between the two groups, although there was a general increase in EGF concentrations in the meniscal injury group (p=0.27) (Figure 4.2). There was also no significant difference between groups in terms of cortisol concentration (p=0.45). There was one outlier in the group without meniscal injury, but there was no obvious reason for this in terms of difference in sample, laboratory technique or clinical differences of the donor (Pollet and van der Meij, 2017). Statistical analysis with removal of the outlier also did not show any significant changes between groups (p=0.9).

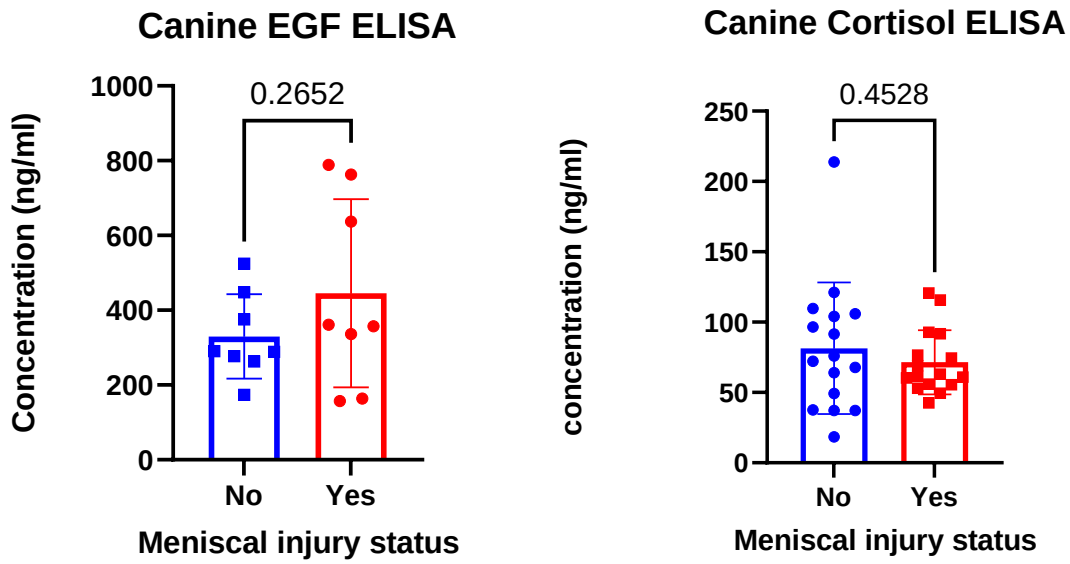

Figure 4.2. Scatter plot with bar graph showing results of canine epidermal growth factor (EGF) and canine cortisol ELISA examining canine synovial fluid from dogs with cranial cruciate ligament rupture (CCLR) with or without meniscal injury. *Individual sample results are shown, with mean and standard deviation. P values from t-test results shown.*

4.3.3. Investigation of protein concentrations in canine synovial fluid with meniscal injury

The ELISAs for histidine rich glycoprotein, tenascin C and cartilage acidic protein 1 were carried out on a separate cohort of canine SF samples from dogs with and without meniscal injuries to the samples used in section 4.3.1.

- Histidine rich glycoprotein

Sixteen samples were included (n=8 per group). All samples were within the detection range of the assay, and concentrations ranged from 0.7 to 2.7ng/ml. There was no significant difference between groups (p=0.32) (Figure 4.3).

- Tenascin C

Seventeen samples were included (n=9) for the group with meniscal injury, n=8 for the group without meniscal injury). Six samples were below the level of detection for the assay. Of the remaining, five samples belonged to group with meniscal injury, and four were samples of SF without meniscal injury. Of these samples that were within the level of detection, there was no significant difference (p=0.43) between groups.

- Cartilage acidic protein 1

Seventeen samples were included (n=9 with meniscal injury, n=8 without meniscal injury). Only one sample reached the threshold for detection.

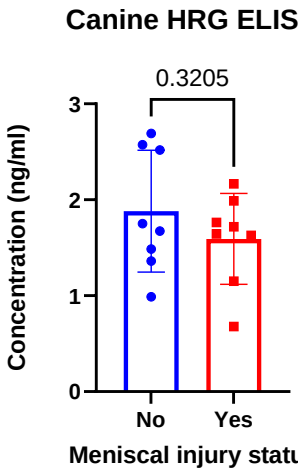

Figure 4.3. Scatter plot with bar graph showing results of canine histidine rich glycoprotein (HRG) ELISA carried out on canine synovial fluid from dogs with CCLR with or without meniscal injury. *Individual sample results are shown, with mean and standard deviation. P value after t-test shown.*

4.4. Discussion

4.4.1. Signalling pathways altered in canine SF with CCLR depending on meniscal injury status

This is the first study to examine pathway alterations in canine SF due to the presence of meniscal injury using luciferase reporter assays. Of the 13-response element examined in this study, three were found to be significantly upregulated when stimulated by canine SF from dogs with meniscal injury compared to those without meniscal injury. Two of these, the AP1RE and SRE, had a low level of significance ($p=0.028$ and 0.012 respectively), and therefore the biological relevance of these is difficult to conclude due to the small degree of change. One of the significantly upregulated response elements was the glucocorticoid response element (GRE), which showed a high level of significance ($p<0.0001$). GRE is found in a number of target genes that respond to glucocorticoid (Necela and Cidlowski, 2004). Glucocorticoid receptors (GR) exist in the cytoplasm bound to heat shock protein 90 (hsp90). When glucocorticoids, such as cortisol, bind to the GR, it disassociated from hsp90, and forms a dimer with another GR. This dimer then moves to the cell nucleus, where it binds to the GRE and stimulates the transcription of glucocorticoid responsive genes (Necela and Cidlowski, 2004). Glucocorticoids are regulated both systemically and locally in mammalian systems (Figure 4.4). Systemic regulation is via the hypothalamic-pituitary axis (Macfarlane *et al*., 2020). Local regulation involves the conversion of inactive cortisone to active cortisol via the enzyme 11-beta-hydroxysteroid dehydrogenase-1 (11β-HSD1) (Loerz and Maser, 2017). This enzyme is expressed in a variety of tissues, including adipose tissue, bone, gonads, and in stromal mesenchymal cells such as fibroblasts (Tomlinson and Stewart, 2001). 11β-HSD1 is upregulated in response to pro-inflammatory cytokines IL-1β and TNFα (Escher *et al*., 1997). Previous work has found TNFα to be increased in injured human meniscal tissue compared to normal meniscal tissue (Ogura *et al*., 2016), and increased in human SF with meniscal injury (Bigoni *et al*., 2017). Therefore, it could be hypothesised that this increase in TNFα could lead to the upregulation of 11β-HSD1, which in turn leads to the conversion of cortisone to cortisol, which then binds to the GR and stimulates the GRE.

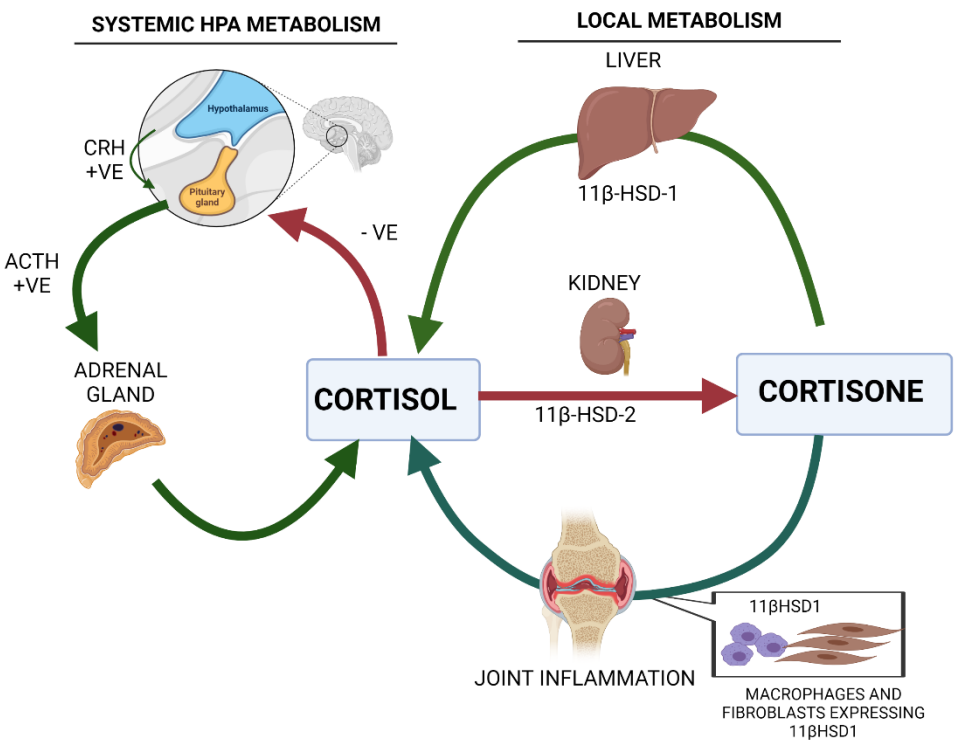

Figure 4.4. Figure to show the systemic regulation of cortisol via the hypothalamic pituitary adrenal axis, and local regulation via the enzyme 11 beta hydroxysteroid dehydrogenase (11ϐHSD). *Corticotrophin-releasing hormone (CRH) is released from the hypothalamus, stimulating the release of adrenocorticotropic hormone (ACTH) from the pituitary gland, which in turn stimulated the release of cortisol from the adrenal gland. Locally, cortisol is inactivated to cortisone via 11ϐHSD2 in the kidneys, and cortisone is turned into the active cortisol by 11ϐHSD1 in the liver. During joint inflammation, joint macrophages and fibroblasts expressing 11ϐHSD1 reactivates cortisone to cortisol. Figure adapted from Hardy et al. (2014).*

To test this hypothesis, ELISAs were carried out to establish whether the concentration on TNFα was increased in the SF with meniscal injury. As the concentration of TNFα failed to be detected on the assay, this remains an area for further work. Cortisol was found not to be significantly altered using an ELISA between the canine SF with and without meniscal injury, therefore the cause of the increased stimulation of the GRE in canine SF with meniscal injury compared to that without meniscal injury remains unknown.

Mechanisms other than an increase in cortisol concentrations in the synovial fluid could also be hypothesised to contribute towards the significant increase in GRE stimulation within the

canine SF with meniscal injury. Heat shock proteins hsp90 and hsp70 are both involved in the activation of GR, with hsp70 promoting GR ligand release and inactivation by partial folding, and Hsp90 binding to GR and ATP hydrolysis on Hsp90 activating ligand binding on the GR (Kirschke et al., 2014). As the GR is regulated by these Hsp chaperone cycles, alterations in Hsp70 and Hsp90 concentrations in cells could therefore affect the regulation of the GR (Kirschke et al., 2014). The transcription of Hsp90 is regulated by heat shock factor 1, which is itself subject to regulation by a complex set of biological mechanisms (Anckar and Sistonen, 2011). Post-transcriptional control of Hsp90 is also affected by a number of factors, including a variety of enzymes, such as kinases, phosphatases and histone acetylases and deacetylases that are, as yet, not fully identified (Prodromou, 2016). It is possible that these Hsps can also impact upon the changes found to GRE in canine SF with meniscal injury, although the exact mechanisms for this are unknown.

Another potential factor impacting the upregulation of GRE in canine SF with meniscal injury could be other hormones such as the androgen, testosterone (Spaanderman et al., 2019). There were more entire (non-castrated) male dogs in the group with meniscal injury (n=5) compared to without meniscal injury (n=1). There were also less entire females in the meniscal injury group (n= 0) than the non-meniscal injury group (n=2). Sex hormones have been found to interact with the expression and activity of GR (Bourke et al., 2012). Estradiol has been found to decrease GR expression in cells, and progesterone can agonise a protein (FKBP5) that can block GR translocation from the cytoplasm to cell nucleus (Krishnan et al., 2001). Testosterone and estradiol can increase the expression of another protein, steroid receptor coactivator-1, that facilitates GRE related gene expression (Charlier et al., 2006). Testosterone, however, has also been found to have an inhibitory effect on the HPA axis (Rubinow et al., 2005). It is possible that the differences in the signalment of the dogs in terms of their sex and neuter status has therefore had an impact on GRE expression, which could be taken into consideration in future studies, ensuring a balance of the sex of dogs between groups.

The GR, as well as binding to GRE to activate transcription, can also bind to other response elements that were also examined in this study, leading to the regulation of the expression of other genes (Necela and Cidlowski, 2004). It can inhibit the expression of genes mediated by activator protein 1 (AP-1) and Nuclear factor-kappa B (NFkB), and enhances STAT regulated gene transcription (Necela and Cidlowski, 2004). AP1- RE, however, was found to be upregulated upon stimulation with canine SF with meniscal injury. AP-1 is involved in a number of cellular processes, such as cellular growth, proliferation, senescence,

differentiation and apoptosis (Shaulian and Karin, 2002). AP-1 is a key mediator of cytokine signalling, and is needed for the activation of several pro-inflammatory genes (Wisdom, 1999). Cytokines and growth factors such as TNFα and EGF have been found to stimulate AP-1 via their association with their respective receptors (Westwick *et al*., 1994).

EGF can also stimulate upregulation of the third response element found to be increased upon stimulation with the canine SF, namely serum response element (SRE), via EGF receptor signalling to the mitogen activated protein kinase (MAPK)/ERK pathways (Lowe Jr *et al*., 1997). Although TNFα concentrations were unable to be elucidated in this study, ELISA examining EGF concentrations in the canine SF was successful. Although there was a general increase in EGF in the meniscal injury samples, this was not significant (p=0.27), although the sample sizes were small with eight per group.

4.4.2. Exploration of protein abundances in canine SF with CCLR depending on meniscal injury status

The study of the proteins histidine rich glycoprotein, tenascin C and cartilage acidic protein 1 were part of an exploratory investigation based on previous findings of these proteins having higher abundance in human knee joint SF with OA, and having the highest mean significant detection in meniscal tissue secretome compared to other tissue types (Timur *et al*., 2021). The hypothesis was that with damage to the meniscal tissue, these proteins could be increased in the canine SF. Previous reports of the concentrations of these proteins within canine SF are lacking in the literature. As both tenascin C and cartilage acidic protein 1 were below the level of detection for this assay, and the lowest standard being a concentration of zero, it is possible that these were not present in the canine SF, or present in very low abundances.

Glycoproteins play a lubricating role in canine SF (Swann *et al*., 1981) and HRG has been found to have roles in immunity, clearance of necrotic cells, and angiogenesis as well as potentially acting as a prothrombotic (Poon *et al*., 2011). Histidine rich glycoprotein was detected by ELISA in the canine SF but found to not be significantly altered depending on meniscal injury status.

4.4.3. Limitations

The canine SF samples were from dogs undergoing surgery for CCLR. Therefore, they had multiple pathologies within the joint that could have confounding effects on the proteome, including CCLR and OA. The examination of the effects of meniscal injury on the pathways and proteins studied could have been affected by these factors. Another limitation is the relatively small sample size, with eight to sixteen samples per group depending on the test being carried out. Furthermore, due to a limited volume of SF per donor, the ELISAs carried out on TNFα and EGF were from separate dogs to those carried out on the other proteins, so direct comparisons between these biological replicates could not be made.

4.5. Conclusions

The findings of differentially regulated response elements and how this relates to upstream signallers is an area for future work that could have potential in yielding definitive biomarkers of meniscal injury within SF.

5. General discussion

Meniscal injuries are a cause of pain and lameness in both dogs and humans (Krupkova *et al*., 2018). In dogs, meniscal injuries and LMI after CCLR stabilisation surgery can be a challenge to diagnose in veterinary practice, with current non-surgical means of diagnosis being either expensive, needing specialised equipment or technical skill, and/or being relatively insensitive (Mahn *et al*., 2005, Arnault *et al*., 2009, Tivers *et al*., 2009). This thesis has investigated the possibility of using NMR metabolomic techniques to identify differentially abundant metabolites within the stifle joint SF of dogs with CCLR in order to examine whether any metabolite could be a potential biomarker for meniscal injuries (Clarke *et al*., 2020).

The hypothesis set out at the start of this thesis was that the NMR metabolomic profile of canine stifle joint synovial fluid will differ depending on the presence of meniscal injuries in dogs with CCLR. It was also hypothesised that this difference in the canine SF metabolome could then identify potential metabolite biomarker(s) that could be used to develop a simple, minimally invasive diagnostic test for meniscal injuries in dogs. Over the course of this thesis, it has been shown that the NMR metabolomic profile differs in canine stifle joint SF from dogs with CCLR depending on the presence of meniscal injuries (Chapter 3). As mobile lipids were differentially abundant depending on meniscal injury status, a lipidomic study was carried out on a subset of samples to elucidate whether any lipid species could be used as a diagnostic biomarker. No lipid was found to be significantly altered to the degree that it could be reliably used as a diagnostic biomarker, although statistical power could be improved by increasing the sample size in the lipidomic study. Other sources of biomarkers were investigated, including proteins, TNFα, EGF and cortisol, although none were found to be significantly different depending on meniscal injury status.

5.1. Using canine stifle joint synovial fluid to develop a diagnostic test for meniscal injuries in dogs with cranial cruciate ligament rupture

In clinical practice, there is often a variety of times between sample collection and laboratory processing. In order to develop any potential diagnostic test, it is important to understand how these delays between collection and processing could affect metabolites with SF (Bernini *et al*., 2011). Previous studies have examined pre-processing delays in metabolome of serum and urine (Bernini *et al*., 2011), but optimisation studies on SF have focused on

other important factors, such as how different methods of centrifugation and freezing affects the metabolome (Anderson *et al*., 2020).

To first investigate the effect of different times from collection to processing of SF, in Chapter 2 of this thesis I have presented the first study investigating whether the ^{1}H NMR metabolomic profiles of both equine and canine SF change with increased length of refrigerated storage time pre-processing.

It was found that the metabolome of equine and canine SF has relatively few significant alterations in metabolites for the first 48 hours of storage at 4°C before centrifugation and freezing prior to NMR spectroscopy. With the equine SF, taken post-mortem from a horse with no gross pathological changes to the metacarpophalangeal joint, the SF remained relatively stable for up to 48 hours of refrigerated storage pre-processing. In the canine SF, evidence of glycolysis was seen within 48 hours, but only two out of 52 metabolites assigned to the spectra became significantly differentially abundant over this time period. Between 48 hours and one week of storage time, further changes were seen in the canine SF metabolome, concluding that samples stored over 48 hours before processing should be excluded from future studies.

It is unknown whether the differences between the equine and canine SF findings were due to species differences, or due to the fact that the equine fluid was collected post-mortem (Donaldson and Lamont, 2015), and the canine SF was from a dog with joint pathologies of CCLR and OA .

The findings of this optimisation study therefore hold importance for future metabolomic studies of SF, as well as potential development of any diagnostic tests using canine and equine SF, as short delays of less than 48 hours from collection to processing were not found to have large effects on the metabolome. The findings also impacted the inclusion of clinical samples of canine SF up to 48 hours of refrigerated storage pre-processing with the remaining chapters of this thesis.

5.2. The metabolomic profile of canine stifle joint synovial fluid from dogs with CCLR differs depending on the presence of meniscal injuries

The hypothesis that the metabolomic profile of canine SF will differ depending on the presence of CCLR and meniscal injuries was proven in Chapter three of this thesis. In Chapter

three, the first study of its kind to examine metabolomic and lipidomic changes in canine stifle joint SF with CCLR depending on the presence of meniscal injuries is presented. There have been no previous studies examining the changes in metabolome of SF specifically depending on the presence of meniscal injury in any species. This study is also novel in the number and scale of canine participants, with 65 SF samples from dogs with CCLR and meniscal injury and 72 SF samples from dogs with CCLR without meniscal injury. Due to this well profiled set of samples, differences in the metabolome depending on clinical features such as age, weight and sex were also able to be examined within the canine SF for the first time.

One finding of interest was that of an increase in mobile lipids between groups. Mobile lipids are NMR visible lipid resonances arising from relatively non-restricted molecules, such as methyl and methylene groups belonging to lipid acyl chains (Delikatny *et al*., 2011). Lipids have gained increasing attention over recent years in their crucial role in a number of biological processes, such as cell necrosis and apoptosis, malignancy, inflammation, and energy metabolism (Hakumäki and Kauppinen, 2000). Meniscal injuries could lead to an increase in lipid concentration in SF due to a number of possible mechanisms, including damage to phospholipid membranes (Uysal *et al*., 2008), release of lipid droplets from cells as mediators of inflammation (Melo *et al*., 2011), or increased lipid production by fibroblast like synoviocytes in order to aid with joint lubrication (Sluzalska *et al*., 2017).

To validate the findings of NMR mobile lipid increases in canine SF with meniscal injury in comparison to canine SF with CCLR but no meniscal injury, a subset of 26 samples (n=13 of each group) underwent NMR spectroscopy on SF lipid extracts. It was generally observed that there was an increase in the majority of lipids in the canine stifle joint SF with meniscal injury compared to without meniscal injury. Although no lipid reached statistical significance between groups, one lipid species of interest with the greatest fold change between groups appears to be a phospholipid species with a choline head group, namely phosphatidylcholine. This lipid has been found to be the most abundant within animal cells (Vance, 2015), with a role in lubrication within SF (Siódmiak *et al*., 2017) as well being a main component of cell membranes and playing a role in lipoprotein production and cellular signalling (van der Veen *et al*., 2017).

As the first study to highlight lipid abnormalities within canine stifle joints with CCLR and meniscal injuries, the findings highlight areas for potential future work to examine in more detail the mechanisms related to these changes.

5.3. Differential expression of response elements and their upstream signallers in canine SF with CCLR with and without meniscal injuries

To investigate alternative sources of biomarkers, and to improve the understanding of signalling pathways that are altered in the presence of meniscal injuries, a study examining the upregulation of certain response elements within canine SF with and without meniscal injuries was carried out. Of the thirteen response elements investigated, three were found to be significantly upregulated upon stimulation with canine SF with CCLR and meniscal injuries compared to CCLR without meniscal injury. These were GRE, AP1-RE and SRE. Upstream signallers for these pathways include glucocorticoids, cytokine and growth factor signalling, and growth factor signalling respectively. In order to investigate upstream signallers for these pathways, ELISAs examining TNFα, EGF and cortisol were undertaken on the canine SF. Of these, TNFα failed to reach the lower limit of detection for the assay, and neither EGF nor cortisol were significantly different between groups. Previous studies have found an increase in TNFα in human meniscal tear tissue (Ogura *et al*., 2016). Also, TNFα and growth factors have been hypothesised by previous authors to be involved in the biosynthesis and release of phosphatidylcholine by fibroblast-like synoviocytes (Sluzalska *et al*., 2017). TNFα can also upregulate the production of cortisol from cortisone via the enzyme 11βHSD1 (Loerz and Maser, 2017). It is also known that glucocorticoids can have an effect on lipid metabolism, with an acute increase in cortisol levels leading to lipolysis (Djurhuus *et al*., 2002), potentially linking with the results of increased lipids observed in Chapter three. However, as ELISAs did not find significant differences between groups with any of the upstream signallers studied, further work to elucidate the mechanisms behind these upregulated pathways is required.

5.4. Investigation of proteins within canine SF with CCLR depending on meniscal injury status

An additional study in Chapter four was undertaken to examine whether proteins that have previously been found to be increased in the protein secretome of meniscal tissue compared to other joint structures were significantly raised in the canine SF with meniscal injury (Timur *et al*., 2021). One protein that was detected by ELISA in the canine SF was HRG, but this was not statistically different between groups. Further work, potentially utilising more sensitive methods of protein detection such as mass spectrometry, could be of use to investigate protein biomarkers of meniscal injury within SF in the future (Peffers *et al*., 2015).

5.5. Future work

Several areas for future work in the detection of biomarkers of CCLR and meniscal injury have been highlighted by this study. Firstly, increasing the number of canine SF samples from non-CCLR affected dogs within the NMR metabolomics study could allow for greater exploration of metabolite biomarkers of CCLR, increasing our knowledge of the metabolite pathways that become altered with CCLR in dogs. Secondly, increasing the number of canine SF samples included in the NMR lipidomics study could increase the power of this study, potentially increasing the likelihood of statistically significant findings (Riffenburgh, 2012). Thirdly, future work examining the relevance of the upregulated response elements and their associated pathways in meniscal injury would be of benefit. This could involve further analysis of cytokines and growth factors within the SF samples, using increased sample numbers and further methods of detecting cortisol and proteins within the SF, such as mass spectrometry (Lee *et al*., 2014, Peffers *et al*., 2015). As no reliable biomarker for the diagnosis of meniscal injuries exists in other species, including humans, NMR metabolomic and lipidomic studies using SF from human subjects with and without meniscal injuries could be of use to examine whether these finding are translatable to human medicine.

5.6. Conclusions

Within this thesis, NMR spectroscopy has been successfully used for the first time to determine differences in the metabolome of canine stifle joint SF from dogs with CCLR depending on the presence of meniscal injuries. Mobile lipids were found to be significantly increased in canine stifle joint SF with CCLR and meniscal injury compared to CCLR without meniscal injury. To investigate the lipidome of canine SF with CCLR with and without meniscal injury further, a subset of samples underwent lipid extraction and NMR lipidomics. Although no lipids were found to be statistically significantly differentially abundant in this subset, it was found that the majority of lipid species were increased in the canine SF with CCLR and meniscal injury. Furthermore, signalling pathways relating to glucocorticoids, cytokines and growth factors were found to be significantly altered between groups, although the examination of upstream signallers TNFα, EGF and cortisol were not found to be significantly altered between groups.

The findings of increased lipids within canine stifle joint SF with CCLR depending on meniscal injury is of interest in future work focusing on biomarker discovery for meniscal injuries.

6. References

ADACHI, N., OCHI, M., UCHIO, Y., IWASA, J., RYOKE, K. & KURIWAKA, M. 2002. Mechanoreceptors in the anterior cruciate ligament contribute to the joint position sense. *Acta Orthopaedica Scandinavica,* 73**,** 330-334.

ADAMS, M. E. & BRANDT, K. D. 1991. Hypertrophic repair of canine articular cartilage in osteoarthritis after anterior cruciate ligament transection. *J Rheumatol,* 18**,** 428-35.

ADAMS, P., BOLUS, R., MIDDLETON, S., MOORES, A. P. & GRIERSON, J. 2011. Influence of signalment on developing cranial cruciate rupture in dogs in the UK. *J Small Anim Pract,* 52**,** 347-52.

ADAMS, S. B., NETTLES, D. L., JONES, L. C., MILLER, S. D., GUYTON, G. P. & SCHON, L. C. 2014. Inflammatory Cytokines and Cellular Metabolites as Synovial Fluid Biomarkers of Posttraumatic Ankle Arthritis. *Foot & Ankle International,* 35**,** 1241-1249.

AHMED, S., DUBEY, D., CHOWDHURY, A., CHAURASIA, S., GULERIA, A., KUMAR, S., SINGH, R., KUMAR, D. & MISRA, R. 2019. Nuclear magnetic resonance-based metabolomics reveals similar metabolomics profiles in undifferentiated peripheral spondyloarthritis and reactive arthritis. *International Journal of Rheumatic Diseases,* 22**,** 725-733.

AHN, J. K., KIM, J., CHEONG, Y. E., KIM, K. H. & CHA, H. S. 2020. Variation in the synovial fluid metabolome according to disease activity of rheumatoid arthritis. *Clin Exp Rheumatol,* 38**,** 500-507.

AHN, J. K., KIM, S., KIM, J., HWANG, J., KIM, K. H. & CHA, H.-S. 2015. A Comparative Metabolomic Evaluation of Behcet's Disease with Arthritis and Seronegative Arthritis Using Synovial Fluid. *PLOS ONE,* 10**,** e0135856.

AKGUN, U., KOCAOGLU, B., ORHAN, E. K., BASLO, M. B. & KARAHAN, M. 2008. Possible reflex pathway between medial meniscus and semimembranosus muscle: an experimental study in rabbits. *Knee Surg Sports Traumatol Arthrosc,* 16**,** 809-14.

AKHBARI, P., JAGGARD, M. K., BOULANGÉ, C. L., VAGHELA, U., GRAÇA, G., BHATTACHARYA, R., LINDON, J. C., WILLIAMS, H. R. T. & GUPTE, C. M. 2019. Differences in the composition of hip and knee synovial fluid in osteoarthritis: a nuclear magnetic resonance (NMR) spectroscopy study of metabolic profiles. *Osteoarthritis and Cartilage,* 27**,** 1768-1777.

AKRAM, M. 2013. Mini-review on Glycolysis and Cancer. *Journal of Cancer Education,* 28**,** 454-457.

AMIEL, D., FRANK, C., HARWOOD, F., FRONEK, J. & AKESON, W. 1984. Tendons and ligaments: a morphological and biochemical comparison. *J Orthop Res,* 1**,** 257-65.

AN, Z., SHI, C., LI, P. & LIU, L. 2021. Stability of amino acids and related amines in human serum under different preprocessing and pre-storage conditions based on iTRAQ®-LC-MS/MS. *Biology Open,* 10.

ANCKAR, J. & SISTONEN, L. 2011. Regulation of HSF1 function in the heat stress response: implications in aging and disease. *Annu Rev Biochem,* 80**,** 1089-115.

ANDERSON, D., NEWMAN, A. & DANIELS, A. 1993. In vitro load transmission in the canine knee: the effect of medial meniscectomy and varus rotation. *Knee Surgery, Sports Traumatology, Arthroscopy,* 1**,** 44-50.

ANDERSON, J. R., CHOKESUWATTANASKUL, S., PHELAN, M. M., WELTING, T. J. M., LIAN, L. Y., PEFFERS, M. J. & WRIGHT, H. L. 2018a. (1)H NMR Metabolomics Identifies Underlying Inflammatory Pathology in Osteoarthritis and Rheumatoid Arthritis Synovial Joints. *J Proteome Res,* 17**,** 3780-3790.

ANDERSON, J. R., PHELAN, M. M., CLEGG, P. D., PEFFERS, M. J. & RUBIO-MARTINEZ, L. M. 2018b. Synovial Fluid Metabolites Differentiate between Septic and Nonseptic Joint Pathologies. *Journal of proteome research,* 17**,** 2735-2743.

ANDERSON, J. R., PHELAN, M. M., RUBIO-MARTINEZ, L. M., FITZGERALD, M. M., JONES, S. W., CLEGG, P. D. & PEFFERS, M. J. 2020. Optimization of Synovial Fluid Collection and Processing for NMR Metabolomics and LC-MS/MS Proteomics. *Journal of Proteome Research,* 19**,** 2585-2597.

ANDERSON, K. L., O'NEILL, D. G., BRODBELT, D. C., CHURCH, D. B., MEESON, R. L., SARGAN, D., SUMMERS, J. F., ZULCH, H. & COLLINS, L. M. 2018c. Prevalence, duration and risk factors for appendicular osteoarthritis in a UK dog population under primary veterinary care. *Scientific Reports,* 8**,** 5641.

ANTONACCI, J. M., SCHMIDT, T. A., SERVENTI, L. A., CAI, M. Z., SHU, Y. L., SCHUMACHER, B. L., MCILWRAITH, C. W. & SAH, R. L. 2012. Effects of equine joint injury on boundary lubrication of articular cartilage by synovial fluid: role of hyaluronan. *Arthritis Rheum,* 64**,** 2917-26.

ARCAND, M. A., RHALMI, S. & RIVARD, C. H. 2000. Quantification of mechanoreceptors in the canine anterior cruciate ligament. *International Orthopaedics,* 24**,** 272-275.

ARNAULT, F., CAUVIN, E., VIGUIER, E., KRAFT, E., SONET, J. & CAROZZO, C. 2009. Diagnostic value of ultrasonography to assess stifle lesions in dogs after cranial cruciate ligament rupture : 13 cases. *Vet Comp Orthop Traumatol,* 22**,** 479-485.

ARNOCZKY, S., MARSHALL, J., JOSEPH, A., JAHRE, C. & YOSHIOKA, M. 1980. Meniscal diffusion–an experimental study in the dog. *Trans Orthop Res Soc,* 5**,** 42.

ARNOCZKY, S. P. & MARSHALL, J. L. 1977. The cruciate ligaments of the canine stifle: an anatomical and functional analysis. *Am J Vet Res,* 38**,** 1807-14.

ARNOCZKY, S. P. & WARREN, R. F. 1983. The microvasculature of the meniscus and its response to injury: an experimental study in the dog. *The American journal of sports medicine,* 11**,** 131-141.

ARON, D. N. 1988. Traumatic dislocation of the stifle joint: Treatment of 12 dogs and one cat. *Journal of the American Animal Hospital Association,* 24**,** 333-340.

BAIRD, A. E., CARTER, S. D., INNES, J. F., OLLIER, W. E. & SHORT, A. D. 2014. Genetic basis of cranial cruciate ligament rupture (CCLR) in dogs. *Connect Tissue Res,* 55**,** 275-81.

BAKER, L. A., MOMEN, M., MCNALLY, R., BERRES, M. E., BINVERSIE, E. E., SAMPLE, S. J. & MUIR, P. 2021. Biologically Enhanced Genome-Wide Association Study Provides Further Evidence for Candidate Loci and Discovers Novel Loci That Influence Risk of Anterior Cruciate Ligament Rupture in a Dog Model. *Front Genet,* 12**,** 593515.

BAKER, L. A., ROSA, G. J. M., HAO, Z., PIAZZA, A., HOFFMAN, C., BINVERSIE, E. E., SAMPLE, S. J. & MUIR, P. 2018. Multivariate genome-wide association analysis identifies novel and relevant variants associated with anterior cruciate ligament rupture risk in the dog model. *BMC Genetics,* 19**,** 39.

BANSAL, S., PELOQUIN, J. M., KEAH, N. M., O'REILLY, O. C., ELLIOTT, D. M., MAUCK, R. L. & ZGONIS, M. H. 2020. Structure, function, and defect tolerance with maturation of the radial tie fiber network in the knee meniscus. *J Orthop Res,* 38**,** 2709-2720.

BARGER, B., PIAZZA, A. & MUIR, P. 2016. Treatment of stable partial cruciate rupture (Grade 1 sprain) in five dogs with tibial plateau levelling osteotomy. *Veterinary Record Case Reports,* 4**,** e000315.

BENNETT, D. & MAY, C. 1991. Meniscal damage associated with cruciate disease in the dog. *Journal of Small Animal Practice,* 32**,** 111-117.

BERENBAUM, F. & WALKER, C. 2020. Osteoarthritis and inflammation: a serious disease with overlapping phenotypic patterns. *Postgraduate Medicine,* 132**,** 377-384.

BERNINI, P., BERTINI, I., LUCHINAT, C., NINCHERI, P., STADERINI, S. & TURANO, P. 2011. Standard operating procedures for pre-analytical handling of blood and urine for metabolomic studies and biobanks. *Journal of Biomolecular NMR,* 49**,** 231-243.

BEXFIELD, N. & LEE, K. 2014. *BSAVA Guide to Procedures in Small Animal Practice,* Gloucester, UNITED KINGDOM, British Small Animal Veterinary Association (B S A V A).

BIGONI, M., TURATI, M., SACERDOTE, P., GADDI, D., PIATTI, M., CASTELNUOVO, A., FRANCHI, S., GANDOLLA, M., PEDROCCHI, A., OMELJANIUK, R. J., BRESCIANI, E., LOCATELLI, V. & TORSELLO, A. 2017. Characterization of synovial fluid cytokine profiles in chronic meniscal tear of the knee. *Journal of Orthopaedic Research,* 35**,** 340-346.

BILLE, C., AUVIGNE, V., LIBERMANN, S., BOMASSI, E., DURIEUX, P. & RATTEZ, E. 2012. Risk of anaesthetic mortality in dogs and cats: an observational cohort study of 3546 cases. *Veterinary anaesthesia and analgesia,* 39**,** 59-68.

BIOMARKERS DEFINITIONS WORKING GROUP 2001. Biomarkers and surrogate endpoints: Preferred definitions and conceptual framework. *Clinical Pharmacology & Therapeutics,* 69**,** 89-95.

BIRD, M. D. & SWEET, M. B. 1988. Canals in the semilunar meniscus: brief report. *The Journal of Bone and Joint Surgery. British volume,* 70-B**,** 839-839.

BLEEDORN, J. A., GREUEL, E. N., MANLEY, P. A., SCHAEFER, S. L., MARKEL, M. D., HOLZMAN, G. & MUIR, P. 2011. Synovitis in dogs with stable stifle joints and incipient cranial cruciate ligament rupture: a cross-sectional study. *Vet Surg,* 40**,** 531-43.

BLEWIS, M., NUGENT-DERFUS, G., SCHMIDT, T., SCHUMACHER, B. & SAH, R. 2007. A model of synovial fluid lubricant composition in normal and injured joints. *Eur Cell Mater,* 13**,** 26-39.

BLOND, L., THRALL, D. E., ROE, S. C., CHAILLEUX, N. & ROBERTSON, I. D. 2008. Diagnostic accuracy of magnetic resonance imaging for meniscal tears in dogs affected with naturally occuring cranial cruciate ligament rupture. *Vet Radiol Ultrasound,* 49**,** 425-31.

BODENHAUSEN, G., FREEMAN, R., NIEDERMEYER, R. & TURNER, D. L. 1977. Double Fourier transformation in high-resolution NMR. *Journal of Magnetic Resonance (1969),* 26**,** 133-164.

BOFFA, A., MERLI, G., ANDRIOLO, L., LATTERMANN, C., SALZMANN, G. M. & FILARDO, G. 2020. Synovial fluid biomarkers in knee osteoarthritis: a systematic review and quantitative evaluation using BIPEDs criteria. *Cartilage***,** 1947603520942941.

BOGAERTS, E., VAN DER VEKENS, E., VERHOEVEN, G., DE ROOSTER, H., VAN RYSSEN, B., SAMOY, Y., PUTCUYPS, I., VAN TILBURG, J., DEVRIENDT, N., WEEKERS, F., BERTAL, M., HOUDELLIER, B., SCHEEMAEKER, S., VERSTEKEN, J., LAMERAND, M., FEENSTRA, L., PEELMAN, L., NIEUWERBURGH, F. V., SAUNDERS, J. H. & BROECKX, B. J. G. 2018. Intraobserver and interobserver agreement on the radiographical diagnosis of canine cranial cruciate ligament rupture. *Vet Rec,* 182**,** 484.

BOLAND, L., DANGER, R., CABON, Q., RABILLARD, M., BROUARD, S., BOUVY, B. & GAUTHIER, O. 2014. MMP-2 as an early synovial biomarker for cranial cruciate ligament disease in dogs. *Vet Comp Orthop Traumatol,* 27**,** 210-215.

BÖTTCHER, P., BRÜHSCHWEIN, A., WINKELS, P., WERNER, H., LUDEWIG, E., GREVEL, V. & OECHTERING, G. 2010. Value of low-field magnetic resonance imaging in diagnosing meniscal tears in the canine stifle: a prospective study evaluating sensitivity and specificity in naturally occurring cranial cruciate ligament deficiency with arthroscopy as the gold standard. *Vet Surg,* 39**,** 296-305.

BOURKE, C. H., HARRELL, C. S. & NEIGH, G. N. 2012. Stress-induced sex differences: Adaptations mediated by the glucocorticoid receptor. *Hormones and Behavior,* 62**,** 210-218.

BROPHY, R. H., SANDELL, L. J., CHEVERUD, J. M. & RAI, M. F. 2017a. Gene expression in human meniscal tears has limited association with early degenerative changes in knee articular cartilage. *Connective Tissue Research,* 58**,** 295-304.

BROPHY, R. H., SANDELL, L. J. & RAI, M. F. 2017b. Traumatic and Degenerative Meniscus Tears Have Different Gene Expression Signatures. *Am J Sports Med,* 45**,** 114-120.

BRYDGES, N. M., ARGYLE, D. J., MOSLEY, J. R., DUNCAN, J. C., FLEETWOOD-WALKER, S. & CLEMENTS, D. N. 2012. Clinical assessments of increased sensory sensitivity in dogs with cranial cruciate ligament rupture. *The Veterinary Journal,* 193**,** 545-550.

BUJAK, R., STRUCK-LEWICKA, W., MARKUSZEWSKI, M. J. & KALISZAN, R. 2015. Metabolomics for laboratory diagnostics. *Journal of Pharmaceutical and Biomedical Analysis,* 113**,** 108-120.

BULLOUGH, P. G., MUNUERA, L., MURPHY, J. & WEINSTEIN, A. M. 1970. The strength of the menisci of the knee as it relates to their fine structure. *J Bone Joint Surg Br,* 52**,** 564-7.

BURKS, R. T., HAUT, R. C. & LANCASTER, R. L. 1990. Biomechanical and histological observations of the dog patellar tendon after removal of its central one-third. *Am J Sports Med,* 18**,** 146-53.

CARLSON, A. K., RAWLE, R. A., ADAMS, E., GREENWOOD, M. C., BOTHNER, B. & JUNE, R. K. 2018. Application of global metabolomic profiling of synovial fluid for osteoarthritis biomarkers. *Biochem Biophys Res Commun,* 499**,** 182-188.

CARLSON, A. K., RAWLE, R. A., WALLACE, C. W., ADAMS, E., GREENWOOD, M. C., BOTHNER, B. & JUNE, R. K. 2019a. Global metabolomic profiling of human synovial fluid for rheumatoid arthritis biomarkers. *Clin Exp Rheumatol,* 37**,** 393-399.

CARLSON, A. K., RAWLE, R. A., WALLACE, C. W., BROOKS, E. G., ADAMS, E., GREENWOOD, M. C., OLMER, M., LOTZ, M. K., BOTHNER, B. & JUNE, R. K. 2019b. Characterization of synovial fluid metabolomic phenotypes of cartilage morphological changes associated with osteoarthritis. *Osteoarthritis Cartilage,* 27**,** 1174-1184.

CARPENTER JR, D. H. & COOPER, R. C. 2000. Mini Review of Canine Stifle Joint Anatomy. *Anatomia, Histologia, Embryologia,* 29**,** 321-329.

CARR, H. Y. & PURCELL, E. M. 1954. Effects of diffusion on free precession in nuclear magnetic resonance experiments. *Physical Review,* 94**,** 630-638.

CARTER, M. & SHIEH, J. 2015. Chapter 15 - Biochemical Assays and Intracellular Signaling. *In:* CARTER, M. & SHIEH, J. (eds.) *Guide to Research Techniques in Neuroscience (Second Edition).* San Diego: Academic Press.

CASE, J. B., HULSE, D., KERWIN, S. C. & PEYCKE, L. E. 2008. Meniscal injury following initial cranial cruciate ligament stabilization surgery in 26 dogs (29 stifles). *Vet Comp Orthop Traumatol,* 21**,** 365-7.

CHARLIER, T. D., BALL, G. F. & BALTHAZART, J. 2006. Plasticity in the expression of the steroid receptor coactivator 1 in the Japanese quail brain: Effect of sex, testosterone, stress and time of the day. *Neuroscience,* 140**,** 1381-1394.

CHEUNG, A. P. & OLSON, L. L. 1990. 1H-NMR assay of phosphatidylcholine and phosphatidylethanolamine in AL721. *Journal of Pharmaceutical and Biomedical Analysis,* 8**,** 729-734.

CHRISTOPHER, S. A., BEETEM, J. & COOK, J. L. 2013. Comparison of Long-Term Outcomes Associated With Three Surgical Techniques for Treatment of Cranial Cruciate Ligament Disease in Dogs. *Veterinary Surgery,* 42**,** 329-334.

CHUANG, C., RAMAKER, M. A., KAUR, S., CSOMOS, R. A., KRONER, K. T., BLEEDORN, J. A., SCHAEFER, S. L. & MUIR, P. 2014. Radiographic risk factors for contralateral rupture

in dogs with unilateral cranial cruciate ligament rupture. *PloS one,* 9**,** e106389-e106389.
CLAIR, A. J., KINGERY, M. T., ANIL, U., KENNY, L., KIRSCH, T. & STRAUSS, E. J. 2019. Alterations in Synovial Fluid Biomarker Levels in Knees With Meniscal Injury as Compared With Asymptomatic Contralateral Knees. *The American Journal of Sports Medicine,* 47**,** 847-856.
CLARKE, E. J., ANDERSON, J. R. & PEFFERS, M. J. 2020. Nuclear magnetic resonance spectroscopy of biofluids for osteoarthritis. *British Medical Bulletin,* 137**,** 28-41.
COMERFORD, E., FORSTER, K., GORTON, K. & MADDOX, T. 2013. Management of cranial cruciate ligament rupture in small dogs: a questionnaire study. *Vet Comp Orthop Traumatol,* 26**,** 493-7.
COMERFORD, E. J., SMITH, K. & HAYASHI, K. 2011. Update on the aetiopathogenesis of canine cranial cruciate ligament disease. *Vet Comp Orthop Traumatol,* 24**,** 91-8.
COMERFORD, E. J., TARLTON, J. F., AVERY, N. C., BAILEY, A. J. & INNES, J. F. 2006. Distal femoral intercondylar notch dimensions and their relationship to composition and metabolism of the canine anterior cruciate ligament. *Osteoarthritis Cartilage,* 14**,** 273-8.
COMERFORD, E. J., TARLTON, J. F., INNES, J. F., JOHNSON, K. A., AMIS, A. A. & BAILEY, A. J. 2005. Metabolism and composition of the canine anterior cruciate ligament relate to differences in knee joint mechanics and predisposition to ligament rupture. *Journal of Orthopaedic Research,* 23**,** 61-66.
COOK, J. L., LUTHER, J. K., BEETEM, J., KARNES, J. & COOK, C. R. 2010. Clinical comparison of a novel extracapsular stabilization procedure and tibial plateau leveling osteotomy for treatment of cranial cruciate ligament deficiency in dogs. *Vet Surg,* 39**,** 315-23.
COSTA DOS SANTOS JUNIOR, G., PEREIRA, C. M., KELLY DA SILVA FIDALGO, T. & VALENTE, A. P. 2020. Saliva NMR-based metabolomics in the war against COVID-19. *Analytical Chemistry,* 92**,** 15688-15692.
COX, J. S., NYE, C. E., SCHAEFER, W. W. & WOODSTEIN, I. J. 1975. The degenerative effects of partial and total resection of the medial meniscus in dogs' knees. *Clinical orthopaedics and related research***,** 178-183.
CROVACE, A., LACITIGNOLA, L., MIOLO, A. & FANIZZI, F. P. 2006. Surgery plus chondroprotection for canine cranial cruciate ligament (CCL) rupture. *Vet Comp Orthop Traumatol,* 19**,** 239-245.
CRUZAT, V., MACEDO ROGERO, M., NOEL KEANE, K., CURI, R. & NEWSHOLME, P. 2018. Glutamine: Metabolism and Immune Function, Supplementation and Clinical Translation. *Nutrients,* 10**,** 1564.
DAMYANOVICH, A. Z., STAPLES, J. R., CHAN, A. D. & MARSHALL, K. W. 1999a. Comparative study of normal and osteoarthritic canine synovial fluid using 500 MHz 1H magnetic resonance spectroscopy. *J Orthop Res,* 17**,** 223-31.
DAMYANOVICH, A. Z., STAPLES, J. R., CHAN, A. D. M. & MARSHALL, K. W. 1999b. Comparative study of normal and osteoarthritic canine synovial fluid using 500 MHz 1H magnetic resonance spectroscopy. *Journal of Orthopaedic Research,* 17**,** 223-231.
DAMYANOVICH, A. Z., STAPLES, J. R. & MARSHALL, K. W. 1999c. 1H NMR investigation of changes in the metabolic profile of synovial fluid in bilateral canine osteoarthritis with unilateral joint denervation. *Osteoarthritis and Cartilage,* 7**,** 165-172.
DAMYANOVICH, A. Z., STAPLES, J. R. & MARSHALL, K. W. 2000. The effects of freeze/thawing on human synovial fluid observed by 500 MHz 1H magnetic resonance spectroscopy. *The Journal of rheumatology,* 27**,** 746-752.

DE BAKKER, E., STROOBANTS, V., VANDAEL, F., VAN RYSSEN, B. & MEYER, E. 2017. Canine synovial fluid biomarkers for early detection and monitoring of osteoarthritis. *Veterinary Record,* 180**,** 328-329.

DE BRUIN, T., DE ROOSTER, H., BOSMANS, T., DUCHATEAU, L., VAN BREE, H. & GIELEN, I. 2007a. Radiographic assessment of the progression of osteoarthrosis in the contralateral stifle joint of dogs with a ruptured cranial cruciate ligament. *Vet Rec,* 161**,** 745-50.

DE BRUIN, T., DE ROOSTER, H., VAN BREE, H. & COX, E. 2007b. Evaluation of anticollagen type I antibody titers in synovial fluid of both stifle joints and the left shoulder joint of dogs with unilateral cranial cruciate disease. *Am J Vet Res,* 68**,** 283-9.

DE BRUIN, T., DE ROOSTER, H., VAN BREE, H., DUCHATEAU, L. & COX, E. 2007c. Cytokine mRNA expression in synovial fluid of affected and contralateral stifle joints and the left shoulder joint in dogs with unilateral disease of the stifle joint. *American Journal of Veterinary Research,* 68**,** 953-961.

DE ROOSTER, H., COX, E. & BREE, H. V. 2000. Prevalence and relevance of antibodies to type-I and-II collagen in synovial fluid of dogs with cranial cruciate ligament damage. *American journal of veterinary research,* 61**,** 1456-1461.

DE SOUSA, E. B., DOS SANTOS JUNIOR, G. C., AGUIAR, R. P., DA COSTA SARTORE, R., DE OLIVEIRA, A. C. L., ALMEIDA, F. C. L., NETO, V. M. & AGUIAR, D. P. 2019. Osteoarthritic Synovial Fluid Modulates Cell Phenotype and Metabolic Behavior In Vitro. *Stem Cells International,* 2019**,** 8169172.

DELIKATNY, E. J., CHAWLA, S., LEUNG, D.-J. & POPTANI, H. 2011. MR-visible lipids and the tumor microenvironment. *NMR in Biomedicine,* 24**,** 592-611.

DESJARDIN, C., RIVIERE, J., VAIMAN, A., MORGENTHALER, C., DIRIBARNE, M., ZIVY, M., ROBERT, C., LE MOYEC, L., WIMEL, L., LEPAGE, O., JACQUES, C., CRIBIU, E. & SCHIBLER, L. 2014. Omics technologies provide new insights into the molecular physiopathology of equine osteochondrosis. *BMC Genomics,* 15**,** 947.

DIETERLE, F., ROSS, A., SCHLOTTERBECK, G. & SENN, H. 2006. Probabilistic Quotient Normalization as Robust Method to Account for Dilution of Complex Biological Mixtures. Application in 1H NMR Metabonomics. *Analytical Chemistry,* 78**,** 4281-4290.

DILLON, D. E., GORDON-EVANS, W. J., GRIFFON, D. J., KNAP, K. M., BUBB, C. L. & EVANS, R. B. 2014. Risk factors and diagnostic accuracy of clinical findings for meniscal disease in dogs with cranial cruciate ligament disease. *Vet Surg,* 43**,** 446-50.

DING, J., NIU, X., SU, Y. & LI, X. 2017. Expression of synovial fluid biomarkers in patients with knee osteoarthritis and meniscus injury. *Exp Ther Med,* 14**,** 1609-1613.

DJURHUUS, C. B., GRAVHOLT, C. H., NIELSEN, S., MENGEL, A., CHRISTIANSEN, J. S., SCHMITZ, O. E. & MØLLER, N. 2002. Effects of cortisol on lipolysis and regional interstitial glycerol levels in humans. *American Journal of Physiology-Endocrinology and Metabolism,* 283**,** E172-E177.

DONALDSON, A. E. & LAMONT, I. L. 2015. Metabolomics of post-mortem blood: identifying potential markers of post-mortem interval. *Metabolomics,* 11**,** 237-245.

DORAL, M. N., BILGE, O., HURI, G., TURHAN, E. & VERDONK, R. 2018. Modern treatment of meniscal tears. *EFORT Open Reviews,* 3**,** 260-268.

DOROKHOV, Y. L., SHINDYAPINA, A. V., SHESHUKOVA, E. V. & KOMAROVA, T. V. 2015. Metabolic Methanol: Molecular Pathways and Physiological Roles. *Physiological Reviews,* 95**,** 603-644.

DUBEY, D., CHAURASIA, S., GULERIA, A., KUMAR, S., MODI, D. R., MISRA, R. & KUMAR, D. 2019. Metabolite assignment of ultrafiltered synovial fluid extracted from knee joints of reactive arthritis patients using high resolution NMR spectroscopy. *Magnetic Resonance in Chemistry,* 57**,** 30-43.

DUERR, F. M., DUNCAN, C. G., SAVICKY, R. S., PARK, R. D., EGGER, E. L. & PALMER, R. H. 2007. Risk factors for excessive tibial plateau angle in large-breed dogs with cranial cruciate ligament disease. *J Am Vet Med Assoc,* 231**,** 1688-91.

DUERR, F. M., MARTIN, K. W., RISHNIW, M., PALMER, R. H. & SELMIC, L. E. 2014. Treatment of canine cranial cruciate ligament disease. A survey of ACVS Diplomates and primary care veterinarians. *Vet Comp Orthop Traumatol,* 27**,** 478-83.

DUNHAM, J., SHACKLETON, D. R., BILLINGHAM, M. E., BITENSKY, L., CHAYEN, J. & MUIR, I. H. 1988. A reappraisal of the structure of normal canine articular cartilage. *Journal of anatomy,* 157**,** 89-99.

DYCE, K., SACK, W. & WENSING, C. 2002. The Locomotor Apparatus. 58-66. *Textbook of Veterinary Anatomy. Saunders-Elsevier Science, Philadelphia*.

EMWAS, A.-H., ROY, R., MCKAY, R. T., TENORI, L., SACCENTI, E., GOWDA, G. A. N., RAFTERY, D., ALAHMARI, F., JAREMKO, L., JAREMKO, M. & WISHART, D. S. 2019. NMR Spectroscopy for Metabolomics Research. *Metabolites,* 9**,** 123.

ESCHER, G., GALLI, I., VISHWANATH, B. S., FREY, B. M. & FREY, F. J. 1997. Tumor necrosis factor alpha and interleukin 1beta enhance the cortisone/cortisol shuttle. *The Journal of experimental medicine,* 186**,** 189-198.

ESKO, T., HIRSCHHORN, J. N., FELDMAN, H. A., HSU, Y. H., DEIK, A. A., CLISH, C. B., EBBELING, C. B. & LUDWIG, D. S. 2017. Metabolomic profiles as reliable biomarkers of dietary composition. *Am J Clin Nutr,* 105**,** 547-554.

EVANS, H. E. & DE LAHUNTA, A. 2013. *Miller's anatomy of the dog-E-Book*, Elsevier Health Sciences.

FEICHTENSCHLAGER, C., GERWING, M., FAILING, K., PEPPLER, C., KÁSA, A., KRAMER, M. & VON PÜCKLER, K. H. 2018. Magnetic Resonance Imaging Assessment of Intra-Articular Structures in the Canine Stifle Joint after Implantation of a Titanium Tibial Plateau Levelling Osteotomy Plate. *Vet Comp Orthop Traumatol,* 31**,** 261-272.

FENG, L., NIAN, S., TONG, Z., ZHU, Y., LI, Y., ZHANG, C., BAI, X., LUO, X., WU, M. & YAN, Z. 2020. Age-related trends in lipid levels: a large-scale cross-sectional study of the general Chinese population. *BMJ Open,* 10**,** e034226.

FITZPATRICK, N. & SOLANO, M. A. 2010. Predictive variables for complications after TPLO with stifle inspection by arthrotomy in 1000 consecutive dogs. *Vet Surg,* 39**,** 460-74.

FLINIAUX, O., GAILLARD, G., LION, A., CAILLEU, D., MESNARD, F. & BETSOU, F. 2011. Influence of common preanalytical variations on the metabolic profile of serum samples in biobanks. *Journal of Biomolecular NMR,* 51**,** 457-465.

FOX, D. B. & COOK, J. L. 2001. Synovial fluid markers of osteoarthritis in dogs. *Journal of the American Veterinary Medical Association,* 219**,** 756-761.

FRANKLIN, S. P., COOK, J. L., COOK, C. R., SHAIKH, L. S., CLARKE, K. M. & HOLMES, S. P. 2017a. Comparison of ultrasonography and magnetic resonance imaging to arthroscopy for diagnosing medial meniscal lesions in dogs with cranial cruciate ligament deficiency. *Journal of the American Veterinary Medical Association,* 251**,** 71-79.

FRANKLIN, S. P., COOK, J. L. & POZZI, A. 2017b. Surgical Treatment of Concurrent Meniscal Injury. *Advances in the Canine Cranial Cruciate Ligament.*

FRANKLIN, S. P., GILLEY, R. S. & PALMER, R. H. 2010. Meniscal injury in dogs with cranial cruciate ligament rupture. *Compend Contin Educ Vet,* 32**,** E1-E10.

FUJITA, Y., HARA, Y., NEZU, Y., ORIMA, H. & TAGAWA, M. 2012. Biomarkers in dogs surgically treated for ruptured cranial cruciate ligaments. *Vet Rec,* 171**,** 426.

FULMER, G. R., MILLER, A. J. M., SHERDEN, N. H., GOTTLIEB, H. E., NUDELMAN, A., STOLTZ, B. M., BERCAW, J. E. & GOLDBERG, K. I. 2010. NMR Chemical Shifts of Trace Impurities: Common Laboratory Solvents, Organics, and Gases in Deuterated Solvents Relevant to the Organometallic Chemist. *Organometallics,* 29**,** 2176-2179.

GALLOWAY, R. & LESTER, S. 1995. Histopathological evaluation of canine stifle joint synovial membrane collected at the time of repair of cranial cruciate ligament rupture. *Journal of the American Animal Hospital Association,* 31**,** 289-294.
GEELS, J. J., ROUSH, J. K., HOSKINSON, J. J. & MCLAUGHLIN, R. M. 2000. Evaluation of an intracapsular technique for the treatment of cranial cruciate ligament rupture. *Vet Comp Orthop Traumatol,* 13**,** 197-203.
GERMAN, A. J., HOLDEN, S. L., MOXHAM, G. L., HOLMES, K. L., HACKETT, R. M. & RAWLINGS, J. M. 2006. A Simple, Reliable Tool for Owners to Assess the Body Condition of Their Dog or Cat. *The Journal of Nutrition,* 136**,** 2031S-2033S.
GHADIALLY, F. N. & LALONDE, J. M. 1981. Intramatrical lipidic debris and calcified bodies in human semilunar cartilages. *J Anat,* 132**,** 481-90.
GHOSH, P. 1994. The role of hyaluronic acid (hyaluronan) in health and disease: interactions with cells, cartilage and components of synovial fluid. *Clin Exp Rheumatol,* 12**,** 75-82.
GIBSON, D. S. & ROONEY, M. E. 2007. The human synovial fluid proteome: A key factor in the pathology of joint disease. *PROTEOMICS – Clinical Applications,* 1**,** 889-899.
GILBERTSON, E. M. 1975. Development of periarticular osteophytes in experimentally induced osteoarthritis in the dog. A study using microradiographic, microangiographic, and fluorescent bone-labelling techniques. *Ann Rheum Dis,* 34**,** 12-25.
GLEASON, H. E., HUDSON, C. C. & CERRONI, B. 2020. Meniscal click in cranial cruciate deficient stifles as a predictor of specific meniscal pathology. *Veterinary Surgery,* 49**,** 155-159.
GONZALO-ORDEN, J., ALTONAGA, J., GONZALO-CORDERO, J., MILLAN, L. & ASUNCION ORDEN, M. 2001. Magnetic resonance imaging in 50 dogs with stifle lameness. *Euro J Comp Anim Pract,* 11**,** 115-118.
GRAHAM, R., ANDERSON, J. R., PHELAN, M. M., CILLAN-GARCIA, E., BLADON, B. M. & TAYLOR, S. E. 2020. Metabolomic analysis of synovial fluid from Thoroughbred racehorses diagnosed with palmar osteochondral disease using magnetic resonance imaging. *Equine Vet J,* 52**,** 384-390.
GRAHAM, S. F., HOLSCHER, C. & GREEN, B. D. 2014. Metabolic signatures of human Alzheimer's disease (AD): 1 H NMR analysis of the polar metabolome of post-mortem brain tissue. *Metabolomics,* 10**,** 744-753.
GRANET, C., MASLINSKI, W. & MIOSSEC, P. 2004. Increased AP-1 and NF-κB activation and recruitment with the combination of the proinflammatory cytokines IL-1β, tumor necrosis factor alpha and IL-17 in rheumatoid synoviocytes. *Arthritis Res Ther,* 6**,** R190.
GRIFFON, D. J., CUNNINGHAM, D., GORDON-EVANS, W. J., TANAKA, R., BRUECKER, K. A. & BOUDRIEAU, R. J. 2017. Evaluation of a scoring system based on conformation factors to predict cranial cruciate ligament disease in Labrador Retrievers. *Vet Surg,* 46**,** 206-212.
GUTHRIE, J. W., KEELEY, B. J., MADDOCK, E., BRIGHT, S. R. & MAY, C. 2012a. Effect of signalment on the presentation of canine patients suffering from cranial cruciate ligament disease. *J Small Anim Pract,* 53**,** 273-7.
GUTHRIE, J. W., KEELEY, B. J., MADDOCK, E., BRIGHT, S. R. & MAY, C. 2012b. Effect of signalment on the presentation of canine patients suffering from cranial cruciate ligament disease. *Journal of Small Animal Practice,* 53**,** 273-277.
HAKUMÄKI, J. M. & KAUPPINEN, R. A. 2000. 1H NMR visible lipids in the life and death of cells. *Trends in Biochemical Sciences,* 25**,** 357-362.
HANS, E. C., BARNHART, M. D., KENNEDY, S. C. & NABER, S. J. 2017. Comparison of complications following tibial tuberosity advancement and tibial plateau levelling

osteotomy in very large and giant dogs 50 kg or more in body weight. *Vet Comp Orthop Traumatol,* 30**,** 299-305.
HARASEN, G. 2008. Canine cranial cruciate ligament rupture in profile: 2002–2007. *The Canadian Veterinary Journal,* 49**,** 193.
HARDY, R. S., RAZA, K. & COOPER, M. S. 2014. Glucocorticoid metabolism in rheumatoid arthritis. *Annals of the New York Academy of Sciences,* 1318**,** 18-26.
HARVEY, N. D. 2021. How old is my dog? Identification of rational age groupings in pet dogs based upon normative age-linked processes. *Frontiers in Veterinary Science,* 8**,** 321.
HASIN, Y., SELDIN, M. & LUSIS, A. 2017. Multi-omics approaches to disease. *Genome Biology,* 18**,** 83.
HAYASHI, K., FRANK, J. D., DUBINSKY, C., ZHENGLING, H., MARKEL, M. D., MANLEY, P. A. & MUIR, P. 2003. Histologic changes in ruptured canine cranial cruciate ligament. *Vet Surg,* 32**,** 269-77.
HAYES, G. M., LANGLEY-HOBBS, S. J. & JEFFERY, N. D. 2010. Risk factors for medial meniscal injury in association with cranial cruciate ligament rupture. *Journal of Small Animal Practice,* 51**,** 630-634.
HEALEY, E., MURPHY, R. J., HAYWARD, J. J., CASTELHANO, M., BOYKO, A. R., HAYASHI, K., KROTSCHECK, U. & TODHUNTER, R. J. 2019. Genetic mapping of distal femoral, stifle, and tibial radiographic morphology in dogs with cranial cruciate ligament disease. *PLoS One,* 14**,** e0223094.
HEARD, B. J., MARTIN, L., RATTNER, J. B., FRANK, C. B., HART, D. A. & KRAWETZ, R. 2012. Matrix metalloproteinase protein expression profiles cannot distinguish between normal and early osteoarthritic synovial fluid. *BMC Musculoskeletal Disorders,* 13**,** 126.
HEFFRON, L. E. & CAMPBELL, J. R. 1978. Morphology, histology and functional anatomy of the canine cranial cruciate ligament. *Vet Rec,* 102**,** 280-3.
HENDERSON, R. 1978. The tibial compression mechanism: a diagnostic aid in stifle injuries. *JAAHA,* 4**,** 474-478.
HENROTIN, Y., MARTEL-PELLETIER, J., MSIKA, P., GUILLOU, G. B. & DEBERG, M. 2012. Usefulness of specific OA biomarkers, Coll2-1 and Coll2-1NO₂, in the anterior cruciate ligament OA canine model. *Osteoarthritis and Cartilage,* 20**,** 787-790.
HOELZLER, M. G., MILLIS, D. L., FRANCIS, D. A. & WEIGEL, J. P. 2004. Results of arthroscopic versus open arthrotomy for surgical management of cranial cruciate ligament deficiency in dogs. *Veterinary surgery,* 33**,** 146-153.
HOLLANDER, J., REGINATO, A. & TORRALBA, T. P. 1966. Examination of Synovial Fluid as a Diagnostic Aid in Arthritis. *Medical Clinics of North America,* 50**,** 1281-1293.
HORE, P. J. 1999. NMR Principles. *In:* LINDON, J. C. (ed.) *Encyclopedia of Spectroscopy and Spectrometry.* Oxford: Elsevier.
HOULT, D. I. 1976. Solvent peak saturation with single phase and quadrature fourier transformation. *Journal of Magnetic Resonance (1969),* 21**,** 337-347.
HU, Y., WU, Q., QIAO, Y., ZHANG, P., DAI, W., TAO, H. & CHEN, S. 2020. Disturbances in Metabolic Pathways and the Identification of a Potential Biomarker Panel for Early Cartilage Degeneration in a Rabbit Anterior Cruciate Ligament Transection Model. *Cartilage***,** 1947603520921434.
HULSE, D. & JOHNSON, S. 1988. Isolated Lateral Meniscal Tear in the Dog. *Vet Comp Orthop Traumatol,* 01**,** 152-154.
HYYTIÄINEN, H. K., MÖLSÄ, S. H., JUNNILA, J. T., LAITINEN-VAPAAVUORI, O. M. & HIELM-BJÖRKMAN, A. K. 2013. Ranking of physiotherapeutic evaluation methods as outcome measures of stifle functionality in dogs. *Acta Veterinaria Scandinavica,* 55**,** 29.

ICHINOHE, T., YAMAKAWA, S., SHIMADA, M., KANNO, N., FUJITA, Y., HARADA, Y., FUJIE, H. & HARA, Y. 2021. Investigation of the effects of excessive tibial plateau angle and changes in load on ligament tensile forces in the stifle joints of dogs. *Am J Vet Res,* 82**,** 459-466.

ICHINOSE, Y., EGUCHI, K., MIGITA, K., KAWABE, Y., TSUKADA, T., KOJI, T., ABE, K., AOYAGI, T., NAKAMURA, H. & NAGATAKI, S. 1998. Apoptosis induction in synovial fibroblasts by ceramide: in vitro and in vivo effects. *J Lab Clin Med,* 131**,** 410-6.

INAUEN, R., KOCH, D., BASS, M. & HAESSIG, M. 2009. Tibial tuberosity conformation as a risk factor for cranial cruciate ligament rupture in the dog. *Vet Comp Orthop Traumatol,* 22**,** 16-20.

INNES, J. F., COSTELLO, M., BARR, F. J., RUDORF, H. & BARR, A. R. S. 2004. Radiographic Progression of Osteoarthritis of the Canine Stifle Joint: A Prospective Study. *Veterinary Radiology & Ultrasound,* 45**,** 143-148.

JANOVEC, J., KYLLAR, M., MIDGLEY, D. & OWEN, M. 2017. Conformation of the proximal tibia and cranial cruciate ligament disease in small breed dogs. *Vet Comp Orthop Traumatol,* 30**,** 178-183.

JEONG, J., JEONG, S. M., KIM, S. E., LEWIS, D. D. & LEE, H. 2021. Subsequent meniscal tears following tibial tuberosity advancement and tibial plateau leveling osteotomy in dogs with cranial cruciate ligament deficiency: An in vivo experimental study. *Vet Surg,* 50**,** 966-974.

JOHNSTON, S. A. 1997. Osteoarthritis. Joint anatomy, physiology, and pathobiology. *Vet Clin North Am Small Anim Pract,* 27**,** 699-723.

JONES, R. S., KEENE, G. C. R., LEARMONTH, D. J. A., BICKERSTAFF, D., NAWANA, N. S., COSTI, J. J. & PEARCY, M. J. 1996. Direct measurement of hoop strains in the intact and torn human medial meniscus. *Clinical Biomechanics,* 11**,** 295-300.

KAISER, R. 1963. Use of the Nuclear Overhauser Effect in the Analysis of High-Resolution Nuclear Magnetic Resonance Spectra. *The Journal of Chemical Physics,* 39**,** 2435-2442.

KAMBIC, H. E. & MCDEVITT, C. A. 2005. Spatial organization of types I and II collagen in the canine meniscus. *J Orthop Res,* 23**,** 142-9.

KANG, K. Y., LEE, S. H., JUNG, S. M., PARK, S.-H., JUNG, B.-H. & JU, J. H. 2015. Downregulation of Tryptophan-related Metabolomic Profile in Rheumatoid Arthritis Synovial Fluid. *The Journal of Rheumatology,* 42**,** 2003-2011.

KEELER, J. 2011. *Understanding NMR spectroscopy*, John Wiley & Sons.

KENNEDY, A. D., WITTMANN, B. M., EVANS, A. M., MILLER, L. A. D., TOAL, D. R., LONERGAN, S., ELSEA, S. H. & PAPPAN, K. L. 2018. Metabolomics in the clinic: A review of the shared and unique features of untargeted metabolomics for clinical research and clinical testing. *J Mass Spectrom,* 53**,** 1143-1154.

KENNEDY, S. C., DUNNING, D., BISCHOFF, M. G., KURIASHKIN, I. V., PIJANOWSKI, G. J. & SCHAEFFER, D. J. 2005. The effect of axial and abaxial release on meniscal displacement in the dog. *Vet Comp Orthop Traumatol,* 18**,** 227-234.

KIM, H.-R., LEE, J.-H., KIM, K.-W., KIM, B.-M. & LEE, S.-H. 2016. The relationship between synovial fluid VEGF and serum leptin with ultrasonographic findings in knee osteoarthritis. *International Journal of Rheumatic Diseases,* 19**,** 233-240.

KIM, J.-H., HEO, S.-Y. & LEE, H.-B. 2017a. Arthroscopic detection of medial meniscal injury with the use of a joint distractor in small-breed dogs. *jvs,* 18**,** 515-520.

KIM, S., HWANG, J., KIM, J., AHN, J. K., CHA, H.-S. & KIM, K. H. 2017b. Metabolite profiles of synovial fluid change with the radiographic severity of knee osteoarthritis. *Joint Bone Spine,* 84**,** 605-610.

KIM, S., HWANG, J., XUAN, J., JUNG, Y. H., CHA, H.-S. & KIM, K. H. 2014. Global Metabolite Profiling of Synovial Fluid for the Specific Diagnosis of Rheumatoid Arthritis from Other Inflammatory Arthritis. *PLOS ONE,* 9**,** e97501.

KINOSHITA, E., FUMOTO, S., HORI, Y., YOSHIKAWA, N., MIYAMOTO, H., SASAKI, H., NAKAMURA, J., TANAKA, T. & NISHIDA, K. 2019. Monitoring method for transgene expression in target tissue by blood sampling. *Biotechnol Rep (Amst),* 24**,** e00401.

KIRSCHKE, E., GOSWAMI, D., SOUTHWORTH, D., GRIFFIN, P. R. & AGARD, D. A. 2014. Glucocorticoid receptor function regulated by coordinated action of the Hsp90 and Hsp70 chaperone cycles. *Cell,* 157**,** 1685-1697.

KOLDE, R. 2012. Pheatmap: pretty heatmaps. *R package version,* 1**,** 726.

KOSINSKA, M. K., LIEBISCH, G., LOCHNIT, G., WILHELM, J., KLEIN, H., KAESSER, U., LASCZKOWSKI, G., RICKERT, M., SCHMITZ, G. & STEINMEYER, J. 2013. A Lipidomic Study of Phospholipid Classes and Species in Human Synovial Fluid. *Arthritis & Rheumatism,* 65**,** 2323-2333.

KOSINSKA, M. K., LUDWIG, T. E., LIEBISCH, G., ZHANG, R., SIEBERT, H.-C., WILHELM, J., KAESSER, U., DETTMEYER, R. B., KLEIN, H., ISHAQUE, B., RICKERT, M., SCHMITZ, G., SCHMIDT, T. A. & STEINMEYER, J. 2015. Articular Joint Lubricants during Osteoarthritis and Rheumatoid Arthritis Display Altered Levels and Molecular Species. *PLOS ONE,* 10**,** e0125192.

KOSINSKA, M. K., MASTBERGEN, S. C., LIEBISCH, G., WILHELM, J., DETTMEYER, R. B., ISHAQUE, B., RICKERT, M., SCHMITZ, G., LAFEBER, F. P. & STEINMEYER, J. 2016. Comparative lipidomic analysis of synovial fluid in human and canine osteoarthritis. *Osteoarthritis Cartilage,* 24**,** 1470-8.

KRAUSE, W. R., POPE, M. H., JOHNSON, R. J. & WILDER, D. G. 1976. Mechanical changes in the knee after meniscectomy. *J Bone Joint Surg Am,* 58**,** 599-604.

KRIAT, M., CONFORT-GOUNY, S., VION-DURY, J., SCIAKY, M., VIOUT, P. & COZZONE, P. J. 1992. Quantitation of metabolites in human blood serum by proton magnetic resonance spectroscopy. A comparative study of the use of formate and TSP as concentration standards. *NMR in Biomedicine,* 5**,** 179-184.

KRISHNAN, A. V., SWAMI, S. & FELDMAN, D. 2001. Estradiol inhibits glucocorticoid receptor expression and induces glucocorticoid resistance in MCF-7 human breast cancer cells. *The Journal of Steroid Biochemistry and Molecular Biology,* 77**,** 29-37.

KROTSCHECK, U., NELSON, S. A., TODHUNTER, R. J., STONE, M. & ZHANG, Z. 2016. Long Term Functional Outcome of Tibial Tuberosity Advancement vs. Tibial Plateau Leveling Osteotomy and Extracapsular Repair in a Heterogeneous Population of Dogs. *Veterinary Surgery,* 45**,** 261-268.

KRUPKOVA, O., SMOLDERS, L., WUERTZ-KOZAK, K., COOK, J. & POZZI, A. 2018. The Pathobiology of the Meniscus: A Comparison Between the Human and Dog. *Frontiers in veterinary science,* 5**,** 73-73.

KUROKI, K., WILLIAMS, N. & COOK, J. L. 2021. Histologic evidence for a humoral immune response in synovitis associated with cranial cruciate ligament disease in dogs. *Veterinary Surgery,* 50**,** 1032-1041.

LAFAVER, S., MILLER, N. A., STUBBS, W. P., TAYLOR, R. A. & BOUDRIEAU, R. J. 2007. Tibial tuberosity advancement for stabilization of the canine cranial cruciate ligament-deficient stifle joint: surgical technique, early results, and complications in 101 dogs. *Veterinary surgery,* 36**,** 573-586.

LAFLAMME, D. 1997. Development and validation of a body condition score system for dogs. *Canine practice.,* 22**,** 10-15.

LAFOND, E., BREUR, G. J. & AUSTIN, C. C. 2002. Breed susceptibility for developmental orthopedic diseases in dogs. *Journal of the American Animal Hospital Association,* 38**,** 467-477.

LAMBERT, J. B. & MAZZOLA, E. Nuclear magnetic resonance spectroscopy : an introduction to principles, applications, and experimental methods. 2004.
LAO, T. D. & LE, T. A. H. 2021. Data Integration Reveals the Potential Biomarkers of Circulating MicroRNAs in Osteoarthritis. *Diagnostics (Basel),* 11.
LE GALL, G. 2015. NMR spectroscopy of biofluids and extracts. *Metabonomics.* Springer.
LEE, S., LIM, H.-S., SHIN, H.-J., KIM, S.-A., PARK, J., KIM, H.-C., KIM, H., KIM, H. J., KIM, Y.-T., LEE, K.-R. & KIM, Y.-J. 2014. Simultaneous Determination of Cortisol and Cortisone from Human Serum by Liquid Chromatography-Tandem Mass Spectrometry. *Journal of Analytical Methods in Chemistry,* 2014**,** 787483.
LEESON, T. S., LEESON, C. R. & PAPARO, A. A. 1988. Text atlas of histology.
LI, J., MA, C., HUANG, Y., LUO, J. & HUANG, C. 2003. Differential requirement of EGF receptor and its tyrosine kinase for AP-1 transactivation induced by EGF and TPA. *Oncogene,* 22**,** 211-9.
LINDHORST, E., VAIL, T. P., GUILAK, F., WANG, H., SETTON, L. A., VILIM, V. & KRAUS, V. B. 2000. Longitudinal characterization of synovial fluid biomarkers in the canine meniscectomy model of osteoarthritis. *Journal of Orthopaedic Research,* 18**,** 269-280.
LIU, B., GOODE, A. P., CARTER, T. E., UTTURKAR, G. M., HUEBNER, J. L., TAYLOR, D. C., MOORMAN, C. T., 3RD, GARRETT, W. E., KRAUS, V. B., GUILAK, F., DEFRATE, L. E. & MCNULTY, A. L. 2017. Matrix metalloproteinase activity and prostaglandin E2 are elevated in the synovial fluid of meniscus tear patients. *Connective tissue research,* 58**,** 305-316.
LOERZ, C. & MASER, E. 2017. The cortisol-activating enzyme 11β-hydroxysteroid dehydrogenase type 1 in skeletal muscle in the pathogenesis of the metabolic syndrome. *J Steroid Biochem Mol Biol,* 174**,** 65-71.
LOWE JR, W. L., FU, R. & BANKO, M. 1997. Growth factor-induced transcription via the serum response element is inhibited by cyclic adenosine 3', 5'-monophosphate in MCF-7 breast cancer cells. *Endocrinology,* 138**,** 2219-2226.
MACFARLANE, E., SEIBEL, M. J. & ZHOU, H. 2020. Arthritis and the role of endogenous glucocorticoids. *Bone Research,* 8**,** 33.
MAHN, M. M., COOK, J. L., COOK, C. R. & BALKE, M. T. 2005. Arthroscopic verification of ultrasonographic diagnosis of meniscal pathology in dogs. *Vet Surg,* 34**,** 318-23.
MALEK, S., WENG, H.-Y., MARTINSON, S. A., ROCHAT, M. C., BÉRAUD, R. & RILEY, C. B. 2020. Evaluation of serum MMP-2 and MMP-3, synovial fluid IL-8, MCP-1, and KC concentrations as biomarkers of stifle osteoarthritis associated with naturally occurring cranial cruciate ligament rupture in dogs. *PloS one,* 15**,** e0242614.
MAN, G. S. & MOLOGHIANU, G. 2014. Osteoarthritis pathogenesis - a complex process that involves the entire joint. *J Med Life,* 7**,** 37-41.
MANNECHEZ, A., REUNGPATTHANAPHONG, P., DE CERTAINES, J. D., LERAY, G. & LE MOYEC, L. 2005. Proton NMR visible mobile lipid signals in sensitive and multidrug-resistant K562 cells are modulated by rafts. *Cancer Cell International,* 5**,** 2.
MANSON, T. T. & COSGAREA, A. J. 2004. Meniscal injuries in active patients. *Adv Stud Med,* 4**,** 545-552.
MARSHALL, K. W., MANOLOPOULOS, V., MANCER, K., STAPLES, J. & DAMYANOVICH, A. 2000. Amelioration of disease severity by intraarticular hylan therapy in bilateral canine osteoarthritis. *Journal of Orthopaedic Research,* 18**,** 416-425.
MARTINI, F. M., BRANDSTETTER DE BELLESINI, A., MIOLO, A., DEL COCO, L., FANIZZI, F. P. & CROVACE, A. 2017. Combining a joint health supplement with tibial plateau leveling osteotomy in dogs with cranial cruciate ligament rupture. An exploratory controlled trial. *International Journal of Veterinary Science and Medicine,* 5**,** 105-112.

MATCHWICK, A. I., BRIDGES, J. P., SCRIMGEOUR, A. B. & WORTH, A. J. 2021. A retrospective evaluation of complications associated with forkless tibial tuberosity advancement performed in primary care practice. *Veterinary Surgery,* 50**,** 121-132.

MATEOS, J., LOURIDO, L., FERNÁNDEZ-PUENTE, P., CALAMIA, V., FERNÁNDEZ-LÓPEZ, C., OREIRO, N., RUIZ-ROMERO, C. & BLANCO, F. J. 2012. Differential protein profiling of synovial fluid from rheumatoid arthritis and osteoarthritis patients using LC–MALDI TOF/TOF. *Journal of Proteomics,* 75**,** 2869-2878.

MCCREADY, D. J. & NESS, M. G. 2016a. Diagnosis and management of meniscal injury in dogs with cranial cruciate ligament rupture: a systematic literature review. *Journal of Small Animal Practice,* 57**,** 59-66.

MCCREADY, D. J. & NESS, M. G. 2016b. Systematic review of the prevalence, risk factors, diagnosis and management of meniscal injury in dogs: Part 2. *Journal of Small Animal Practice,* 57**,** 194-204.

MEIBOOM, S. & GILL, D. 1958. Modified spin-echo method for measuring nuclear relaxation times. *Review of Scientific Instruments,* 29**,** 688-691.

MELO, R. C., D'AVILA, H., WAN, H. C., BOZZA, P. T., DVORAK, A. M. & WELLER, P. F. 2011. Lipid bodies in inflammatory cells: structure, function, and current imaging techniques. *J Histochem Cytochem,* 59**,** 540-56.

METELMAN, A. L., SCHWARZ, P. D., SALMAN, M. & ALVIS, M. R. 1995a. An Evaluation of Three Different Cranial Cruciate Ligament Surgical Stabilization Procedures As They Relate to Postoperative Meniscal Injuries. *Vet Comp Orthop Traumatol,* 08**,** 118-123.

METELMAN, L., SCHWARZ, P., SALMAN, M. & ALVIS, M. 1995b. An Evaluation of Three Different Cranial Cruciate Ligament Surgical Stabilization Procedures As They Relate to Postoperative Meniscal Injuries. *Veterinary and Comparative Orthopaedics and Traumatology,* 08**,** 118-123.

MICKIEWICZ, B., HEARD, B. J., CHAU, J. K., CHUNG, M., HART, D. A., SHRIVE, N. G., FRANK, C. B. & VOGEL, H. J. 2015. Metabolic profiling of synovial fluid in a unilateral ovine model of anterior cruciate ligament reconstruction of the knee suggests biomarkers for early osteoarthritis. *Journal of Orthopaedic Research,* 33**,** 71-77.

MIELOCH, A. A., RICHTER, M., TRZECIAK, T., GIERSIG, M. & RYBKA, J. D. 2019. Osteoarthritis Severely Decreases the Elasticity and Hardness of Knee Joint Cartilage: A Nanoindentation Study. *Journal of clinical medicine,* 8**,** 1865.

MIGHT, K. R., BACHELEZ, A., MARTINEZ, S. A. & GAY, J. M. 2013. Evaluation of the drawer test and the tibial compression test for differentiating between cranial and caudal stifle subluxation associated with cruciate ligament instability. *Vet Surg,* 42**,** 392-7.

MILLER, C. & PRESNELL, K. 1985. EXAMINATION OF THE CANINE STIFLE-ARTHROSCOPY VERSUS ARTHROTOMY. *Journal of the American Animal Hospital Association,* 21**,** 623-629.

MITTENDORFER, B., GORE, D. C., HERNDON, D. N. & WOLFE, R. R. 1999. Accelerated glutamine synthesis in critically ill patients cannot maintain normal intramuscular free glutamine concentration. *JPEN J Parenter Enteral Nutr,* 23**,** 243-50; discussion 250-2.

MOBASHERI, A. & BATT, M. 2016. An update on the pathophysiology of osteoarthritis. *Annals of Physical and Rehabilitation Medicine,* 59**,** 333-339.

MOBASHERI, A. & CASSIDY, J. P. 2010. Biomarkers in veterinary medicine: Towards targeted, individualised therapies for companion animals. *Vet J,* 185**,** 1-3.

MOORE, S. C., MATTHEWS, C. E., SAMPSON, J. N., STOLZENBERG-SOLOMON, R. Z., ZHENG, W., CAI, Q., TAN, Y. T., CHOW, W. H., JI, B. T., LIU, D. K., XIAO, Q., BOCA, S. M., LEITZMANN, M. F., YANG, G., XIANG, Y. B., SINHA, R., SHU, X. O. & CROSS, A. J. 2014. Human metabolic correlates of body mass index. *Metabolomics,* 10**,** 259-269.

MORGAN, R. 2019. *Understanding the role of HACD enzymes and very long chain fatty acids in muscle development and disease*, The University of Liverpool (United Kingdom).
MOSES, P. A. 2002. A technique for the surgical repair of caudal peripheral detachment and longitudinal peripheral tears of the medial meniscus in dogs. *Veterinary and Comparative Orthopaedics and Traumatology,* 15**,** 92-96.
MOSTAFA, A. A., CUNNINGHAM, D. P., BOUDRIEAU, R. J., KOWALESKI, M. P. & GRIFFON, D. J. 2018. Influence of radiographic techniques on the measurement of femoral anteversion angles and a conformation score of pelvic limbs in Labrador retrievers. *Vet Surg,* 47**,** 421-430.
MUHAMMED, H., KUMAR, D., DUBEY, D., KUMAR, S., CHAURASIA, S., GULERIA, A., MAJUMDER, S., SINGH, R., AGARWAL, V. & MISRA, R. 2019. Metabolomics analysis revealed significantly higher synovial Phe/Tyr ratio in reactive arthritis and undifferentiated spondyloarthropathy. *Rheumatology,* 59**,** 1587-1590.
MUIR, P. 2017. History and Clinical Signs of Cruciate Ligament Rupture. *Advances in the Canine Cranial Cruciate Ligament.*
MUIR, P., DANOVA, N. A., ARGYLE, D. J., MANLEY, P. A. & HAO, Z. 2005. Collagenolytic protease expression in cranial cruciate ligament and stifle synovial fluid in dogs with cranial cruciate ligament rupture. *Vet Surg,* 34**,** 482-90.
MUIR, P., SCHWARTZ, Z., MALEK, S., KREINES, A., CABRERA, S. Y., BUOTE, N. J., BLEEDORN, J. A., SCHAEFER, S. L., HOLZMAN, G. & HAO, Z. 2011. Contralateral cruciate survival in dogs with unilateral non-contact cranial cruciate ligament rupture. *PLoS One,* 6**,** e25331.
MURAKAMI, K., MAEDA, S., YONEZAWA, T. & MATSUKI, N. 2016. Synovial fluid matrix metalloproteinase-2 and -9 activities in dogs suffering from joint disorders. *Journal of Veterinary Medical Science,* 78**,** 1051-1054.
NEAL, B. A., TING, D., BONCZYNSKI, J. J. & YASUDA, K. 2015. Evaluation of Meniscal Click for Detecting Meniscal Tears in Stifles with Cranial Cruciate Ligament Disease. *Veterinary Surgery,* 44**,** 191-194.
NECELA, B. M. & CIDLOWSKI, J. A. 2004. Mechanisms of Glucocorticoid Receptor Action in Noninflammatory and Inflammatory Cells. *Proceedings of the American Thoracic Society,* 1**,** 239-246.
NEEFJES, M., HOUSMANS, B. A. C., VAN DEN AKKER, G. G. H., VAN RHIJN, L. W., WELTING, T. J. M. & VAN DER KRAAN, P. M. 2021. Reporter gene comparison demonstrates interference of complex body fluids with secreted luciferase activity. *Scientific Reports,* 11**,** 1359.
NELSON, S. A., KROTSCHECK, U., RAWLINSON, J., TODHUNTER, R. J., ZHANG, Z. & MOHAMMED, H. 2013. Long-Term Functional Outcome of Tibial Plateau Leveling Osteotomy Versus Extracapsular Repair in a Heterogeneous Population of Dogs. *Veterinary Surgery,* 42**,** 38-50.
OGURA, T., SUZUKI, M., SAKUMA, Y., YAMAUCHI, K., ORITA, S., MIYAGI, M., ISHIKAWA, T., KAMODA, H., OIKAWA, Y., KANISAWA, I., TAKAHASHI, K., SAKAI, H., NAGAMINE, T., FUKUDA, H., TAKAHASHI, K., OHTORI, S. & TSUCHIYA, A. 2016. Differences in levels of inflammatory mediators in meniscal and synovial tissue of patients with meniscal lesions. *Journal of experimental orthopaedics,* 3**,** 7-7.
OLIVE, J., D'ANJOU, M. A., CABASSU, J., CHAILLEUX, N. & BLOND, L. 2014. Fast presurgical magnetic resonance imaging of meniscal tears and concurrent subchondral bone marrow lesions. Study of dogs with naturally occurring cranial cruciate ligament rupture. *Vet Comp Orthop Traumatol,* 27**,** 1-7.
ONAL, G., KUTLU, O., GOZUACIK, D. & DOKMECI EMRE, S. 2017. Lipid Droplets in Health and Disease. *Lipids in Health and Disease,* 16**,** 128.

OVERMYER, K. A., MUIR, P. & COON, J. J. 2018. Discovery metabolomics and lipidomics of canine synovial fluid and serum. *Osteoarthritis and Cartilage,* 26**,** S172.

PAATSAMA, S. 1952. *Ligament injuries in the canine stifle joint: a clinical and experimental study*, Veterinary College.

PANG, Z., CHONG, J., ZHOU, G., DE LIMA MORAIS, D. A., CHANG, L., BARRETTE, M., GAUTHIER, C., JACQUES, P.-É., LI, S. & XIA, J. 2021. MetaboAnalyst 5.0: narrowing the gap between raw spectra and functional insights. *Nucleic Acids Research,* 49**,** W388-W396.

PARK, R. 1979. Radiographic evaluation of the canine stifle joint. *Compend Contin Educ Pract Vet,* 1**,** 833-842.

PEARSON, M. J., HERNDLER-BRANDSTETTER, D., TARIQ, M. A., NICHOLSON, T. A., PHILP, A. M., SMITH, H. L., DAVIS, E. T., JONES, S. W. & LORD, J. M. 2017. IL-6 secretion in osteoarthritis patients is mediated by chondrocyte-synovial fibroblast cross-talk and is enhanced by obesity. *Scientific Reports,* 7**,** 3451.

PEFFERS, M. J., MCDERMOTT, B., CLEGG, P. D. & RIGGS, C. M. 2015. Comprehensive protein profiling of synovial fluid in osteoarthritis following protein equalization. *Osteoarthritis Cartilage,* 23**,** 1204-13.

PLESMAN, R., GILBERT, P. & CAMPBELL, J. 2013. Detection of meniscal tears by arthroscopy and arthrotomy in dogs with cranial cruciate ligament rupture: a retrospective, cohort study. *Vet Comp Orthop Traumatol,* 26**,** 42-6.

PLICKERT, H. D., BONDZIO, A., EINSPANIER, R., TICHY, A. & BRUNNBERG, L. 2013. Hyaluronic acid concentrations in synovial fluid of dogs with different stages of osteoarthritis. *Res Vet Sci,* 94**,** 728-34.

POLLET, T. V. & VAN DER MEIJ, L. 2017. To remove or not to remove: the impact of outlier handling on significance testing in testosterone data. *Adaptive Human Behavior and Physiology,* 3**,** 43-60.

PONNURANGAM, S., MONDALEK, F. G., GOVIND, J., SUBRAMANIAM, D., HOUCHEN, C. W., ANANT, S., PANTAZIS, P. & RAMANUJAM, R. P. 2010. Urine and serum analysis of consumed curcuminoids using an IkappaB-luciferase surrogate marker assay. *In Vivo,* 24**,** 861-4.

POON, I. K. H., PATEL, K. K., DAVIS, D. S., PARISH, C. R. & HULETT, M. D. 2011. Histidine-rich glycoprotein: the Swiss Army knife of mammalian plasma. *Blood,* 117**,** 2093-2101.

POZZI, A. & COOK, J. L. 2017. Meniscal Structure and Function. *Advances in the Canine Cranial Cruciate Ligament.*

POZZI, A., HILDRETH, B. E., 3RD & RAJALA-SCHULTZ, P. J. 2008a. Comparison of arthroscopy and arthrotomy for diagnosis of medial meniscal pathology: an ex vivo study. *Vet Surg,* 37**,** 749-55.

POZZI, A., KIM, S. E. & LEWIS, D. D. 2010a. Effect of transection of the caudal menisco-tibial ligament on medial femorotibial contact mechanics. *Vet Surg,* 39**,** 489-95.

POZZI, A., KOWALESKI, M. P., APELT, D., MEADOWS, C., ANDREWS, C. M. & JOHNSON, K. A. 2006. Effect of medial meniscal release on tibial translation after tibial plateau leveling osteotomy. *Vet Surg,* 35**,** 486-94.

POZZI, A., LITSKY, A. S., FIELD, J., APELT, D., MEADOWS, C. & JOHNSON, K. A. 2008b. Pressure distributions on the medial tibial plateau after medial meniscal surgery and tibial plateau levelling osteotomy in dogs. *Vet Comp Orthop Traumatol,* 21**,** 8-14.

POZZI, A., TONKS, C. A. & LING, H. Y. 2010b. Femorotibial contact mechanics and meniscal strain after serial meniscectomy. *Vet Surg,* 39**,** 482-8.

PRODROMOU, C. 2016. Mechanisms of Hsp90 regulation. *The Biochemical journal,* 473**,** 2439-2452.

R CORE TEAM 2020. R: A Language and Environment for Statistical Computing, R Foundation for Statistical Computing, Vienna, Austria. https://www.R.project.org/.
RAI, M. F., BROPHY, R. H. & ROSEN, V. 2020. Molecular biology of meniscus pathology: Lessons learned from translational studies and mouse models. *Journal of Orthopaedic Research,* 38**,** 1895-1904.
RANJAN, R. & SINHA, N. 2019. Nuclear magnetic resonance (NMR)-based metabolomics for cancer research. *NMR Biomed,* 32**,** e3916.
READIOFF, R., GERAGHTY, B., ELSHEIKH, A. & COMERFORD, E. 2020. Viscoelastic characteristics of the canine cranial cruciate ligament complex at slow strain rates. *PeerJ,* 8**,** e10635.
REINKE, J. 1982. Cruciate ligament avulsion injury in the dog [Surgical techniques]. *Journal American Animal Hospital Association*.
RIFFENBURGH, R. H. 2012. Chapter 18 - Sample Size Estimation and Meta-Analysis. *In:* RIFFENBURGH, R. H. (ed.) *Statistics in Medicine (Third Edition).* San Diego: Academic Press.
RITZO, M. E., RITZO, B. A., SIDDENS, A. D., SUMMERLOTT, S. & COOK, J. L. 2014. Incidence and Type of Meniscal Injury and Associated Long-Term Clinical Outcomes in Dogs Treated Surgically for Cranial Cruciate Ligament Disease. *Veterinary Surgery,* 43**,** 952-958.
ROGATKO, C. P., WARNOCK, J. J., BOBE, G. & VERPAALEN, V. D. 2018. Comparison of iatrogenic articular cartilage injury in canine stifle arthroscopy versus medial parapatellar mini-arthrotomy in a cadaveric model. *Veterinary Surgery,* 47**,** O6-O14.
ROLLER, B. L., MONIBI, F., STOKER, A. M., BAL, B. S. & COOK, J. L. 2016. Identification of Novel Synovial Fluid Biomarkers Associated with Meniscal Pathology. *J Knee Surg,* 29**,** 47-62.
ROPES, M. W., ROSSMEISL, E. C. & BAUER, W. 1940. THE ORIGIN AND NATURE OF NORMAL HUMAN SYNOVIAL FLUID. *The Journal of clinical investigation,* 19**,** 795-799.
ROUSH, J. K. 1993. Canine Patellar Luxation. *Veterinary Clinics of North America: Small Animal Practice,* 23**,** 855-868.
ROVESTI, G. L., DEVESA, V., BERTORELLI, L. & RODRIGUEZ-QUIROS, J. 2018. Facilitation of arthroscopic visualization and treatment of meniscal tears using a stifle joint distractor in the dog. *BMC Veterinary Research,* 14**,** 212.
RUBINOW, D. R., ROCA, C. A., SCHMIDT, P. J., DANACEAU, M. A., PUTNAM, K., CIZZA, G., CHROUSOS, G. & NIEMAN, L. 2005. Testosterone Suppression of CRH-Stimulated Cortisol in Men. *Neuropsychopharmacology,* 30**,** 1906-1912.
RUDD GARCES, G., ARIZMENDI, A., BARRIENTOS, L. S., CRESPI, J. A., MORALES, H., PERAL GARCÍA, P., PADULA, G. & GIOVAMBATTISTA, G. 2021. Epidemiology of Cranial Cruciate Ligament Rupture and Patellar Luxation in Dogs from the Province of Buenos Aires, Argentina. *Vet Comp Orthop Traumatol,* 34**,** 024-031.
SAENGSOI, W. 2018. *The Role of Adipose Tissue in Canine Cranial Cruciate Ligament Disease*, The University of Liverpool (United Kingdom).
SAKAGUCHI, C. A., NIEMAN, D. C., SIGNINI, E. F., ABREU, R. M. & CATAI, A. M. 2019. Metabolomics-Based Studies Assessing Exercise-Induced Alterations of the Human Metabolome: A Systematic Review. *Metabolites,* 9.
SAMII, V. F., DYCE, J., POZZI, A., DROST, W. T., MATTOON, J. S., GREEN, E. M., KOWALESKI, M. P. & LEHMAN, A. M. 2009. Computed tomographic arthrography of the stifle for detection of cranial and caudal cruciate ligament and meniscal tears in dogs. *Vet Radiol Ultrasound,* 50**,** 144-50.
SAMPLE, S. J., RACETTE, M. A., HANS, E. C., VOLSTAD, N. J., HOLZMAN, G., BLEEDORN, J. A., SCHAEFER, S. L., WALLER, K. R., III, HAO, Z., BLOCK, W. F. & MUIR, P. 2017. Radiographic and magnetic resonance imaging predicts severity of cruciate

ligament fiber damage and synovitis in dogs with cranial cruciate ligament rupture. *PLOS ONE,* 12**,** e0178086.

SANTAROSSA, A., GIBSON, T. W. G., KERR, C., MONTEITH, G. J., DURZI, T., GOWLAND, S. & VERBRUGGHE, A. 2020. Body composition of medium to giant breed dogs with or without cranial cruciate ligament disease. *Veterinary Surgery,* 49**,** 1144-1153.

SAYGI, B., YILDIRIM, Y., BERKER, N., OFLUOGLU, D., KARADAG-SAYGI, E. & KARAHAN, M. 2005. Evaluation of the neurosensory function of the medial meniscus in humans. *Arthroscopy,* 21**,** 1468-72.

SCAVELLI, T. D., SCHRADER, S. C., MATTHIESEN, D. T. & SKORUP, D. E. 1990. Partial rupture of the cranial cruciate ligament of the stifle in dogs: 25 cases (1982-1988). *J Am Vet Med Assoc,* 196**,** 1135-8.

SCAVENIUS, C., POULSEN, E. C., THØGERSEN, I. B., ROEBUCK, M., FROSTICK, S., BOUGHARIOS, G., YAMAMOTO, K., DELEURAN, B. & ENGHILD, J. J. 2019. Matrix-degrading protease ADAMTS-5 cleaves inter-α-inhibitor and releases active heavy chain 2 in synovial fluids from arthritic patients. *J Biol Chem,* 294**,** 15495-15504.

SCHMIDLI, M. R., FUHRER, B., KURT, N., SENN, D., DRÖGEMÜLLER, M., RYTZ, U., SPRENG, D. E. & FORTERRE, S. 2018. Inflammatory pattern of the infrapatellar fat pad in dogs with canine cruciate ligament disease. *BMC veterinary research,* 14**,** 1-13.

SCHWARZ, I. & HILLS, B. 1996a. Synovial surfactant: lamellar bodies in type B synoviocytes and proteolipid in synovial fluid and the articular lining. *Rheumatology,* 35**,** 821-827.

SCHWARZ, I. M. & HILLS, B. A. 1996b. Synovial surfactant: lamellar bodies in type B synoviocytes and proteolipid in synovial fluid and the articular lining. *Br J Rheumatol,* 35**,** 821-7.

SCUDERI, G. J., WOOLF, N., DENT, K., GOLISH, S. R., CUELLAR, J. M., CUELLAR, V. G., YEOMANS, D. C., CARRAGEE, E. J., ANGST, M. S., BOWSER, R. & HANNA, L. S. 2010. Identification of a complex between fibronectin and aggrecan G3 domain in synovial fluid of patients with painful meniscal pathology. *Clinical Biochemistry,* 43**,** 808-814.

SELLAM, J. & BERENBAUM, F. 2010. The role of synovitis in pathophysiology and clinical symptoms of osteoarthritis. *Nature Reviews Rheumatology,* 6**,** 625-635.

SEO, S.-B., RAHMAN, M. M. & JEONG, I. S. 2017. Importance of meniscal injury diagnosis and surgical management in dogs during reconstruction of cranial cruciate ligament rupture: a retrospective study. *Journal of Advanced Veterinary and Animal Research,* 4**,** 311-318.

SHAHID, M., MANCHI, G., BRUNNBERG, L. & RAILA, J. 2018. Use of proteomic analysis to determine the protein constituents of synovial fluid samples from the stifle joints of dogs with and without osteoarthritis secondary to cranial cruciate ligament rupture. *Am J Vet Res,* 79**,** 397-403.

SHAULIAN, E. & KARIN, M. 2002. AP-1 as a regulator of cell life and death. *Nature Cell Biology,* 4**,** E131-E136.

SHOWIHEEN, S. A. A., SUN, A. R., WU, X., CRAWFORD, R., XIAO, Y., WELLARD, R. M. & PRASADAM, I. 2019. Application of Metabolomics to Osteoarthritis: from Basic Science to the Clinical Approach. *Curr Rheumatol Rep,* 21**,** 26.

SIÓDMIAK, J., BEŁDOWSKI, P., AUGÉ, W. K., LEDZIŃSKI, D., ŚMIGIEL, S. & GADOMSKI, A. 2017. Molecular Dynamic Analysis of Hyaluronic Acid and Phospholipid Interaction in Tribological Surgical Adjuvant Design for Osteoarthritis. *Molecules (Basel, Switzerland),* 22**,** 1436.

SLAUTERBECK, J. R., PANKRATZ, K., XU, K. T., BOZEMAN, S. C. & HARDY, D. M. 2004. Canine ovariohysterectomy and orchiectomy increases the prevalence of ACL injury. *Clin Orthop Relat Res***,** 301-5.

SLOCUM, B. & SLOCUM, T. D. 1993. Tibial plateau leveling osteotomy for repair of cranial cruciate ligament rupture in the canine. *Vet Clin North Am Small Anim Pract,* 23**,** 777-95.

SLUZALSKA, K. D., LIEBISCH, G., LOCHNIT, G., ISHAQUE, B., HACKSTEIN, H., SCHMITZ, G., RICKERT, M. & STEINMEYER, J. 2017. Interleukin-1β affects the phospholipid biosynthesis of fibroblast-like synoviocytes from human osteoarthritic knee joints. *Osteoarthritis and Cartilage,* 25**,** 1890-1899.

SMITH, K. D., CLEGG, P. D., INNES, J. F. & COMERFORD, E. J. 2014. Elastin content is high in the canine cruciate ligament and is associated with degeneration. *The Veterinary Journal,* 199**,** 169-174.

SMITH, K. D., VAUGHAN-THOMAS, A., SPILLER, D. G., CLEGG, P. D., INNES, J. F. & COMERFORD, E. J. 2012. Variations in cell morphology in the canine cruciate ligament complex. *The Veterinary Journal,* 193**,** 561-566.

SOETERS, P. B. & GRECU, I. 2012. Have We Enough Glutamine and How Does It Work? A Clinician's View. *Annals of Nutrition and Metabolism,* 60**,** 17-26.

SOININEN, P., KANGAS, A. J., WÜRTZ, P., TUKIAINEN, T., TYNKKYNEN, T., LAATIKAINEN, R., JÄRVELIN, M. R., KÄHÖNEN, M., LEHTIMÄKI, T., VIIKARI, J., RAITAKARI, O. T., SAVOLAINEN, M. J. & ALA-KORPELA, M. 2009. High-throughput serum NMR metabonomics for cost-effective holistic studies on systemic metabolism. *Analyst,* 134**,** 1781-5.

SOKOLOVE, J. & LEPUS, C. M. 2013. Role of inflammation in the pathogenesis of osteoarthritis: latest findings and interpretations. *Therapeutic advances in musculoskeletal disease,* 5**,** 77-94.

SONG, Z., WANG, H., YIN, X., DENG, P. & JIANG, W. 2019. Application of NMR metabolomics to search for human disease biomarkers in blood. *Clinical Chemistry and Laboratory Medicine (CCLM),* 57**,** 417-441.

SPAANDERMAN, D. C. E., NIXON, M., BUURSTEDE, J. C., SIPS, H. H. C. M., SCHILPEROORT, M., KUIPERS, E. N., BACKER, E. A., KOOIJMAN, S., RENSEN, P. C. N., HOMER, N. Z. M., WALKER, B. R., MEIJER, O. C. & KROON, J. 2019. Androgens modulate glucocorticoid receptor activity in adipose tissue and liver. *Journal of Endocrinology,* 240**,** 51-63.

STEIN, S. & SCHMOEKEL, H. 2008. Short-term and eight to 12 months results of a tibial tuberosity advancement as treatment of canine cranial cruciate ligament damage. *J Small Anim Pract,* 49**,** 398-404.

STEPHAN, J. S., MCLAUGHLIN, R. M. & GRIFFITH, G. 1998. Water content and glycosaminoglycan disaccharide concentration of the canine meniscus. *American journal of veterinary research,* 59**,** 213-216.

STEVENS, V. L., HOOVER, E., WANG, Y. & ZANETTI, K. A. 2019. Pre-Analytical Factors that Affect Metabolite Stability in Human Urine, Plasma, and Serum: A Review. *Metabolites,* 9.

SUMNER, L. W., AMBERG, A., BARRETT, D., BEALE, M. H., BEGER, R., DAYKIN, C. A., FAN, T. W. M., FIEHN, O., GOODACRE, R., GRIFFIN, J. L., HANKEMEIER, T., HARDY, N., HARNLY, J., HIGASHI, R., KOPKA, J., LANE, A. N., LINDON, J. C., MARRIOTT, P., NICHOLLS, A. W., REILY, M. D., THADEN, J. J. & VIANT, M. R. 2007. Proposed minimum reporting standards for chemical analysis Chemical Analysis Working Group (CAWG) Metabolomics Standards Initiative (MSI). *Metabolomics : Official journal of the Metabolomic Society,* 3**,** 211-221.

SWANN, D. A., HENDREN, R. B., RADIN, E. L. & SOTMAN, S. L. 1981. The lubricating activity of synovial fluid glycoproteins. *Arthritis & Rheumatism,* 24**,** 22-30.

TAN, A. L., TOUMI, H., BENJAMIN, M., GRAINGER, A. J., TANNER, S. F., EMERY, P. & MCGONAGLE, D. 2006. Combined high-resolution magnetic resonance imaging and

histological examination to explore the role of ligaments and tendons in the phenotypic expression of early hand osteoarthritis. *Annals of the Rheumatic Diseases,* 65**,** 1267-1272.

TANEGASHIMA, K., EDAMURA, K., AKITA, Y., YAMAZAKI, A., YASUKAWA, S., SEKI, M., ASANO, K., NAKAYAMA, T., KATSURA, T. & HAYASHI, K. 2019. Functional Anatomy of the Craniomedial and Caudolateral Bundles of the Cranial Cruciate Ligament in Beagle Dogs. *Vet Comp Orthop Traumatol,* 32**,** 182-191.

TAO, H., HU, Y., QIAO, Y., XIE, Y., CHEN, T. & CHEN, S. 2019. Alternations of Metabolic Profiles in Synovial Fluids and the Correlation with T2 Relaxation Times of Cartilage and Meniscus—A Study on Anterior Cruciate Ligament- (ACL-) Injured Rabbit Knees at Early Stage. *BioMed Research International,* 2019**,** 8491301.

TAYLOR-BROWN, F. E., MEESON, R. L., BRODBELT, D. C., CHURCH, D. B., MCGREEVY, P. D., THOMSON, P. C. & O'NEILL, D. G. 2015. Epidemiology of Cranial Cruciate Ligament Disease Diagnosis in Dogs Attending Primary-Care Veterinary Practices in England. *Vet Surg,* 44**,** 777-83.

TERREROS, A. & DAYE, R. M. 2020. Modified cranial closing wedge osteotomy to treat cranial cruciate ligament deficient stifles with excessive tibial plateau angles: Complications, owner satisfaction, and midterm to long-term outcomes. *Vet Surg,* 49**,** 1109-1117.

TESTUZ, J., HOWARD, J., POZZI, A., RYTZ, U., KRUDEWIG, C., SPRENG, D. & FORTERRE, S. 2016. Evaluation of surface blood flow in intact and ruptured canine cruciate ligaments using laser Doppler flowmetry. *Vet Comp Orthop Traumatol,* 29**,** 361-368.

THIEMAN, K. M., POZZI, A., LING, H.-Y. & LEWIS, D. 2010. Comparison of Contact Mechanics of Three Meniscal Repair Techniques and Partial Meniscectomy in Cadaveric Dog Stifles. *Veterinary Surgery,* 39**,** 355-362.

THIEMAN, K. M., POZZI, A., LING, H.-Y., LEWIS, D. D. & HORODYSKI, M. 2009. Contact Mechanics of Simulated Meniscal Tears in Cadaveric Canine Stifles. *Veterinary Surgery,* 38**,** 803-810.

TIMUR, U. T., JAHR, H., ANDERSON, J., GREEN, D. C., EMANS, P. J., SMAGUL, A., VAN RHIJN, L. W., PEFFERS, M. J. & WELTING, T. J. M. 2021. Identification of tissue-dependent proteins in knee OA synovial fluid. *Osteoarthritis and Cartilage,* 29**,** 124-133.

TIVERS, M. S., MAHONEY, P. N., BAINES, E. A. & CORR, S. A. 2009. Diagnostic accuracy of positive contrast computed tomography arthrography for the detection of injuries to the medial meniscus in dogs with naturally occurring cranial cruciate ligament insufficiency. *J Small Anim Pract,* 50**,** 324-32.

TOMLINSON, J. W. & STEWART, P. M. 2001. Cortisol metabolism and the role of 11β-hydroxysteroid dehydrogenase. *Best Practice & Research Clinical Endocrinology & Metabolism,* 15**,** 61-78.

TORRES DE LA RIVA, G., HART, B. L., FARVER, T. B., OBERBAUER, A. M., MESSAM, L. L., WILLITS, N. & HART, L. A. 2013. Neutering dogs: effects on joint disorders and cancers in golden retrievers. *PLoS One,* 8**,** e55937.

TROY, J. R. & BERGH, M. S. 2015. Development and Efficacy of a Canine Pelvic Limb Model Used to Teach the Cranial Drawer and Tibial Compression Tests in the Stifle Joint. *J Vet Med Educ,* 42**,** 127-32.

TYNKKYNEN, T. 2012. *^{1}H NMR analysis of serum lipids.* Itä-Suomen yliopisto.

ULRICH, E. L., AKUTSU, H., DORELEIJERS, J. F., HARANO, Y., IOANNIDIS, Y. E., LIN, J., LIVNY, M., MADING, S., MAZIUK, D., MILLER, Z., NAKATANI, E., SCHULTE, C. F., TOLMIE, D. E., KENT WENGER, R., YAO, H. & MARKLEY, J. L. 2007. BioMagResBank. *Nucleic Acids Research,* 36**,** D402-D408.

UM, S. Y., CHUNG, M. W., KIM, K. B., KIM, S. H., OH, J. S., OH, H. Y., LEE, H. J. & CHOI, K. H. 2009. Pattern recognition analysis for the prediction of adverse effects by nonsteroidal anti-inflammatory drugs using 1H NMR-based metabolomics in rats. *Anal Chem,* 81**,** 4734-41.

UYSAL, M., AKPINAR, S., BOLAT, F., CEKIN, N., CıNAR, M. & CESUR, N. 2008. Apoptosis in the traumatic and degenerative tears of human meniscus. *Knee Surgery, Sports Traumatology, Arthroscopy,* 16**,** 666.

VAN DER SAR, S. A., ZIELMAN, R., TERWINDT, G. M., VAN DEN MAAGDENBERG, A. M. J. M., DEELDER, A. M., MAYBORODA, O. A., MEISSNER, A. & FERRARI, M. D. 2015. Ethanol contamination of cerebrospinal fluid during standardized sampling and its effect on (1)H-NMR metabolomics. *Analytical and bioanalytical chemistry,* 407**,** 4835-4839.

VAN DER VEEN, J. N., KENNELLY, J. P., WAN, S., VANCE, J. E., VANCE, D. E. & JACOBS, R. L. 2017. The critical role of phosphatidylcholine and phosphatidylethanolamine metabolism in health and disease. *Biochimica et Biophysica Acta (BBA) - Biomembranes,* 1859**,** 1558-1572.

VAN GESTEL, M. 1985. Diagnostic accuracy of stifle arthroscopy in the dog. *Journal of the American Animal Hospital Association,* 21**,** 757-763.

VANCE, J. E. 2015. Phospholipid Synthesis and Transport in Mammalian Cells. *Traffic,* 16**,** 1-18.

VASSEUR, P. B. & ARNOCZKY, S. P. 1981. Collateral ligaments of the canine stifle joint: anatomic and functional analysis. *Am J Vet Res,* 42**,** 1133-7.

WANG, Y., GLUDISH, D. W., HAYASHI, K., TODHUNTER, R. J., KROTSCHECK, U., JOHNSON, P. J., CUMMINGS, B. P., SU, J. & REESINK, H. L. 2020. Synovial fluid lubricin increases in spontaneous canine cruciate ligament rupture. *Scientific Reports,* 10**,** 16725.

WESSELY, M., BRÜHSCHWEIN, A. & SCHNABL-FEICHTER, E. 2017. Evaluation of Intra- and Inter-observer Measurement Variability of a Radiographic Stifle Osteoarthritis Scoring System in Dogs. *Vet Comp Orthop Traumatol,* 30**,** 377-384.

WESTWICK, J. K., WEITZEL, C., MINDEN, A., KARIN, M. & BRENNER, D. A. 1994. Tumor necrosis factor alpha stimulates AP-1 activity through prolonged activation of the c-Jun kinase. *Journal of Biological Chemistry,* 269**,** 26396-26401.

WILKE, V. L., ROBINSON, D. A., EVANS, R. B., ROTHSCHILD, M. F. & CONZEMIUS, M. G. 2005. Estimate of the annual economic impact of treatment of cranial cruciate ligament injury in dogs in the United States. *J Am Vet Med Assoc,* 227**,** 1604-7.

WISDOM, R. 1999. AP-1: One Switch for Many Signals. *Experimental Cell Research,* 253**,** 180-185.

WISE, C. M., WHITE, R. E. & AGUDELO, C. A. 1987. Synovial fluid lipid abnormalities in various disease states: Review and classification. *Seminars in Arthritis and Rheumatism,* 16**,** 222-230.

WISHART, D. S. 2008. Quantitative metabolomics using NMR. *TrAC Trends in Analytical Chemistry,* 27**,** 228-237.

WISHART, D. S., BIGAM, C. G., YAO, J., ABILDGAARD, F., DYSON, H. J., OLDFIELD, E., MARKLEY, J. L. & SYKES, B. D. 1995. 1 H, 13 C and 15 N chemical shift referencing in biomolecular NMR. *Journal of biomolecular NMR,* 6**,** 135-140.

WISHART, D. S., FEUNANG, Y. D., MARCU, A., GUO, A. C., LIANG, K., VÁZQUEZ-FRESNO, R., SAJED, T., JOHNSON, D., LI, C., KARU, N., SAYEEDA, Z., LO, E., ASSEMPOUR, N., BERJANSKII, M., SINGHAL, S., ARNDT, D., LIANG, Y., BADRAN, H., GRANT, J., SERRA-CAYUELA, A., LIU, Y., MANDAL, R., NEVEU, V., PON, A., KNOX, C., WILSON, M., MANACH, C. & SCALBERT, A. 2018. HMDB 4.0: the human metabolome database for 2018. *Nucleic Acids Res,* 46**,** D608-d617.

WITSBERGER, T. H., VILLAMIL, J. A., SCHULTZ, L. G., HAHN, A. W. & COOK, J. L. 2008. Prevalence of and risk factors for hip dysplasia and cranial cruciate ligament deficiency in dogs. *J Am Vet Med Assoc,* 232**,** 1818-24.

WOJDASIEWICZ, P., PONIATOWSKI, Ł. A. & SZUKIEWICZ, D. 2014. The Role of Inflammatory and Anti-Inflammatory Cytokines in the Pathogenesis of Osteoarthritis. *Mediators of Inflammation,* 2014**,** 561459.

WOLF, R. E., SCAVELLI, T. D., HOELZLER, M. G., FULCHER, R. P. & BASTIAN, R. P. 2012. Surgical and postoperative complications associated with tibial tuberosity advancement for cranial cruciate ligament rupture in dogs: 458 cases (2007-2009). *J Am Vet Med Assoc,* 240**,** 1481-7.

WON, W. W., LEE, A. M., BUTLER, J. R., WILLS, R. W. & BRINKMAN, E. L. 2020. Association of meniscal injury to joint space width on standard tibial plateau leveling osteotomy lateral radiographic projections of the canine stifle. *Veterinary Radiology & Ultrasound,* 61**,** 16-24.

WOOD, R. D. & GIBSON, T. 2020. Synovial Fluid Analysis of the Dog and Cat. *Veterinary Cytology.*

WU, C.-L., KIMMERLING, K. A., LITTLE, D. & GUILAK, F. 2017. Serum and synovial fluid lipidomic profiles predict obesity-associated osteoarthritis, synovitis, and wound repair. *Scientific Reports,* 7**,** 44315.

XU, X. & VEENSTRA, T. D. 2008. Analysis of biofluids for biomarker research. *PROTEOMICS – Clinical Applications,* 2**,** 1403-1412.

YAHIA, L. H. & DROUIN, G. 1989. Microscopical investigation of canine anterior cruciate ligament and patellar tendon: collagen fascicle morphology and architecture. *J Orthop Res,* 7**,** 243-51.

YANG, X. Y., ZHENG, K. D., LIN, K., ZHENG, G., ZOU, H., WANG, J. M., LIN, Y. Y., CHUKA, C. M., GE, R. S., ZHAI, W. & WANG, J. G. 2015. Energy Metabolism Disorder as a Contributing Factor of Rheumatoid Arthritis: A Comparative Proteomic and Metabolomic Study. *PLOS ONE,* 10**,** e0132695.

YOSHIHARA, Y., NAKAMURA, H., OBATA, K., YAMADA, H., HAYAKAWA, T., FUJIKAWA, K. & OKADA, Y. 2000. Matrix metalloproteinases and tissue inhibitors of metalloproteinases in synovial fluids from patients with rheumatoid arthritis or osteoarthritis. *Ann Rheum Dis,* 59**,** 455-61.

ZAR, T., GRAEBER, C. & PERAZELLA, M. A. 2007. Recognition, treatment, and prevention of propylene glycol toxicity. *Semin Dial,* 20**,** 217-9.

ZHAN, X., WU, H. & WU, H. 2020. Joint Synovial Fluid Metabolomics Method to Decipher the Metabolic Mechanisms of Adjuvant Arthritis and Geniposide Intervention. *Journal of Proteome Research,* 19**,** 3769-3778.

ZHANG, A., SUN, H., YAN, G., WANG, P. & WANG, X. 2016. Mass spectrometry-based metabolomics: applications to biomarker and metabolic pathway research. *Biomedical Chromatography,* 30**,** 7-12.

ZHANG, W., LIKHODII, S., ZHANG, Y., AREF-ESHGHI, E., HARPER, P. E., RANDELL, E., GREEN, R., MARTIN, G., FUREY, A., SUN, G., RAHMAN, P. & ZHAI, G. 2014. Classification of osteoarthritis phenotypes by metabolomics analysis. *BMJ Open,* 4**,** e006286.

ZHENG, K., SHEN, N., CHEN, H., NI, S., ZHANG, T., HU, M., WANG, J., SUN, L. & YANG, X. 2017a. Global and targeted metabolomics of synovial fluid discovers special osteoarthritis metabolites. *J Orthop Res,* 35**,** 1973-1981.

ZHENG, K., SHEN, N., CHEN, H., NI, S., ZHANG, T., HU, M., WANG, J., SUN, L. & YANG, X. 2017b. Global and targeted metabolomics of synovial fluid discovers special osteoarthritis metabolites. *Journal of Orthopaedic Research,* 35**,** 1973-1981.

ZOU, Y.-C., CHEN, L.-H., YE, Y.-L., YANG, G.-G., MAO, Z., LIU, D.-D., CHEN, J.-Q., CHEN, J.-J. & LIU, G. 2016. Attenuated synovial fluid ghrelin levels are linked with cartilage

damage, meniscus injury, and clinical symptoms in patients with knee anterior cruciate ligament deficiency. *Discovery medicine,* 22**,** 325-335.

7. Supplementary Material

S1. Veterinary surgeon information sheet

S2. Veterinary surgeon consent form

S3. Owner information sheet

S4. Owner consent form

S5. Radiographic scoring systems

S6. Pattern File for canine synovial fluid 1H NMR spectroscopy

S7. R scripts developed for analysis of PCA in respect to variable

S8. 2D NMR spectra

S9. Pattern file for canine lipid NMR spectra

S1.

VETERINARY SURGEON INFORMATION SHEET
Version 1.0
November 2020

Title of Research: Determining predictive metabolomic biomarkers for meniscal injuries in dogs with cranial cruciate ligament disease using stifle joint synovial fluid.

(*Identification of biomarkers in the knee joint fluid from dogs that could be used to identify meniscal injuries)*

You are being asked for permission to participate in a research project. Before you decide whether to participate, it is important for you to understand why the research is being done and what it will involve. Please take time to read the following information carefully and feel free to ask us if you would like more information or if there is anything that you do not understand. Please also feel free to discuss this with your friends, relatives and veterinary colleagues if you wish. We would like to stress that you do not have to accept this invitation and should only agree to take part if you want to. Thank you for reading this.

1. **What is the purpose of the study?**

The aim of this study is to investigate molecules in the knee joint fluid of dogs, in order to identify differences in these molecules in dogs with different knee joint problems. This could lead to the development of inexpensive and non-invasive (so without surgery) diagnostic tests for damage to cartilage structures in the joint and identify targets for future treatments.

We are requesting your permission to participate in this study by recruiting dogs that meet the inclusion criteria (dogs with cranial cruciate ligament ruptures that are surgical managed) within your practice.

2. **Why have I been chosen to take part?**

You are being asked for permission for your dog to take part in a research study because you are a veterinary surgeon that commonly performs surgery for rupture of an important knee ligament, or for surgery for a common kneecap problem in dogs.

3. **Do I have to take part?**

No, your participation is voluntary, and you may withdraw for any reason at any time. If you do not wish to participate you do not have to provide any reason for your decision. If you decide to take part, you are still free to withdraw at any time.

4. **What will happen if I take part?**

At the beginning of surgery for the disorders listed above, you will remove normally discard joint fluid from the affected stifle joint as directed in a standard operating procedure (SOP) sent to you by the Masters student, Ms. Christine Pye. This fluid will then be collected by Christine at a time suitable to you.

5. **Expenses and / or payments.**

There will be no cost to you for your participation in the research study. You will receive no reimbursement for the participation in the research study but we will debrief all participants in the research in a virtual session at the end of the study.

6. **Are there any risks in taking part?**

There are no risks associated with this study. Only the discarded clinical waste will be used in this research study.

7. **Are there any benefits in taking part?**

There will be no direct benefit to you . However, by taking part, you will be contributing to research which will help us better understand disease processes in the stifle joints of dogs, and ultimately help develop future diagnostic tests and treatment that would benefit animals with stifle joint problems.

8. **What if I am unhappy or if there is a problem?**

If you are unhappy, or if there is a problem, please feel free to let us know by contacting Professor Eithne Comerford by email at eithne.comerford@liverpool.ac.uk and we will try to help. If you remain unhappy or have a complaint which you feel you cannot come to us with then you should contact the Research Governance Officer on 0151 794 8290 (ethics@liv.ac.uk). When contacting the Research Governance Officer, please provide details of the name or description of the study (so that it can be identified), the researcher(s) involved, and the details of the complaint you wish to make.

9. **Will my participation be kept confidential?**

All information will be strictly confidential. No identification of individuals will be made when reporting or publishing the data arising from this study.

10. **What will happen to the results of the study?**

We hope to publish our findings in a scientific journal. You can be provided with a copy of the paper should you wish.

11. **What will happen if I want to stop taking part?**

You are free to withdraw your animal at anytime, without explanation. Results up to the period of withdrawal may be used, if you are happy for this to be done. Otherwise you may request that they are destroyed and no further use is made of them.

12. **Who can I contact if I have further questions**

If you would like more information about the research please contact:

Professor Eithne Comerford
Professor of Small Animal Surgery
Institute of Life Course and Medical Sciences and School of Veterinary Science
Faculty of Health and Life Sciences
Leahurst Campus
Chester High Road
Neston
CH64 7TE
Email:
Thank you for considering taking part in our research.

S2.

UNIVERSITY OF LIVERPOOL

VETERINARY SURGEON CONSENT FORM

Title of Research Project: Determining predictive metabolomic biomarkers for meniscal injuries in dogs with cranial cruciate ligament disease using stifle joint synovial fluid.

(*Identification of biomarkers in the knee joint fluid from dogs that could be used to identify meniscal injuries)*

Researcher(s): **Professors Eithne Comerford and Mandy Peffers and Ms. Christine Pye**

1. I confirm that I have read and have understood the information sheet dated November 2020 for the above study. I have had the opportunity to consider the information, ask questions and have had these answered satisfactorily. ☐

2. I understand that my participation is voluntary and that I am free to withdraw at any time without giving any reason, without my rights being affected. ☐

3. I understand that, under the Data Protection Act, I can at any time ask for access to the information I provide and I can also request the destruction of that information if I wish. ☐

4. I agree to take part in the above study. ☐

_____	_____	
Participant Name	Date	Signature
_____		
Name of Person taking consent	Date	Signature

The contact details of lead Researcher are:

Professor Eithne Comerford
Professor of Small Animal Surgery
Institute of Life Course and Medical Sciences and School of Veterinary Science
Faculty of Health and Life Sciences
Leahurst Campus
Chester High Road
Neston
CH64 7TE
Email:

S3.

OWNER INFORMATION SHEET
Version 1.0
November 2020

Title of Research: Determining predictive metabolomic biomarkers for meniscal injuries in dogs with cranial cruciate ligament disease using stifle joint synovial fluid.

(*Identification of biomarkers in the knee joint fluid from dogs that could be used to identify meniscal injuries)*

You are being asked for permission for your animal to participate in a research project. Before you decide whether to participate, it is important for you to understand why the research is being done and what it will involve. Please take time to read the following information carefully and feel free to ask us if you would like more information or if there is anything that you do not understand. Please also feel free to discuss this with your friends, relatives and Veterinary Surgeon if you wish. We would like to stress that you do not have to accept this invitation and should only agree to take part if you want to. Thank you for reading this.

2. **What is the purpose of the study?**

The aim of this study is to investigate molecules in the knee joint fluid of dogs, in order to identify differences in these molecules in dogs with different knee joint problems. This could lead to the development of inexpensive and non-invasive (so without surgery) diagnostic tests for damage to cartilage structures in the joint and identify targets for future treatments.

We are requesting your permission to use joint fluid that would normally be discarded during surgery to assist us in this research project.

3. **Why have I been chosen to take part?**

You are being asked for permission for your dog to take part in a research study because your dog is undergoing surgery for rupture of an important knee ligament, or for surgery for a common kneecap problem in dogs.

4. **Do I have to take part?**

No, the participation of your animal is voluntary, and you may withdraw your animal(s) for any reason at any time. If you do not wish to participate you do not have to provide any reason for your decision. If you decide to take part, you are still free to withdraw at any time. Refusal to participate or withdrawal will in no way affect the care to which animal participants are otherwise entitled.

5. **What will happen if I take part?**

At the beginning of surgery for the disorders listed above, the veterinary surgeon will remove some joint fluid from the knee. This fluid would normally be lost once the joint has been opened. If you agree to the participation of your animal in this study, we will ask you to sign a consent form to enable the discarded joint fluid to be used in this research project.

6. **Expenses and / or payments.**

There will be no cost to you for the participation of your animal in the research study. You will not be charged for any of the procedures performed solely for the study's purposes. You will receive no reimbursement for the participation of your animal in the research study but we will debrief all participants in the research in a virtual session at the end of the study.

7. **Are there any risks in taking part?**

There are no risks associated with this study. Only the discarded clinical waste will be used in this research study.

8. **Are there any benefits in taking part?**

There will be no direct benefit to you or your animal. However, by taking part, you will be contributing to research which will help us better understand disease processes in the knee joints of dogs, and ultimately help develop future diagnostic tests and treatment that would benefit animals with knee joint problems.

9. **What if I am unhappy or if there is a problem?**

If you are unhappy, or if there is a problem, please feel free to let us know by contacting Professor Eithne Comerford by email at eithne.comerford@liverpool.ac.uk and we will try to help. If you remain unhappy or have a complaint which you feel you cannot come to us with then you should contact the Research Governance Officer on 0151 794 8290 (ethics@liv.ac.uk). When contacting the Research Governance Officer, please provide details of the name or description of the study (so that it can be identified), the researcher(s) involved, and the details of the complaint you wish to make.

10. **Will my participation be kept confidential?**

All information will be strictly confidential. No identification of individuals will be made when reporting or publishing the data arising from this study.

11. **What will happen to the results of the study?**

We hope to publish our findings in a scientific journal. You can be provided with a copy of the paper should you wish. Otherwise there will be no further interaction with you.

12. **What will happen if I want to stop taking part?**

You are free to withdraw your animal at anytime, without explanation. Results up to the period of withdrawal may be used, if you are happy for this to be done. Otherwise you may request that they are destroyed and no further use is made of them.

13. **Who can I contact if I have further questions**

If you would like more information about the research please contact:
Professor Eithne Comerford
Professor of Small Animal Surgery
Institute of Life Course and Medical Sciences and School of Veterinary Science
Faculty of Health and Life Sciences
Leahurst Campus
Chester High Road
Neston
CH64 7TE
Email:

S4.

UNIVERSITY OF LIVERPOOL

CONSENT FORM

Title of Research Project: Determining predictive metabolomic biomarkers for meniscal injuries in dogs with cranial cruciate ligament disease using stifle joint synovial fluid.

(*Identification of biomarkers in the knee joint fluid from dogs that could be used to identify meniscal injuries)*

Researcher(s): **Professors Eithne Comerford and Mandy Peffers and Ms. Christine Pye**

2. I confirm that I have read and have understood the information sheet dated November 2020 for the above study. I have had the opportunity to consider the information, ask questions and have had these answered satisfactorily. ☐

3. I understand that my participation is voluntary and that I am free to withdraw at any time without giving any reason, without my rights being affected. ☐

4. I understand that, under the Data Protection Act, I can at any time ask for access to the information I provide and I can also request the destruction of that information if I wish. ☐

5. I agree to take part in the above study. ☐

_____ _____

Participant Name Date Signature

_____ _____

Name of Person taking consent Date Signature

The contact details of lead Researcher are:

Professor Eithne Comerford
Professor of Small Animal Surgery
Institute of Life Course and Medical Sciences and School of Veterinary Science
Faculty of Health and Life Sciences
Leahurst Campus
Chester High Road
Neston
CH64 7TE
Email:

S5. Radiographic scoring systems

- **Innes *et al*. (2004)**

Global score for osteoarthritis (0-3)
Joint effusion (0-2)
Osteophytosis (0-3)
Intrarticular mineralisation (02)

- **Mager and Mattis and Colleagues (Wessely *et al*. 2017)**

Assessment of osteophytosis (0-3) on 15 areas on mediolateral and craniocaudal radiograph:

Mediolateral stifle radiograph assessment areas:

1)Patellar apex
2)Patellar base
3)Proximal trochlear ridge
4)Distal trochlear ridge
5) Femoral condule
6)Tibial tuberosity
7)Cranial aspect of tibial plateau
8) Caudal aspect tibial plateau
9) Central aspect tibial plateau
10)Popliteal surface femur
11)Sesamoid bones

Caudocranial stifle radiograph assessment areas:

12)Lateral tibial and femoral condyle
13)Medial tibial and femoral condyle
14)Intercondylar notch
15)Patella

S6. PATTERN FILE FOR CANINE SYNOVIAL FLUID ^{1}H 1D NMR SPECTRA

Higher boundary (ppm)	Lower boundary (ppm)	Metabolite(s) Annotated and bin number
8.4669	8.4456	FORMATE_1
7.9301	7.9154	XANTHINE_2
7.9153	7.8321	4-PYRIDOXATE_ANSERINE_3
7.8309	7.7756	HISTIDINE_4
7.7325	7.7083	dTTP_t-methylhistidine_5
7.6489	7.613	UNKNOWN_6
7.6129	7.5826	UNKNOWN_7
7.5609	7.5265	UNKNOWN_8
7.4536	7.4376	PHENYLALANINE_9
7.4375	7.4259	PHENYLALANINE_10
7.4258	7.4149	PHENYLALANINE_11
7.4148	7.3979	UNKNOWN_12
7.3978	7.3823	PHENYLALANINE_2-PHENYLPROPRIONATE_13
7.3822	7.3711	PHENYLALANINE_2-PHENYLPROPRIONATE_14
7.371	7.3559	PHENYLALANINE_2-PHENYLPROPRIONATE_15
7.3475	7.3336	PHENYLALANINE_16
7.3335	7.3205	PHENYLALANINE_17
7.3204	7.3115	UNKNOWN_18
7.2786	7.2336	UNKNOWN_19
7.2166	7.1978	TYROSINE_20
7.1977	7.1823	TYROSINE_21
7.1674	7.153	UNKNOWN_22
7.1529	7.138	UNKNOWN_23
7.1324	7.0929	UNKNOWN_24
7.0837	7.0525	HISTIDINE_t-METHYLHISTIDINE_25
7.0348	6.9856	UNKNOWN_26
6.9201	6.9056	TYROSINE_ACETAMINOPHEN_O-CRESOL_GLUTAMINE_27
6.9055	6.889	TYROSINE_ACETAMINOPHEN_O-CRESOL_GLUTAMINE_28
6.8493	6.7967	P-CREOSOL_29
6.6654	6.6331	UNKNOWN_30
6.5255	6.5171	UNKNOWN_31
6.2689	6.2621	DTTP_32
5.919	5.9002	UNKNOWN_33
5.8253	5.8022	UNKNOWN_34
5.4086	5.3953	UNKNOWN_35
5.3663	5.3532	UNKNOWN_36
5.3531	5.251	MOBILE UNSATURATED LIPID_37
5.2509	5.2115	GLUCOSE_38

5.1968	5.1783	MANNOSE_39
5.124	5.1094	UNKNOWN_40
5.1093	5.0981	UNKNOWN_41
5.098	5.0883	UNKNOWN_42
4.9087	4.9019	MANNOSE_43
4.4626	4.454	TRIGONELLINE_44
4.3912	4.3821	UNKNOWN_45
4.382	4.3702	UNKNOWN_46
4.3353	4.281	SN-GLYCERO-3-PHOSPHOCHOLINE_47
4.2734	4.2649	THREONINE_48
4.2648	4.2372	THREONINE_49
4.2371	4.2258	UNKNOWN_50
4.2257	4.2172	UNKNOWN_51
4.2076	4.1831	UNKNOWN_52
4.1487	4.1386	UNKNOWN_53
4.1385	4.1327	UNKNOWN_54
4.1326	4.0933	LACTATE_55
4.0932	4.0871	UNKNOWN_56
4.084	4.0778	GALACTOSE_CHOLINE_57
4.0777	4.0733	GALACTOSE_CHOLINE_58
4.0732	4.0667	GALACTOSE_CHOLINE_59
4.0666	4.0603	GALACTOSE_CHOLINE_60
4.0602	4.0489	CREATININE_61
4.0208	4.0092	UNKNOWN_62
4.0091	4.0046	UNKNOWN_63
4.0045	3.999	UNKNOWN_64
3.9989	3.9949	UNKNOWN_65
3.9948	3.9869	UNKNOWN_66
3.9868	3.983	UNKNOWN_67
3.9829	3.9776	UNKNOWN_68
3.9775	3.9664	UNKNOWN_69
3.9663	3.9561	UNKNOWN_70
3.956	3.9482	GLYCOLATE_71
3.9481	3.9327	UNKNOWN_72
3.9326	3.9258	CREATINE_73
3.9257	3.9204	UNKNOWN_74
3.9203	3.9052	GLUCOSE_75
3.9026	3.8858	GLUCOSE_BETAINE_76
3.8857	3.8724	MANNITOL_77
3.8699	3.8639	MANNITOL_78
3.8638	3.8604	MANNITOL_79
3.8603	3.852	GLUCOSE_80
3.8519	3.8466	UNKNOWN_81
3.8465	3.8355	GLUCOSE_82
3.8354	3.8321	GLUCOSE_83
3.832	3.8283	GLUCOSE_84

3.8282	3.8251	GLUCOSE_85
3.825	3.8212	GLUCOSE_86
3.8211	3.8185	GLUCOSE_87
3.8184	3.812	GLUCOSE_MANNITOL_88
3.8119	3.8001	ALANINE_MANNITOL_89
3.8	3.7907	ALANINE_GLUTAMINE_90
3.7906	3.7808	GLUCOSE_ALANINE_MANNITOL_GALACTOSE_GLUCITOL_91
3.7807	3.7752	GLUCOSE_ANSERINE_GALACTOSE_LYCINE_MANNITOL_GLUCITOL_92
3.7751	3.7723	ALANINE_GLUCOSE_GLUCITOL_MANNITOL_93
3.7722	3.7634	GLUCOSE_GALACTOSE_LYCINE_GLUTAMATE_MANNITOL_94
3.7633	3.7552	GLUCOSE_GALACTOSE_LYCINE_GLUTAMATE_GLUCITOL_MANNITOL_95
3.7502	3.7419	GLUCOE_ALLOISOLEUCINE_2-AMINOADIPATE_GALACTOSE_O-ACETYLCHOLINE_LEUCINE_96
3.7418	3.7314	GLUCOSE_O-ACETYLCHOLINE_2-AMINOADIPATE_GALACTOSE_LEUCINE_97
3.7313	3.7257	GLUCOSE_FRUCTOSE_98
3.7256	3.7214	GLUCOSE_99
3.7213	3.718	GLUCOSE_PI-METHYLHISTIDINE_100
3.7179	3.7123	UNKNOWN_101
3.7122	3.6989	GLUCOSE_T-METHYLHISTIDINE_GALACTOSE_MANNITOL_102
3.6988	3.6917	MANNITOL_103
3.6916	3.683	MANNITOL_104
3.6829	3.6766	MANNITOL_105
3.6765	3.6676	ETHANOL_106
3.6675	3.662	GLYCEROL_ETHANOL_107
3.6619	3.6582	UNKNOWN_ETHANOL_108
3.6581	3.6521	ETHANOL_109
3.652	3.6471	GLYCEROL_ETHANOL_110
3.647	3.6437	ETHANOL_111
3.6436	3.6368	UNKNOWN_112
3.6367	3.6299	MYO-INOSITOL_113
3.6298	3.6218	UNKNOWN_114
3.6217	3.6176	MYO-INOSITOL_VALINE_115
3.6175	3.6051	VALINE_THREONINE_116
3.605	3.5921	UNKNOWN_117
3.592	3.5691	UNKNOWN_GLYCEROL_118
3.569	3.5598	GLYCINE_119
3.5597	3.5558	GLYCEROL_120
3.5557	3.5505	GLUCOSE_121
3.5504	3.5433	GLUCOSE_122
3.5432	3.5367	GLUCOSE_123
3.5366	3.5281	GLUCOSE_124
3.5185	3.5068	GLUCOSE_125
3.5067	3.4487	GLUCOSE_126
3.4486	3.4404	UNKNOWN_127

3.4403	3.3815	GLUCOSE_128
3.3706	3.3621	METHANOL_129
3.362	3.3578	UNKNOWN_130
3.3577	3.3451	UNKNOWN_131
3.345	3.3399	UNKNOWN_132
3.3398	3.3324	UNKNOWN_133
3.3323	3.3108	UNKNOWN_134
3.3107	3.3057	PI-METHYLHISTIDINE_135
3.3056	3.301	UNKNOWN_136
3.2988	3.2919	UNKNOWN_137
3.2918	3.28817	UNKNOWN_138
3.2835	3.2741	UNKNOWN_139
3.2832	3.276	UNKNOWN_141
3.2759	3.2736	UNKNOWN_142
3.274	3.2833	UNKNOWN_140
3.2735	3.2738	UNKNOWN_143
3.2727	3.2719	UNKNOWN_144
3.2718	3.2679	UNKNOWN_145
3.2678	3.2645	GLUCOSE_BETAINE_146
3.2644	3.2608	BETAINE_147
3.2607	3.2574	UNKNOWN_BETAINE_GLUCOSE_148
3.2573	3.2491	GLUCOSE_149
3.249	3.2443	UNKNOWN_150
3.2442	3.2379	GLUCOSE_151
3.2378	3.2033	MOBILE LIPID -N(CH3)3_152
3.2032	3.1952	CHOLINE_153
3.1951	3.1809	UNKNOWN_154
3.1763	3.1274	DIMETHYL SULFONE_155
3.1273	3.0975	UNKNOWN_156
3.0518	3.0429	CREATININE_CREATINE_LYSINE_TYROSINE_CREATININE-PHOSPHATE_157
3.0428	3.0369	LYSINE_CREATININE_CREATINE-PHOSPHATE_CREATINE_TYROSINE_158
3.0368	3.0268	LYSINE_159
3.0267	3.0173	LYSINE_160
3.0172	3.0079	UNKNOWN_161
3.0078	2.9992	UNKNOWN_162
2.9991	2.989	UNKNOWN_163
2.9678	2.9478	UNKNOWN_164
2.9477	2.9061	UNKNOWN_165
2.906	2.8951	UNKNOWN_166
2.895	2.8849	UNKNOWN_167
2.872	2.8316	UNKNOWN_168
2.6866	2.6672	UNKNOWN_169
2.6671	2.6522	UNKNOWN_170
2.6521	2.6436	UNKNOWN_171

2.6435	2.6304	UNKNOWN_172
2.5733	2.5565	UNKNOWN_173
2.5564	2.5357	CITRATE_174
2.5356	2.5166	CITRATE_175
2.5165	2.5122	UNKNOWN_176
2.5121	2.5063	UNKNOWN_177
2.5062	2.5003	UNKNOWN_178
2.5002	2.4803	GLUTAMINE_179
2.4802	2.4693	GLUTAMINE_180
2.4692	2.4571	GLUTAMINE_181
2.457	2.4451	GLUTAMINE_182
2.445	2.4344	GLUTAMINE_183
2.4343	2.4229	GLUTAMINE_184
2.4228	2.4085	GLUTAMINE_185
2.4084	2.3964	3-HYDROXY-3-METHYLGLUTARATE_186
2.3963	2.3791	DTTP_GLUTAMATE_ISOBUTYRATE_UNKNOWN_187
2.379	2.3714	PYRUVATE_188
2.3713	2.3681	GLUTAMATE_3-HYDROXYISOVALERATE_189
2.368	2.3352	GLUTAMATE_190
2.2994	2.2869	VALINE_191
2.2868	2.28	ACETOACETATE_VALINE_SUCCINYLACETONE_192
2.2799	2.2706	VALINE_UNKNOWN_193
2.2705	2.2609	VALINE_2-AMINOADIPATE_P-CREOSOL_2-METHYLGLUTARATE_GLYCYLPROLINE_UNKNOWN_194
2.2608	2.2509	2-AMINOADIPATE_THYMOL_VALINE_2-METHYLGLUTARATE_GLYCYLPROLINE_VALINE_P-CRESOL_195
2.2508	2.2364	UNKNOWN_196
2.2363	2.2294	ACETONE_O-CRESOL_197
2.2062	2.1854	UNKNOWN_198
2.1853	2.1726	GLUTAMINE_2-METHYLGLUTARATE_AZELATE_SEBACATE_199
2.1725	2.168	GLUTAMINE_ACETAMINOPHEN_200
2.1679	2.1614	GLUTAMINE_ACETAMINOPHEN_METHIONINE_2-METHYLGLUTARATE_GLUTAMATE_201
2.1613	2.1517	GLUTAMINE_GLUTAMATE_202
2.1516	2.1404	METHIONINE_GLUTAMINE_GLUTAMATE_203
2.1403	2.0939	GLUTAMINE_GLUTAMATE_204
2.0938	2.0708	N-ACETYLCYSTEINE_GLUTAMATE_ALLOISOLEUCINE_205
2.0707	2.0638	GLUTAMATE_206
2.0637	2.0542	GLUTAMATE_207
2.0541	2.0315	N-ACETYLGLUTAMINE_GLUTAMATE_UNKNOWN_208
2.0314	2.0202	UNKNOWN_GLUTAMATE_209
2.0201	1.9363	GLYCYLPROLINE_ISOLEUCINE_UNKNOWN_210
1.9272	1.9149	ACETATE_211
1.9148	1.8691	LYSINE_UKNOWN_212
1.8065	1.7592	UNKNOWN_213
1.7591	1.7036	LYCINE_LEUCINE_214
1.7035	1.6345	LEUCINE_LYSINE_2-HYDROXYVALERATE_215

1.6344	1.5936	2-HYDROXYVALERATE_UNKNOWN_216
1.5935	1.5419	UNKNOWN_217
1.5418	1.4975	LYSINE_218
1.5141	1.4362	ALANINE_219
1.4296	1.4077	2-PHENYLPROPRIONATE_ALLOISOLEUCINE_220
1.4076	1.3774	2-HYDROXYVALERATE_ALLOISOLEUCINE_221
1.3773	1.3474	UNKNOWN_222
1.3473	1.3167	LACTATE_THREONINE_223
1.3166	1.1986	MOBILE LIPID -(CH2)n (VLDL)_224
1.1985	1.1924	ETHANOL_225
1.1889	1.1819	ETHANOL_226
1.1818	1.1671	UNKNOWN_227
1.153	1.1453	PROPYLENE GLYCOL_228
1.1452	1.1361	PROPYLENE GLYCOL_229
1.08	1.0717	METHYLSUCCINATE_2-METHYLGLUTARATE_230
1.0716	1.0625	METHYLSUCCINATE_2-METHYLGLUTARATE_231
1.0563	1.026	VALINE_ISOBUTYRATE_232
1.0202	1.0087	ISOLEUCINE_233
1.0086	1.0004	ISOLEUCINE_234
1.0003	0.9943	VALINE_235
0.9942	0.9905	ALLOISOLEUCINE_VALINE_236
0.9904	0.9841	VALINE_237
0.984	0.9778	ALLOISOLEUCINE_VALINE_238
0.9777	0.9671	LEUCINE_ALLOISOLEUCINE_239
0.967	0.9564	LEUCINE_240
0.9563	0.9432	LEUCINE_ISOLEUCINE_ALLOISOLEUCINE_241
0.9431	0.9334	ALLOISOLEUCINE_ISOLEUCINE_242
0.9333	0.9219	ISOLEUCINE_243
0.9175	0.9063	GLYCOCHOLATE_244
0.9062	0.8977	IBUPROFEN_245
0.8908	0.7892	MOBILE LIPID -CH3(VLDL)_246

S7. R scripts developed for analysis of principal component analysis (PCA) in respect to variable

Function for assessing variance in across principle components developed by Dan Green of the University of Liverpool Computational Biology Department

```
covariate_pc_summary <- function(covar = "Age", prin_comp = "PC1",
pca_data = canine_pca_pcs) {
  if(length(unique(pca_data[,covar])) < 10){

    pca_data[,covar] <- as.factor(pca_data[,covar])

print(paste0("Your covariate is a factor with ",
length(levels(pca_data[,covar])), " levels; "));
print(paste0(levels(pca_data[,covar])))
f <- formula(paste(prin_comp, "~", covar))
x <- summary(aov(f , data = pca_data))
x <- x[[1]]$`Pr(>F)`[1] %>% round(5)
return(x)

  } else {

    pca_data[,covar] <- as.numeric(pca_data[,covar])
    print("Your covariate is numeric, running linear model")
    f <- formula(paste(prin_comp, "~", covar))
    x <- summary(lm(f, data = pca_data))
    x <- x$coefficients[2,4]
    return(x)
}

}
```

S8. ^{1}H ^{13}C HSQC 2D NMR spectra for canine synovial fluid

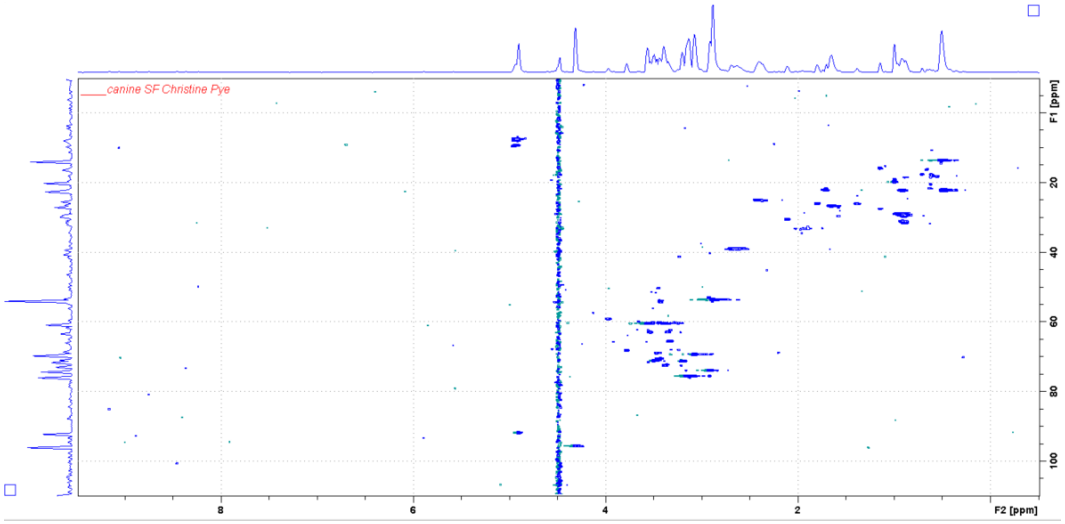

S9. Pattern file used for lipid extract 1H 1D NMR of canine synovial fluid

Bin upper boundary (ppm)	Bin lower boundary (ppm)	Bin number	Annotation
9.974	9.9631	unknown_1	
9.8089	9.7997	unknown_2	
7.9671	7.9229	unknown_3	
7.7965	7.7842	unknown_4	
7.7841	7.7714	unknown_5	
7.7323	7.7249	unknown_6	
7.5438	7.53	unknown_7	
7.5229	7.5119	unknown_8	
7.4593	7.4451	unknown_9	
7.445	7.4283	unknown_10	
7.4282	7.4157	unknown_11	
7.4156	7.4	unknown_12	
7.3948	7.3829	unknown_13	
7.3828	7.3775	unknown_14	
7.3709	7.3623	unknown_15	
7.3588	7.3376	unknown_16	
7.3014	7.2902	unknown_17	
7.2799	7.2721	unknown_18	
7.272	7.2277	Chloroform_19	
7.2276	7.2186	unknown_20	
7.2002	7.183	unknown_21	
7.1829	7.1576	unknown_22	
7.1404	7.1344	unknown_23	
7.1343	7.1283	unknown_24	
7.1282	7.1223	unknown_25	
7.1222	7.1161	unknown_26	
7.116	7.099	unknown_27	
7.0989	7.0651	unknown_28	
6.9877	6.9742	unknown_29	
6.9517	6.9426	unknown_30	
6.844	6.7796	unknown_31	
6.6209	6.5851	unknown_32	
6.5179	6.5039	unknown_33	
6.1558	6.1343	unknown_34	
6.1342	6.1235	unknown_35	
6.1234	6.1113	unknown_36	
6.1112	6.094	unknown_37	
5.8432	5.8217	unknown_38	
5.8216	5.8015	unknown_39	
5.7856	5.7645	unknown_40	
5.7201	5.7106	unknown_41	

5.6354	5.6238	unknown_42	
5.6237	5.59	unknown_43	
5.428	5.2894	unknown_44	
5.2893	5.2001	unknown_45	
5.2	5.1888	unknown_46	
5.0927	5.082	unknown_47	
4.9309	4.9105	unknown_48	
4.9104	4.8975	unknown_49	
4.8806	4.8682	unknown_50	
4.7403	4.7109	unknown_51	
4.7108	4.6861	unknown_52	
4.686	4.6678	unknown_53	
4.6677	4.6556	unknown_54	
4.6555	4.63656	unknown_55	Phospholipids
4.63	4.5685	unknown_56	
4.4428	4.3689	unknown_57	Triacylglycerides
4.3688	4.3159	unknown_58	Triacylglycerides
4.3158	4.2936	unknown_59	
4.2935	4.2601	unknown_60	
4.1723	4.1614	unknown_61	
4.1613	4.1529	unknown_62	
4.1528	4.1443	unknown_63	
4.1442	4.125	unknown_64	
4.1249	4.1046	unknown_65	
4.1045	4.098	unknown_66	Phospholipids
4.0979	4.0896	unknown_67	Phospholipids
4.0895	4.0804	unknown_68	Phospholipids
4.0803	4.0631	unknown_69	Phospholipids
4.0625	4.055	unknown_70	Phospholipids
4.0549	4.0133	unknown_71	Phospholipids
4.0137	3.9142	unknown_72	Phosphatidylcholine
3.8841	3.7715	unknown_73	
3.7714	3.6651	unknown_74	Phosphatidylcholine
3.665	3.5948	unknown_75	
3.5647	3.4725	unknown_76	Free Cholesterol
3.38	3.29	unknown_77	Phosphatidyl choline
3.0097	2.9695	unknown_78	
2.8649	2.8423	unknown_79	
2.8422	2.8332	unknown_80	
2.8331	2.825	unknown_81	
2.8249	2.8176	unknown_82	
2.8177	2.8121	unknown_83	
2.812	2.8068	unknown_84	
2.8067	2.7969	unknown_85	
2.7968	2.7865	unknown_86	
2.7864	2.7751	unknown_87	linoleic acid

2.775	2.7647	unknown_88	linoleic acid
2.7646	2.7419	unknown_89	linoleic acid
2.7183	2.7062	unknown_90	
2.7061	2.6954	unknown_91	
2.6953	2.6834	unknown_92	
2.6669	2.6576	unknown_93	
2.6575	2.6499	unknown_94	
2.6469	2.6411	unknown_95	
2.6289	2.6171	unknown_96	
2.617	2.6131	unknown_97	
2.613	2.607	unknown_98	
2.6069	2.6026	unknown_99	
2.6025	2.5879	unknown_100	
2.5878	2.4944	unknown_101	
2.4943	2.4727	unknown_102	
2.4574	2.4424	unknown_103	
2.4296	2.3943	unknown_104	
2.3581	2.3449	unknown_105	
2.3448	2.3342	unknown_106	
2.3341	2.3246	unknown_107	
2.3245	2.2931	unknown_108	
2.293	2.2858	unknown_109	
2.2857	2.283	unknown_110	
2.2829	2.2726	unknown_111	
2.2725	2.2608	unknown_112	
2.2607	2.245	unknown_113	
2.244	2.2256	unknown_114	
2.2255	2.2017	unknown_115	
2.1826	2.1758	unknown_116	
2.1652	2.1566	unknown_117	
2.1565	2.1474	unknown_118	
2.1311	2.1201	unknown_119	
2.12	2.1108	unknown_120	
2.1107	2.1079	unknown_121	
2.1078	2.1	unknown_122	
2.0999	2.0913	unknown_123	
2.0912	2.0812	unknown_124	
2.0811	2.072	unknown_125	
2.0719	2.0662	unknown_126	
2.0661	2.0562	unknown_127	
2.0561	2.0453	unknown_128	
2.0452	2.0346	unknown_129	
2.0345	2.0262	unknown_130	
2.0261	2.0068	unknown_131	
2.0097	1.9881	unknown_132	
1.988	1.9822	unknown_133	

1.9821	1.9647	unknown_134	
1.9646	1.9207	unknown_135	
1.8836	1.7865	unknown_136	
1.7518	1.7126	unknown_137	
1.7125	1.7012	unknown_138	
1.7011	1.6919	unknown_139	
1.6918	1.6643	unknown_140	
1.6528	1.5521	unknown_141	
1.5449	1.5347	unknown_142	
1.5346	1.5241	unknown_143	
1.524	1.5167	unknown_144	
1.5166	1.5067	unknown_145	
1.5066	1.49641	unknown_146	
1.4963	1.4867	unknown_147	
1.4866	1.4804	unknown_148	
1.4803	1.4725	unknown_149	
1.4724	1.4631	unknown_150	
1.463	1.4483	unknown_151	
1.4482	1.4421	unknown_152	
1.442	1.4347	unknown_153	
1.4346	1.4252	unknown_154	
1.4251	1.4174	unknown_155	
1.4173	1.4092	unknown_156	
1.4091	1.3966	unknown_157	
1.394	1.3667	unknown_158	
1.3666	1.3607	unknown_159	
1.3606	1.3465	unknown_160	
1.3464	1.3266	unknown_161	
1.3265	1.3188	unknown_162	
1.3187	1.3102	unknown_163	
1.3101	1.3	unknown_164	
1.2999	1.2884	unknown_165	
1.2883	1.2791	unknown_166	
1.279	1.2701	unknown_167	
1.27	1.184	unknown_168	
1.183	1.178	unknown_169	
1.1779	1.1657	unknown_170	
1.1656	1.159	unknown_171	
1.1589	1.1521	unknown_172	
1.152	1.1455	unknown_173	
1.1454	1.1409	unknown_174	
1.1408	1.1194	unknown_175	
1.1193	1.111	unknown_176	
1.1109	1.007	unknown_177	
1.006	1.0872	unknown_178	
1.0871	1.0232	unknown_179	

1.0231	1.0099	unknown_180	Cholesteryl ester
1.0098	1.0002	unknown_181	CF
1.0001	0.9918	unknown_182	CF
0.9917	0.923	unknown_183	
0.9229	0.9102	unknown_184	
0.9101	0.9005	unknown_185	
0.9004	0.8934	unknown_186	
0.8933	0.8837	unknown_187	
0.8836	0.8717	unknown_188	
0.8716	0.8662	unknown_189	
0.8661	0.8615	unknown_190	
0.8614	0.8567	unknown_191	
0.8566	0.8502	unknown_192	
0.8501	0.7686	unknown_193	
0.6876	0.6313	unknown_194	Total Cholesterol
0.5971	0.5663	unknown_195	
0.5662	0.345	unknown_196	
0.227	0.193	unknown_197	
0.0782	0.0544	unknown_198	